University of Liège

Faculty of Sciences - Department of Life Sciences

UR InBioS

Centre for Protein Engineering - Laboratory of Biochemistry

Extremophilic cuproxidases: new pattern of temperature adaptation and function of their methionine-rich regions

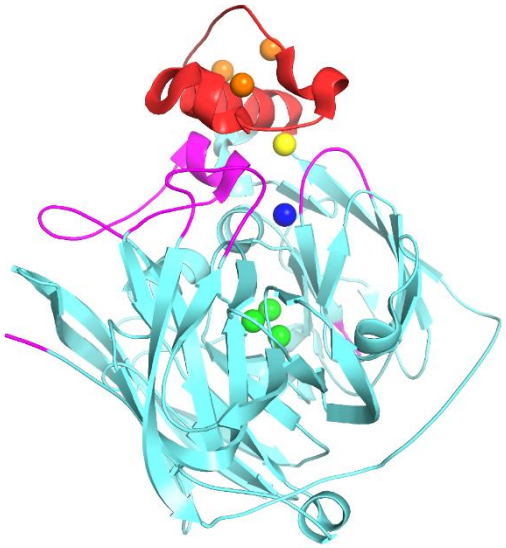

Frédéric Roulling

Thesis presented for the Degree of Doctor of Science (PhD)

Promoter: Dr. Georges Feller

Academic year 2021-2022

Cover page illustration: ribbon diagram of the cuproxidase CueO from *E. coli*. In red, the Met-rich insert in CueO and in magenta, the solvent-exposed loops in which the Met-rich insert has been found in other bacterial cuproxidases. Note the proximity with the blue T1 site. Spheres represent bound copper ions with color code: blue, the T1 Cu; green, the trinuclear center; yellow, the sCu and orange, Cu(I) on the Met-rich region. The N-terminus (magenta) is in front, left and the C-terminus (magenta) is behind the structure. Figure based on PDB entries 3OD3 and 3NT0. (Figure from Roulling *et al.*, 2022).

Summary

On Earth, there are many environments that can be described as extreme from an anthropocentric point of view. This is particularly valid for temperature. These environments are not, however, devoid of life and the organisms that can be found there are called extremophiles. Extremophiles are mainly prokaryotic organisms which have developed cellular components adapted to such extreme conditions. These adaptations can be found in their membranes, their nucleic acids as well as their proteins and the molecular study of these adjustments allows a better understanding of these fundamental molecules of life.

This work is part of a broader effort conducted for several years at the Laboratory of Biochemistry, Center for Protein Engineering, University of Liège, to understand the adaptation of enzymes to temperature. Within this context, many different enzymes have been extensively studied to generate a knowledge that has greatly contributed to establish the activity-stability-flexibility tradeoff hypothesis for temperature adaptation. However, a comparative study of extremophilic enzymes catalyzing electron transfer was still lacking. The first aim of the present work was to investigate this aspect using psychrophilic, mesophilic and thermophilic blue multicopper oxidases (MCOs) as models. Those three enzymes are homologous periplasmic cuproxidases involved in copper resistance mechanisms of bacteria and they display a methionine-rich region with high diversity in both the length and composition. The second aim of this study was to examine the role of this peculiar region.

The model enzymes studied were CueO from the mesophilic bacterium *Escherichia coli*, the thermophilic *Tth*-MCO from *Thermus thermophilus*, and PhaMOx, the corresponding psychrophilic enzyme from the Antarctic bacterium *Pseudoalteromonas haloplanktis*. We have shown that these enzymes demonstrate a specific adaptive pattern, distinct from the one observed in enzymes possessing a well-defined active site and relying on conformational changes such as for the induced fit mechanism. In fact, and in contrast with many previous studies on extremozymes, the stability of the extremophilic cuproxidases examined is correlated with neither activity, nor flexibility. One of the most striking observation is that despite large differences in stability, the flexibility of the cold-adapted PhaMOx and that of the thermophilic *Tth*-MCO are identical. This tends to indicate that the firm and precise bindings of the four catalytic copper ions are essential to ensure the proper functioning of the oxidases, i.e. substrate oxidation by the T1 site, positioned close to the protein surface, and oxygen reduction to water by the trinuclear cluster, located in the core enzyme. Still, the psychrophilic cuproxidase display a low stability and it remains to be clarified if it is due to a lack of selective pressure or if it is an essential component for its function.

The cuproxidases are found in prokaryotes and form a subgroup of the MCO family. Their role is to oxidize toxic Cu(I) ions into less harmful Cu(II) and they are part of the copper resistance mechanism of bacteria. In contrast to other MCOs such as laccase or ascorbate oxidase where a depression near the T1 site creates a substrate specific site for phenolic compounds or ascorbic acid, respectively, cuproxidases display disordered methionine-rich (Met-rich) loops of variable length that restricts accessibility to the T1 site. In CueO, the Met-rich region had been demonstrated to bind Cu(I) ions which are subsequently oxidized by the enzyme. We found that the location of the Met-rich regions in the primary structure is highly variable in bacterial cuproxidases, but always inserted in solvent exposed surface loops, at close proximity of the conserved T1 site. Taking advantage of the large loop length differences in the three model cuproxidases and by studying PhaMOx variants, we showed that the number of Cu(I) bound is nearly proportional to the size of the Met-rich loops and to the number of potential Cu(I) ligands (Met, His, Asp). These results demonstrate that Met-rich loops in cuproxidases are essential components of bacterial copper resistance. They can be seen as tentacles that feed the Cu(I) substrate binding site (sCu), regarded as a beak located between the protein surface and the T1 site, and fancying cuproxidases as molecular octopus chasing toxic cuprous ions in bacterial periplasm.

Résumé

Sur Terre, il existe de nombreux environnements qui peuvent être décrits comme extrêmes d'un point de vue anthropocentrique. Ceci est particulièrement valable pour la température. Ces environnements ne sont néanmoins pas exempts de vie et les organismes qui peuvent y être trouvés sont appelés extrêmophiles. Les extrêmophiles sont principalement des organismes procaryotes qui ont développé des composants cellulaires adaptés à ces conditions extrêmes. Ces adaptations se retrouvent dans leurs membranes, leurs acides nucléiques ainsi que leurs protéines et l'étude moléculaire de ces ajustements permet une meilleure compréhension de ces molécules fondamentales de la vie.

Ce travail s'inscrit dans un effort plus large mené depuis plusieurs années au Laboratoire de Biochimie, Centre d'Ingénierie des Protéines, Université de Liège, pour comprendre l'adaptation des enzymes à la température. Dans ce contexte, de nombreuses enzymes différentes ont été étudiées intensivement pour générer une connaissance qui a grandement contribué à établir l'hypothèse de compromis activité-stabilité-flexibilité pour l'adaptation à la température. Cependant, une étude comparative des enzymes extrêmophiles catalysant le transfert d'électrons faisait encore défaut. Le premier objectif du présent travail était d'étudier cet aspect en utilisant des oxydases multicuivres (MCOs) psychrophile, mésophile et thermophile comme modèles. Ces trois enzymes sont des cuproxidases périplasmiques homologues impliquées dans les mécanismes de résistance au cuivre des bactéries et elles présentent une région riche en méthionine avec une grande diversité tant dans la longueur que dans la composition. Le deuxième objectif de cette étude était d'examiner le rôle de cette région particulière.

Les enzymes modèles étudiées étaient CueO de la bactérie mésophile *Escherichia coli*, la thermophile *Tth*-MCO de *Thermus thermophilus* et PhaMOx, l'enzyme psychrophile correspondante de la bactérie antarctique *Pseudoalteromonas haloplanktis*. Nous avons montré que ces enzymes présentent un schéma adaptatif spécifique, distinct de celui observé dans les enzymes possédant un site actif bien défini et s'appuyant sur des changements conformationnels tels que le mécanisme d'ajustement induit. En fait, et contrairement à de nombreuses études antérieures sur les extrêmozymes, la stabilité des cuproxidases extrêmophiles examinées n'est corrélée ni à l'activité, ni à la flexibilité. L'une des observations les plus frappantes est que malgré de grandes différences de stabilité, la flexibilité de PhaMOx, adaptée au froid, et de *Tth*-MCO, thermophile, est identique. Cela tend à indiquer que les liaisons fermes et précises des quatre ions de cuivre catalytique sont essentielles pour assurer le bon fonctionnement des oxydases, c.-à-d. l'oxydation du substrat par le site T1, positionné près de la surface de la protéine, et la réduction de l'oxygène en eau par le centre trinucléaire, situé dans le corps de l'enzyme. Pourtant, la cuproxidase psychrophile affiche une faible stabilité et il reste à préciser si elle est due à un manque de pression sélective ou si elle est un composant essentiel pour son fonctionnement.

Les cuproxidases sont trouvées chez les procaryotes et forment un sous-groupe de la famille des MCOs. Leur rôle est d'oxyder les ions Cu(I) toxiques en Cu(II) moins nocifs et elles font partie du mécanisme de résistance au cuivre des bactéries. Contrairement à d'autres MCOS comme la laccase ou l'ascorbate oxydase, où une dépression près du site T1 crée un site spécifique au substrat pour les composés phénoliques ou l'acide ascorbique, respectivement, les cuproxidases présentent des boucles désordonnées riches en méthionines (Met-rich) et de longueur variable qui limitent l'accessibilité au site T1. Chez CueO, il a été démontré que la région Met-rich lie les ions Cu(I) qui sont ensuite oxydés par l'enzyme. Nous avons constaté que l'emplacement des régions Met-rich dans la structure primaire est très variable dans les cuproxidases bactériennes, mais qu'elles sont toujours insérées dans des boucles de surface exposées au solvant, à proximité du site T1 conservé. Profitant des grandes différences de longueur de boucle dans les trois cuproxidases modèles et par mutagenèse de PhaMOx, nous avons montré que le nombre de Cu(I) lié est presque proportionnel à la taille des boucles Met-rich et au nombre de ligands potentiels de Cu(I) (Met, His, Asp). Ces résultats démontrent que les boucles Met-rich dans les cuproxidases sont des composants essentiels de la résistance bactérienne au cuivre. Elles peuvent être considérées comme des tentacules qui alimentent le site de liaison du substrat Cu(I) (sCu), vu comme un bec situé entre la surface protéique et le site T1, et les cuproxidases imaginées comme des pieuvres moléculaires chassant les ions cuivreux toxiques dans le périplasme bactérien.

Remerciements

Je souhaite exprimer ma gratitude au Docteur Georges Feller pour la confiance qu'il m'a accordée en m'accueillant dans son laboratoire afin d'y réaliser mon doctorat et sans qui cette thèse n'aurait jamais vu le jour. Georges, merci pour tes conseils avisés, ta patience, tes mots d'encouragement (/rappels à l'ordre), … en condensé, pour ton soutien indéfectible. Objectif atteint : je passe ma thèse avant ta pension !

Je remercie le Professeur André Matagne et le Professeur Moreno Galleni pour m'avoir épaulé pour certaines parties expérimentales et pour leur rôle indispensable dans mon comité de thèse.

Mes remerciements s'adressent aussi au Docteur Tony Collins pour m'avoir initié à la recherche scientifique lors de mon mémoire de deuxième cycle et pour son soutien lors de ma demande de bourse de doctorat.

L'occasion m'est ici également donnée de remercier le FNRS pour la confiance qui m'a été accordée en m'octroyant une bourse FRIA.

Je tiens à témoigner ma reconnaissance à Nicole. Son expérience et ses précieux conseils techniques n'ont d'égal que son énergie et sa bonne humeur inépuisables.

Merci à Fabienne pour son aide administrative, mais surtout pour les pauses cafés riches en discussions diverses et variées, et toujours synonymes de bons moments.

Mes remerciements s'adressent aussi aux membres du laboratoire de biochimie qui ont rythmé la vie du labo et avec qui j'ai partagé d'innombrables, et tout aussi agréables, pauses repas ou cafés, et, bien sûr, dures journées de labeur : Florence, Salvi, Jean-Claude et le Professeur Charles Gerday.

Je pense aussi à mes compagnons de « galère » depuis la licence en biochimie (et oui ça remonte à longtemps, en ce temps-là le master n'avait pas encore remplacé la licence…) et avec qui j'ai continué de partager ce sacré bout de chemin qu'est le doctorat : JS, Seb, Lionel, Marylène, Delphine, Marie-Eve et Séverine.

Je voudrais remercier Iris pour les nombreux séquençages qu'elle a effectués. Ainsi que Fabrice et Andy pour leur aide dans l'utilisation des équipements de purification du CIP.

Merci à mes parents qui m'ont toujours soutenu et continuent de me soutenir dans tous mes choix de vie, ainsi qu'à toute ma famille et belle-famille.

J'adresse une pensée toute particulière aux étudiants et stagiaires que j'ai eu le privilège de superviser au cours de mes années de doctorat : Alex, Cécile, Nicolas, Thomas, Sonia et, bien sûr, Amandine.

Amandine, grâce à toi j'ai pu trouver l'énergie et la volonté d'aller au bout. On touche enfin au but. Je dis « on » car cela a été un vrai travail d'équipe. Tes attentions, tes encouragements m'ont accompagné tout au long de ces années. Je me sens si fier de vivre avec une femme aussi magnifique, intelligente, courageuse et pleine d'humour. Lors de ton stage pendant mon doctorat, je t'ai séduite grâce à mes recherches sur une enzyme bleue qui contient du cuivre. Nous avons fêté nos 10 ans de mariage il y a quelques mois, nous voilà donc passés à l'étain. En effet, l'étain, élément chimique de la famille du carbone, de numéro atomique 50, a été attribué au dixième anniversaire de mariage. Il s'agit d'un matériau métallique gris argenté, malléable mais solide. Il est donc parfaitement adapté aux 10 ans d'union maritale. L'étain possède 5 couches électroniques et existe aux états d'oxydation 0, +II et +IV.

C'est surtout l'élément comportant le plus d'isotopes stables : 10 au total. Tiens, tiens, la voilà surtout l'explication pour symboliser les 10 ans de mariage. Cela a certainement un rapport avec le fait que l'étain possède 50 protons, un nombre magique. Et un nombre magique en physique c'est un nombre de protons ou de neutrons pour lequel un noyau atomique est particulièrement stable. L'étain symbolise donc cette stabilité et ce cap primordial des 10 ans de mariage. Il est là pour renforcer encore plus la relation amoureuse. Quand l'étain, comme principal élément d'alliage, est associé au cuivre, il permet en effet de former du bronze, connu pour sa bonne résistance à l'usure ! Au bout de 10 ans, on considère que le couple est suffisamment solide pour affronter les dix prochaines années, et, espérons, les suivantes encore. Pour tout dire, l'étain est au bronze ce que tu es pour moi : indispensable ! Tu nous as offert trois merveilleux enfants, les voilà bientôt avec deux docteurs à la maison…

Alexia, Maeva, Hugo, merci pour votre compréhension particulièrement ces derniers mois pendant lesquels je me suis moins consacré à vous pour prendre du temps pour achever cette thèse. Sachez qu'à vous trois, vous serez à jamais mon plus bel accomplissement.

It does not matter how slowly you go
as long as you do not stop.

Confucius

Table of contents

List of abbreviations (excluding publications)

PhaMOx	***Pseudoalteromonas haloplanktis* metallo-oxidase**
CueO	**Cu efflux oxidase from *Escherichia coli***
***Tth*-MCO**	***Thermus thermophilus* multicopper oxidase**

ABTS	2,2'-azino-bis(3-ethylbenzothiazoline-6-sulfonic acid)
Bca	Bicinchoninic Acid
BisTris	(2-[Bis(2-hydroxyethyl)amino]-2-(hydroxymethyl)-1,3-propanediol)
Cu	Copper
E^0	Reduction potential
EC	Enzyme Commission
ET	Electron Transfer
EPR	Electron Paramagnetic Resonance
Fe	Iron
GOE	Great Oxidation Event
HSAB	Hard and Soft (Lewis) Acids and Bases
MCO	MultiCopper Oxidase
NMR	Nuclear Magnetic Resonance
sCu	Substrate Cu
SOD	Cu, Zn superoxide dismutase
T1	Type I copper
T2	Type II copper
T3	Type III copper
TNC	TriNuclear Cluster
TR	Tandem Repeats

Preamble

Man is a homeothermic organism. He has to live in a temperate environment in order to be able to maintain his internal temperature constant and allow his cells to perform their functions. The temperature as well as the set of environmental conditions required for human life are well characterized and are somehow considered to be “the standard”. On Earth, there are many environments that can therefore be described as extreme from an anthropocentric point of view. These environments are characterized by a very low or very high temperature, by a high concentration of salts or elements toxic to humans (including metal ions such as copper), by an absence of oxygen, by a very marked acidity or alkalinity, by an absence of light or even by a hydrostatic pressure much higher than atmospheric pressure. Several of these characteristics can also be found in the same place. These environments are not, however, devoid of life and the organisms that can be found there are called extremophiles, as opposed to organisms that live under the so-called standard conditions defined by humans. Extremophiles are mainly prokaryotic organisms which have developed cellular components adapted to such physicochemical properties outside the norm of their habitat. These adaptations can be found in their membranes, their nucleic acids as well as their proteins and the molecular study of these adjustments allows a better understanding of these fundamental molecules of life.
Life at low temperature is far from being anecdotic since cold environments displaying temperature close to 0°C represent about three quarter of the surface of terrestrial and aquatic habitats on Earth. The vast extent of permanently cold environments comprises the polar and alpine regions, the permafrost zone, the glaciers and the deep-sea waters which display under one thousand meters temperatures below 5°C independently of the latitude. The cold loving organisms, named psychrophiles, found in these extreme life conditions are dominated by the prokaryotes but yeasts, algae, invertebrates and lower vertebrates are also encountered.
The Laboratory of Biochemistry in the Center for Protein Engineering at the University of Liège has specialized for many years in the study of enzymes from organisms who encounter permanently low temperatures (mainly microorganisms) by comparing them to their homologs originating from mesophilic and thermophilic organisms or warm-blooded animals.

This study is focused on an oxidative enzyme, a cuproxidase, involved in copper resistance and found in a bacterium isolated in Antarctica. The introduction (**Chapter I**) consists of a first section (I.I) presenting the molecular adaptations generally observed for the enzymes produced by organisms which have to face a permanently cold environment. This section corresponds to a book chapter published in 2011. The second section (I.II) of the introduction presents the importance of copper in biological systems and the mechanisms that bacteria have developed to cope with elevated copper in their environment. It also includes a description of the MultiCopper Oxidases (MCO) family to which the oxidase from this work belongs.
The objective of the work is presented in **Chapter II**. **Chapters III and IV** present the experimental results of the work in the form of two research articles published in peer-reviewed scientific journals. The first one, published in the journal *Extremophiles* in 2016, focuses on the comparative characterization of the psychrophilic enzyme, PhaMOx, with a mesophilic and a thermophilic counterpart, CueO and *Tth*-MCO, respectively. The second research paper, published in the journal *Biochimie* in 2022, is devoted to the investigation of the role of the highly variable methionine-rich region found in cuproxidases, expecially by analyzing the cuprous ion binding capacity of this loop in the three homologous enzymes and in mutants of PhaMOx. The general conclusions and the perspectives of the work are discussed in **Chapter V**.

Chapter I – Introduction

I.I Psychrophilic enzymes: cool responses to chilly problems

Roulling F, Piette F, Cipolla A, Struvay C, Feller G. Psychrophilic enzymes: cool responses to chilly problems. In: Horikoshi K, editor. Extremophiles Handbook. Berlin, Germany: Springer; 2011. pp. 891-916.

6.7 Psychrophilic Enzymes: Cool Responses to Chilly Problems

Frédéric Roulling · Florence Piette · Alexandre Cipolla · Caroline Struvay · Georges Feller
Institute of Chemistry B6, University of Liège, Liège-Sart Tilman, Belgium

Koki Horikoshi (ed.), *Extremophiles Handbook*, DOI 10.1007/978-4-431-53898-1_6.7,

Introduction

Most of the biotopes on Earth are permanently exposed to low temperatures. This includes the Antarctic continent, the Arctic ice floe, the permafrost, the mountain and glacier regions, and the deep-sea waters, the latter covering 70% of the planet surface. If a psychrophile is defined as an organism living permanently at temperatures close to the freezing point of water, in thermal equilibrium with the medium, this definition encompasses a large range of species from Bacteria, Archaea, and Eukaryotes. This aspect underlines that psychrophiles are numerous, taxonomically diverse, and have a widespread distribution. In these organisms, low temperatures are essential for sustained cell metabolism. Some psychrophilic bacteria grown at 4°C have doubling times close to that of *Escherichia coli* at 37°C. Such deep adaptation of course requires a vast array of metabolic and structural adjustments at nearly all organization levels of the cell, which begins to be understood thanks to the availability of genome sequences and of proteomic approaches. Overviews on these various aspects have been recently published (D'Amico et al. 2006a; Gerday and Glansdorff 2007; Margesin et al. 2008; Casanueva et al. 2010).

This chapter focuses on protein structure and mainly on enzyme function at low temperatures. As a general picture, psychrophilic enzymes are all faced to a main constraint, to be active at low temperatures, but the ways to reach this goal are quite diverse. Previous reviews can also be consulted for a complete coverage of this topic (Smalas et al. 2000; Feller and Gerday 2003; Siddiqui and Cavicchioli 2006).

Biocatalysis in the Cold: A Thermodynamic Challenge

The activity of enzymes is strongly dependent on the surrounding temperature. The catalytic constant k_{cat} corresponds to the maximum number of substrate molecules converted to product per active site per unit of time, and the temperature dependence of the catalytic rate constant is given by the relation:

$$k_{cat} = \kappa \frac{k_B T}{h} e^{-\Delta G^{\#}/RT} \qquad (6.7.1)$$

In this equation, κ is the transmission coefficient generally close to 1, k_B is the Bolzmann constant (1.38×10^{-23} J K^{-1}), h the Planck constant (6.63×10^{-34} J s), R the universal gas constant (8.31 J K^{-1} $mole^{-1}$), and $\Delta G^{\#}$ the free energy of activation or the variation of the Gibbs energy between the activated enzyme-substrate complex ES^{*} and the ground state ES (see *Fig. 6.7.8*). Accordingly, the activity k_{cat} is exponentially dependent on the temperature. As a rule of thumb, for a biochemical reaction catalyzed by an enzyme from a mesophile (a bacterium or a warm-blooded vertebrate), a drop in temperature from 37°C to 0°C results in a 20–80 times lower activity. This is the main factor preventing the growth of non-adapted organisms at low temperatures.

The effect of temperature on the activity of psychrophilic and mesophilic enzymes is illustrated in *Fig. 6.7.1*. Equation 6.7.1 is only valid for the exponential rise of activity with temperature on the left limb of the curves. This figure reveals at least three basic features of cold adaptation. (1) In order to compensate for the slow reaction rates at low temperatures, psychrophiles synthesize enzymes having an up to tenfold higher specific activity in this temperature range. This is in fact the main physiological adaptation to cold at the enzyme level. (2) The temperature for apparent maximal activity for cold-active enzymes is shifted

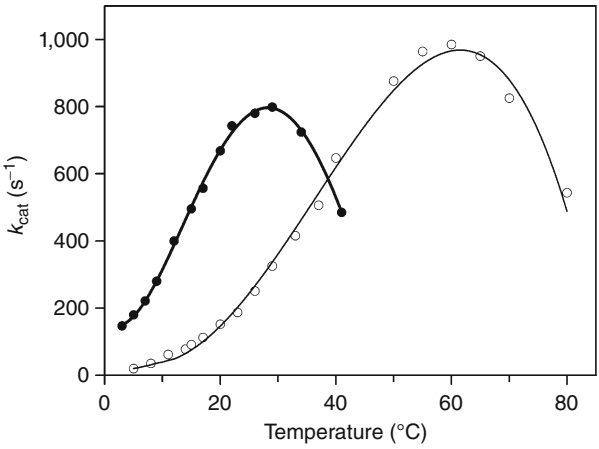

Fig. 6.7.1

Temperature dependence of the activity. The activity of psychrophilic (*filled symbols, heavy line*) and mesophilic (*open symbols*) enzymes recorded at various temperatures illustrates the main properties of cold-active enzymes (see text for details)

toward low temperatures, reflecting the weak stability of these proteins and their unfolding and inactivation at moderate temperatures. (3) Finally, the adaptation to cold is not perfect. It can be seen in *Fig. 6.7.1* that the specific activity of the psychrophilic enzymes at low temperatures, although very high, remains generally lower than that of the mesophilic enzymes at 37°C.

"Flexibility" and "Corresponding States" Hypotheses

Such activity curves have suggested relationships between the activity of the enzyme, the flexibility of the protein, and its stability. Indeed, the high activity at low temperatures seems to arise from an increased flexibility of the protein structure, especially at temperatures that strongly slow down molecular motions, but the consequence of this improved mobility of the protein structure is of course a weak stability. Fluorescence quenching of extremophilic enzymes was used to probe this "flexibility" hypothesis (*Fig. 6.7.2*). It was found that the structure of psychrophilic proteins has an improved propensity to be penetrated by a small quencher molecule, when compared to mesophilic and thermophilic proteins, and therefore revealing a less compact conformation undergoing frequent micro-unfolding events (D'Amico et al. 2003b; Collins et al. 2003; Georlette et al. 2003). The "flexibility" hypothesis has received further support by the quantification of macromolecular dynamics in the whole protein content of psychrophilic, mesophilic, thermophilic, and hyperthermophilic bacteria by neutron scattering (Tehei et al. 2004). This unique tool to study thermal atomic motions has indeed revealed that the resilience (equivalent to macromolecular rigidity in term of a force constant) increases with physiological temperatures. Furthermore, it was also shown that the atomic fluctuation amplitudes (equivalent to macromolecular flexibility) were similar for each microorganism at its physiological temperature. This is in full agreement with

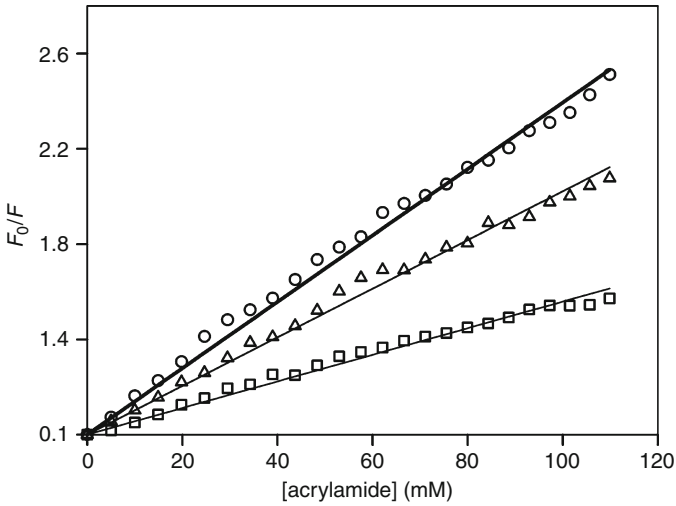

Fig. 6.7.2

Permeability of the protein structure. Fluorescence quenching experiments on psychrophilic (*circles, heavy line*), mesophilic (*triangles*), and heat-stable (*squares*) enzymes. The steep slope recorded for the psychrophilic enzyme indicates that its structure is easily penetrated by a small quencher molecule (acrylamide), resulting in a larger attenuation of the intrinsic fluorescence (F_0/F). This graph shows a clear correlation between this permeability index and the stability of the proteins. Adapted from (D'Amico et al. 2003b)

Somero's "corresponding state" concept (Somero 1995) postulating that enzyme homologues exhibit comparable flexibilities to perform catalysis at their physiologically relevant temperatures.

However, the "flexibility" hypothesis has been challenged from an evolutionary point of view. As a matter of fact, directed evolution (Wintrode and Arnold 2000) and protein engineering (Bae and Phillips 2006) of enzymes have demonstrated that activity and stability are not physically linked in protein. Accordingly, it has been proposed that the low stability of cold-active enzymes is the result of a genetic drift related to the lack of selective pressure for stable proteins (Wintrode and Arnold 2000). Nevertheless, several lines of evidences indicate that the situation is more subtle. For instance, in multi-domain psychrophilic enzymes containing a catalytic and a non-catalytic domain, the catalytic domain is always heat-labile (*Fig. 6.7.3*) whereas the non-catalytic domain can be as stable as mesophilic proteins (Lonhienne et al. 2001; Claverie et al. 2003; Suzuki et al. 2005). It is therefore unlikely that a genetic drift only affects the catalytic domain without modifying other regions of the protein. Furthermore, several directed evolution experiments have shown that when libraries of randomly mutated enzymes are only screened for improved activity at low temperatures without any other constraints, the best candidates invariably display the canonical properties of psychrophilic enzymes (see D'Amico et al. 2002a for discussion) whereas random mutations improving both activity and stability are rare (Giver et al. 1998; Cherry et al. 1999). It follows that improvement of activity at low temperatures associated with loss of stability appears to be the most frequent and accessible event. In conclusion, the current view suggests that the strong evolutionary pressure on psychrophilic enzymes to increase their activity at low temperatures

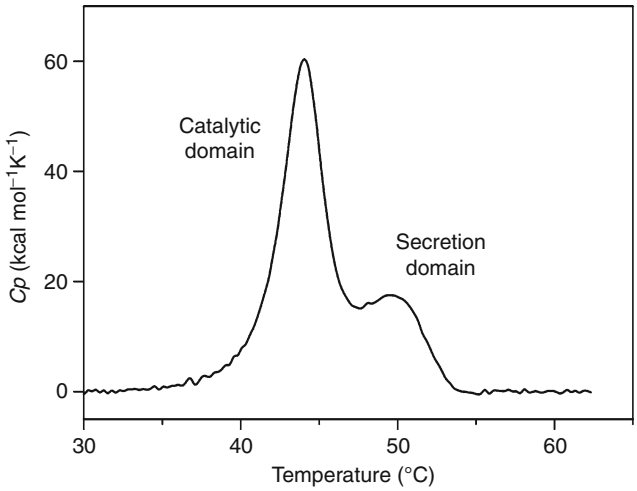

Fig. 6.7.3

Stability of domains in the α-amylase precursor. The precursor is composed by a catalytic domain and a secretion helper. In this thermogram, the top of the transitions corresponds to the melting points and the area under the transitions is roughly proportional to the domain sizes. Assuming that the low stability of psychrophilic enzymes is simply the result of a genetic drift (lack of selection for stable proteins), it is surprising that the more stable non-catalytic domain has not been subjected to the same extent to this drift. Adapted from (Claverie et al. 2003)

can be accommodated for by the lack of selection for stability and represents the simplest adaptive strategy for enzyme catalysis in the cold.

Flexibility and Structural Adaptations at the Active Site

Psychrophilic enzymes all share at least one property: a heat-labile activity, irrespective of the protein structural stability. Furthermore, the active site appears to be the most heat-labile structural element of these proteins (Collins et al. 2003; D'Amico et al. 2003b; Georlette et al. 2003). *Figure 6.7.4* illustrates this significant difference between the stability of the activity and the stability of the structure. The lower panel shows the stability of the structure as recorded by fluorescence. As expected, the structure of the cold-active enzyme is less stable than the mesophilic one. In the upper panel, the activity is recorded under the same experimental conditions and it can be seen that the mesophilic enzyme is inactivated when the protein unfolds. By contrast, activity of the cold-active enzyme is lost before the protein unfolds. This means that the active site is even more heat-labile than the whole protein structure. It was also shown that the active site of the psychrophilic α-amylase is the first structural element that unfolds in transverse urea gradient gel electrophoresis (Siddiqui et al. 2005). All these aspects point to a very unstable and flexible active site and illustrate a central concept in cold adaptation: localized increases in flexibility at the active site are responsible for the high but heat-labile activity (Fields and Somero 1998), whereas other regions of the enzyme might or might not be characterized by low stability when not involved in catalysis (Chiuri et al. 2009).

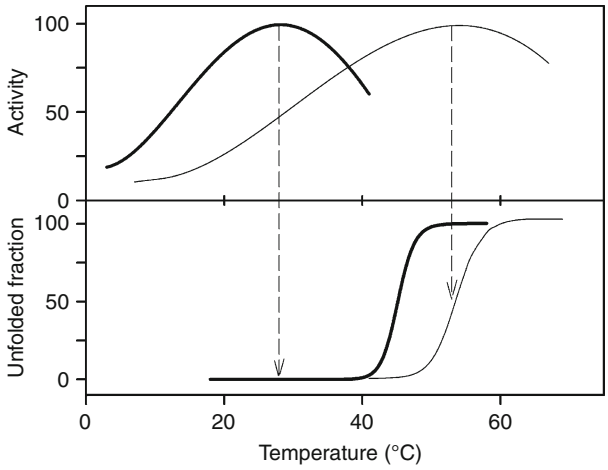

Fig. 6.7.4

Inactivation and unfolding of psychrophilic enzymes. The activity of psychrophilic enzymes (upper panel, *heavy line*) is inactivated by temperature before unfolding of the protein structure (lower panel, *heavy line*) illustrating the pronounced heat-lability of the active site. By contrast, inactivation of mesophilic (*thin lines*) or thermophilic enzymes closely corresponds to the loss of the protein conformation. Adapted from (D'Amico et al. 2003b)

Crystal structures of psychrophilic enzymes were of course of prime importance to investigate the properties of these heat-labile and cold-active catalytic centers. The first basic observation is that all side chains involved in the catalytic mechanism are strictly conserved. Indeed, comparison of the first X-ray structure of a psychrophilic enzyme, the cold-active α-amylase (Aghajari et al. 1998a, b), and of its closest structural homologue from pig both in complex with acarbose, a pseudosaccharide inhibitor mimicking the transition state intermediate (Aghajari et al. 2002; Qian et al. 1994), has shown that all 24 residues forming the catalytic cleft are strictly conserved in the cold-active α-amylase (*Fig. 6.7.5*). This outstanding example of active site identity demonstrates that the specific properties of psychrophilic enzymes can be reached without any amino acid substitution in the reaction center. As a consequence, changes occurring elsewhere in the molecule are responsible for the optimization of the catalytic parameters.

Nevertheless, significant structural adjustments at the active site of psychrophilic enzymes have been frequently reported. In many cases, a larger opening of the catalytic cleft is observed and achieved by various ways, including replacement of bulky side chains for smaller groups, distinct conformation of the loops bordering the active site, or small deletions in these loops, as illustrated by a cold-active citrate synthase (Russell et al. 1998). In the case of a Ca^{2+}, Zn^{2+}-protease from a psychrophilic *Pseudomonas* species, an additional bound Ca^{2+} ion pull the backbone forming the entrance of the site and markedly increases its accessibility when compared with the mesophilic homologue (Aghajari et al. 2003). As a result of such a better accessibility, cold-active enzymes can accommodate substrates at lower energy cost, as far as the conformational changes are concerned, and therefore reduce the activation energy required for the formation of the enzyme-substrate complex. The larger active site may also facilitate easier release and exit of products and thus may alleviate the effect of a rate limiting step on the

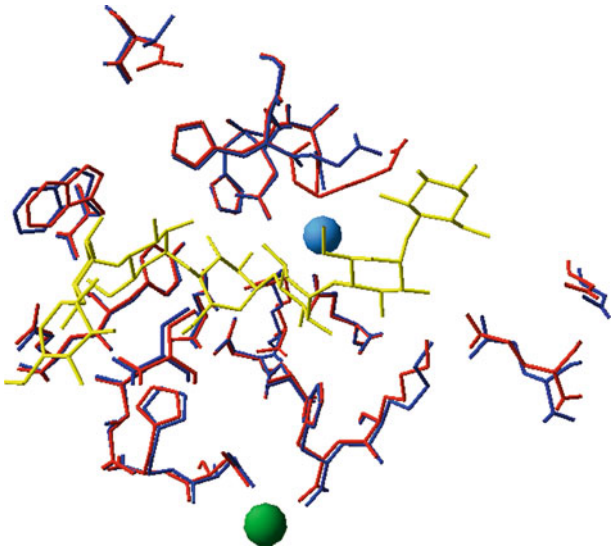

Fig. 6.7.5

Structure of the active site. Superimposition of the active site residues in psychrophilic (*blue*) and mesophilic (*red*) α-amylases. The chloride and calcium ions are shown as blue and green spheres, respectively. The 24 residues performing direct or water-mediated interactions with the substrate analog derived from acarbose (*yellow*) are identical and superimpose perfectly within the resolution of the structures, demonstrating a structural identity in these psychrophilic and mesophilic enzymes

reaction rate. It was also shown that an opening of the active site takes place upon binding of substrate or product in a cold-active xylanase whereas similar large scale movements are not observed in mesophilic or thermophilic structural homologues (De Vos et al. 2006). This can be tentatively related to higher active site mobility in the psychrophilic enzyme.

In addition, differences in electrostatic potentials in and around the active site of psychrophilic enzymes appear to be a crucial parameter for activity at low temperatures. Electrostatic surface potentials generated by charged and polar groups are an essential component of the catalytic mechanism at various stages: as the potential extends out into the medium, a substrate can be oriented and attracted before any contact between enzyme and substrate occurs. Interestingly, the cold-active citrate synthase (Russell et al. 1998), malate dehydrogenase (Kim et al. 1999), uracyl-DNA glycosylase (Leiros et al. 2003), and trypsin (Smalas et al. 2000; Gorfe et al. 2000; Brandsdal et al. 2001) are characterized by marked differences in electrostatic potentials near the active site region compared to their mesophilic or thermophilic counterparts that may facilitate interaction with ligand. In all cases, the differences were caused by discrete substitutions in non-conserved charged residues resulting in local electrostatic potential differing in both sign and magnitude.

Finally, two last examples illustrate the unsuspected diversity of strategies used to improve the activity in psychrophilic enzymes. With few exceptions, β-galactosidases are homotetrameric enzymes bearing four active sites. However, the crystal structure of a cold-active β-galactosidase revealed that it is a homohexamer, therefore possessing six active sites

certainly contributing to improve the activity at low temperatures (Skalova et al. 2005). Cellulases are microbial enzymes displaying a modular organization made of a globular catalytic domain connected by a linker to a cellulose-binding domain. Psychrophilic cellulases were found to possess unusually long linkers about five times longer than in mesophilic cellulases (Garsoux et al. 2004; Violot et al. 2005). The long linker adopts a large number of conformations, and considering the cellulose-binding domain anchored to the cellulose fibers and a rotation of the extended molecule around this axis, it was calculated that the catalytic domain has a 40-fold higher accessible surface area of substrate when compared with a mesophilic cellulase possessing a much shorter linker. Here also, increasing the available surface of the insoluble substrate to the catalytic domain should improve the activity of this enzyme at low temperatures.

Active Site Dynamics

The heat-labile activity of psychrophilic enzymes suggests that the dynamics of the functional side chains at the active site is improved in order to contribute to cold-activity and the above-mentioned structural adaptations seem to favor a better accessibility to the substrate and release of the product (Tsigos et al. 1998; Smalas et al. 2000). This active site flexibility of cold-active enzymes in solution is also well demonstrated by the psychrophilic α-amylase (D'Amico et al. 2006b). In this specific case, the above-mentioned structural identity of the catalytic cleft with its mesophilic homologue from pig precludes the involvement of adaptive mutations within the active site in the analysis of the results. As shown in *Table 6.7.1*, both the psychrophilic and mesophilic α-amylases degrade large macromolecular polysaccharides made

Table 6.7.1

Relative activity of the psychrophilic (AHA) and the mesophilic (PPA) α-amylases on macromolecular polysaccharides and on maltooligasaccharides. Adapted from D'Amico et al., 2006b

Substrate	Relative activity (%)	
	AHA	PPA
Macromolecular substrates		
Starch	100	100
Amylopectin	96	68
Amylose	324	214
Dextrin	108	95
Glycogen	74	59
Short oligosaccharides		
Maltotetraose G4	17	22
Maltopentose G5	69	145
Maltohexaose G6	94	147
Maltoheptaose G7	119	155
Maltooligosaccharides (G4–G10 mix)	64	101

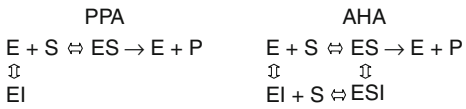

Fig. 6.7.6

Inhibition models of α-amylases. Reaction pathways for the competitive inhibition of starch hydrolysis by maltose for the mesophilic α-amylase PPA and of the mixed type inhibition for the psychrophilic α-amylase AHA. Under identical experimental conditions, the cold-active enzyme forms the ternary complex ESI (D'Amico et al. 2006b)

of glucose units linked by α-1,4 bonds. These substrates have a complex structure and are generally branched. Taking the natural substrate, starch, as the reference, it can be seen that the psychrophilic enzyme is more active on all these large substrates. Being more flexible, the active site can accommodate easily these macromolecular polysaccharides. Considering the small substrates, the reverse situation is observed. Both enzymes are active on short oligosaccharides of at least four glucose units, but in this case, the psychrophilic α-amylase is less active on all these small substrates. Apparently, the flexible active site accommodates less efficiently these short oligosaccharides.

The inhibition patterns provide additional insights into the specific properties of psychrophilic active sites (*Fig. 6.7.6*). Both the mesophilic and the psychrophilic α-amylases are inhibited by maltose, the end product of starch hydrolysis. In the case of the mesophilic enzyme, the enzyme can bind either the substrate (in a productive mode) or the inhibitor, but not both. By contrast, the cold-active enzyme can also bind either the substrate or the inhibitor but also both, forming the ternary complex ESI, once again suggesting a more accessible and flexible active site.

Adaptive Drift and Adaptive Optimization of Substrate Affinity

As a consequence of the improved active site dynamics in cold-active enzymes, substrates bind less firmly in the binding site (if no point mutations have occurred) giving rise to higher K_m values. An example is given in *Table 6.7.2* showing that the psychrophilic α-amylase is more active on its macromolecular substrates whereas the K_m values are up to 30-fold larger, i.e., the affinity for the substrates is up to 30-fold lower. Ideally, a functional adaptation to cold would mean optimizing both k_{cat} and K_m. However, a survey of the available data on psychrophilic enzymes (Xu et al. 2003) showed that optimization of the k_{cat}/K_m ratio is far from a general rule but on the contrary that the majority of cold-active enzymes improve the k_{cat} value at the expense of K_m, therefore leading to suboptimal values of the k_{cat}/K_m ratio, as also shown in *Table 6.7.2*. There is in fact an evolutionary pressure on K_m to increase in order to maximize the overall reaction rate. Such adaptive drift of K_m has been well illustrated by the lactate dehydrogenases from Antarctic fish (Fields and Somero 1998) and by the psychrophilic α-amylase (D'Amico et al. 2001) because both enzymes display rigorously identical substrate binding site and active site architecture when compared with their mesophilic homologues. In both cases, temperature-adaptive increases in k_{cat} occur concomitantly with increases in K_m in cold-active enzymes. As already mentioned, such identity of the sites also implies that adjustments of the kinetic parameters are obtained by structural changes occurring distantly from the

Table 6.7.2

Kinetic parameters for the hydrolysis of polysaccharides at 25°C by the psychrophilic (AHA) and the mesophilic (PPA) α-amylases. Adapted from D'Amico et al., 2006b

Substrate	AHA			PPA		
	k_{cat} s^{-1}	K_m mg l^{-1}	k_{cat}/K_m $s^{-1}mg^{-1}$ l	k_{cat} s^{-1}	K_m mg l^{-1}	k_{cat}/K_m $s^{-1}mg^{-1}$ l
Starch	663	155	4.3	327	41	8.0
Amylopectin	636	258	2.5	222	53	4.2
Amylose	2,148	178	12.1	700	36	19.4
Dextrin	716	586	1.2	311	61	5.1
Glycogen	491	1,344	0.3	193	46	4.2

reaction center. This aspect has received strong experimental support (D'Amico et al. 2003a) as discussed latter in this chapter.

Several enzymes, especially in some cold-adapted fish, counteract this adaptive drift of K_m in order to maintain or to improve the substrate binding affinity by amino acid substitutions within the active site (Smalas et al. 2000). The first reason for these enzymes to react against the drift is obvious when considering the regulatory function associated with K_m, especially for intracellular enzymes. The second reason is related to the temperature dependence of weak interactions. Substrate binding is an especially temperature-sensitive step because both the binding geometry and interactions between binding site and ligand are governed by weak interactions having sometimes opposite temperature dependencies. Hydrophobic interactions form endothermically and are weakened by a decrease in temperature. By contrast, interactions of electrostatic nature (ion pairs, hydrogen bounds, Van der Waals interactions) form exothermically and are stabilized at low temperatures. Therefore low temperatures do not only reduce the enzyme activity (k_{cat}), but can also severely alter the substrate binding mode according to the type of interaction involved.

The chitobiase from an Antarctic bacteria nicely illustrates both aspects, as well as the extent of the kinetic optimization that can be reached during cold adaptation of enzymes (Lonhienne et al. 2001). *Figure 6.7.7* shows that the k_{cat} of the cold-active chitobiase is eight times higher than that of a mesophilic chitobiase at 5°C. However, the K_m for the substrate is 25 times lower at this temperature, and as a result, the k_{cat}/K_m for the cold-active enzyme is nearly 200 times greater at low temperature. Because the cell-bound bacterial chitobiase has to access its substrate in the extracellular medium, the physiological advantage of a high affinity for the substrate is clear. In addition, the cross-shaped plot of K_m shows that the K_m of each enzyme tends to minimal and optimal values in the range of the corresponding environmental temperatures, reflecting the fine tuning of this parameter reached in the course of thermal adaptation. In the case of the mesophilic chitobiase, the 3D-structure indicates that two tryptophan residues are the main substrate binding ligands and perform hydrophobic interactions with the substrate. This can be related to the decrease of K_m with temperature, according to the above-mentioned thermal dependence of hydrophobic interactions. Interestingly, the two tryptophan residues are not found in the cold-active chitobiase but are replaced by polar residues that are able to perform stronger interactions as the temperature is decreased.

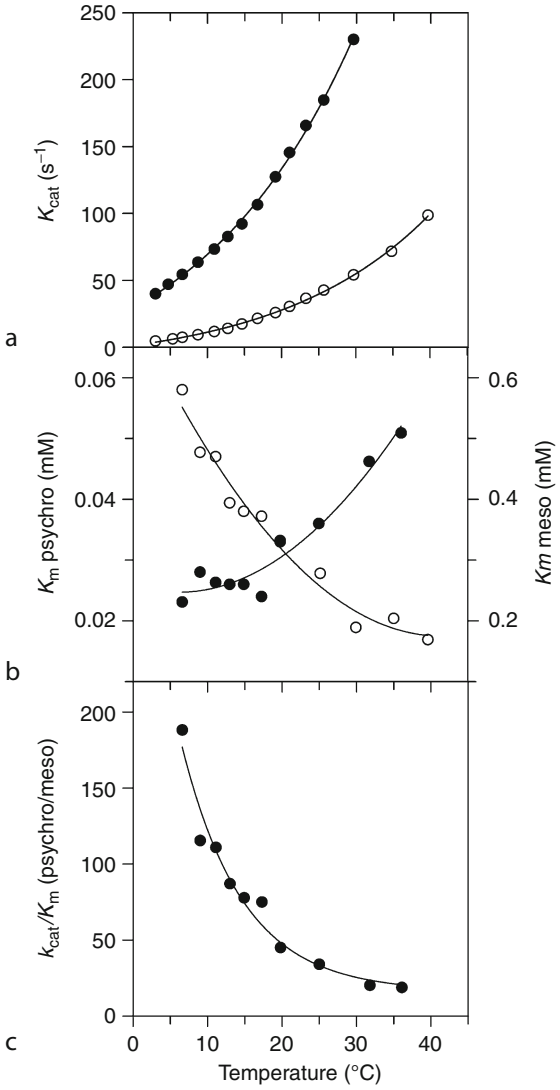

Fig. 6.7.7

Kinetic optimization in a cold-active chitobiase. Temperature dependence of the kinetic parameters for psychrophilic (*closed symbols*) and mesophilic (*open symbols*) chitobiases. Data for (a) the catalytic rate constant k_{cat}; (b) the Michaelis parameter K_m, note the different scales used; and (c) the relative catalytic efficiency k_{cat}/K_m (psychrophile/mesophile). The cold-adapted chitobiase is characterized by a higher activity, an optimal K_m value at low temperatures, and a 200 times higher catalytic efficiency at 7°C. Adapted from (Lonhienne et al. 2001)

Energetics of Activity at Low Temperatures

Referring to Eq. 6.7.1, the high activity of cold-adapted enzymes corresponds to a decrease of the free energy of activation $\Delta G^{\#}$. Two strategies have been highlighted to reduce the height of this energy barrier. *Figure 6.7.8* illustrates the first strategy where an evolutionary pressure increases K_m in order to maximize the reaction rate. According to the transition state theory, when the enzyme encounters its substrate, the enzyme-substrate complex ES falls into an energy pit. For the reaction to proceed, an activated state $ES^{\#}$ has to be reached, which eventually breaks down into the enzyme and the product. The height of the energy barrier between the ground state ES and the transition state $ES^{\#}$ is defined as the free energy of activation $\Delta G^{\#}$: the lower this barrier, the higher the activity as reflected in Eq. 6.7.1. In the case of cold-active enzymes displaying a weak affinity for the substrate, the energy pit for the ES complex is less deep (dashed in *Fig. 6.7.8*). It follows that the magnitude of the energy barrier is reduced and therefore the activity is increased. This thermodynamic link between affinity and activity is valid for most enzymes (extremophilic or not) under saturating substrate concentrations and this link appears to be involved in the improvement of activity at low temperatures in numerous cold-active enzymes (Fields and Somero 1998; Xu et al. 2003).

The second and more general strategy involves the temperature dependence of the reaction catalyzed by cold-active enzymes. *Table 6.7.3* reports the enthalpic and entropic contributions to the free energy of activation in extremophilic α-amylases. The free energy of activation $\Delta G^{\#}$ is calculated from Eq. 6.7.1 using the k_{cat} value at a given temperature and the enthalpy of activation $\Delta H^{\#}$ is obtained by recording the temperature dependence of the activity (Lonhienne et al. 2000). Finally, the entropic contribution $T\Delta S^{\#}$ is deduced from the Gibbs–Helmholtz equation:

$$\Delta G^{\#} = \Delta H^{\#} - T\Delta S^{\#} \tag{6.7.2}$$

The enthalpy of activation $\Delta H^{\#}$ depicts the temperature dependence of the activity: the lower this value, the lower the variation of activity with temperature. The low value found for almost all psychrophilic enzymes demonstrates that their reaction rate is less reduced than for

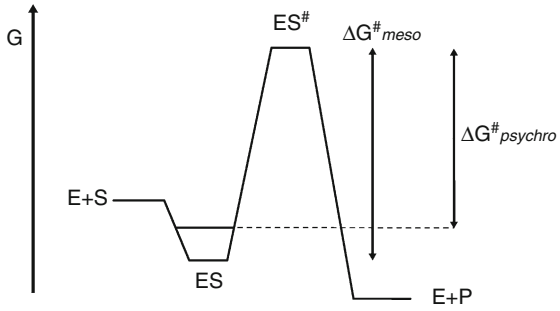

Fig. 6.7.8

Optimization of activity by decreasing substrate affinity in psychrophilic enzymes. Reaction profile for an enzyme-catalyzed reaction with Gibbs energy changes under saturating substrate concentration. Weak substrate binding (*dashed line*) decreases the activation energy ($\Delta G^{\#}$*psychro*) and thereby increases the reaction rate (see text for details)

Table 6.7.3

Activation parameters of the hydrolytic reaction of α-amylases at 10°C. Adapted from (D'Amico et al. 2003b)

	k_{cat} s^{-1}	$\Delta G^{\#}$ kcal mol^{-1}	$\Delta H^{\#}$ kcal mol^{-1}	$T\Delta S^{\#}$ kcal mol^{-1}
Psychrophile	294	13.3	8.3	−5.5
Mesophile	97	14.0	11.1	−2.9
Thermophile	14	15.0	16.8	1.8

other enzymes when the temperature is lowered. Accordingly, the decrease of the activation enthalpy in the enzymatic reaction of psychrophilic enzymes can be considered as the main adaptive character to low temperatures. This decrease is structurally achieved by a decrease in the number of enthalpy-driven interactions that have to be broken during the activation steps. These interactions also contribute to the stability of the protein folded conformation, and, as a corollary, the structural domain of the enzyme bearing the active site should be more flexible. It is interesting to note that such a macroscopic interpretation of the low activation enthalpy in cold-active enzymes fits with the experimental observation of a markedly heat-labile activity illustrated in *Fig. 6.7.4*. *Table 6.7.3* shows that the entropic contribution $T\Delta S^{\#}$ for the cold-active enzyme is larger and negative. This has been interpreted as a large reduction of the apparent disorder between the ground state with its relatively loose conformation and the well organized and compact transition state (Lonhienne et al. 2000). The heat-labile activity of cold-active enzymes suggests a macroscopic interpretation for this thermodynamic parameter. As a consequence of active site flexibility, the enzyme-substrate complex ES occupies a broader distribution of conformational states translated into increased entropy of this state, compared to that of the mesophilic or thermophilic homologues. This assumption has received strong experimental support by using microcalorimetry to compare the stabilities of free extremophilic enzymes with the same enzymes trapped in the transition state conformation by a non-hydrolysable substrate analog (D'Amico et al. 2003b). The larger increase in stability for the psychrophilic enzyme in the transition state conformation demonstrated larger conformational changes between the free and bound states when compared to mesophilic and thermophilic homologues. Furthermore, a broader distribution of the ground state ES should be accompanied by a weaker substrate binding strength, as indeed observed for numerous psychrophilic enzymes.

Conformational Stability of Extremophilic Proteins

Considering the numerous insights for strong relationships between activity and stability in psychrophilic enzymes, the conformational stability of these proteins has been intensively investigated in comparison with mesophilic and thermophilic counterparts. *Figure 6.7.9* displays the calorimetric records of heat-induced unfolding for psychrophilic, mesophilic, and thermophilic proteins. These enzymes clearly show distinct stability patterns that evolve from a simple profile in the unstable psychrophilic proteins to a more complex profile in very stable thermophilic counterparts. The unfolding of the cold-adapted enzymes occurs at lower

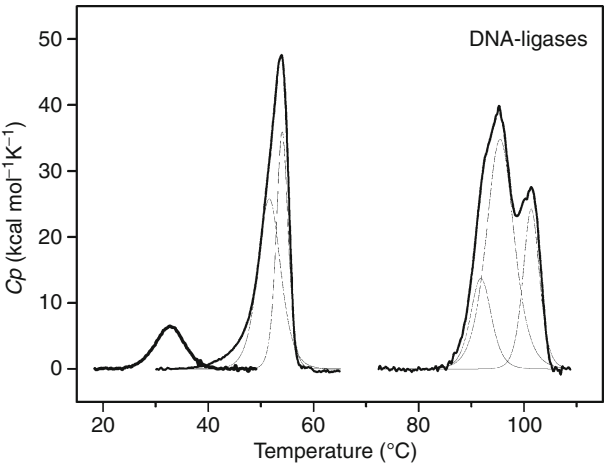

Fig. 6.7.9

Thermal unfolding of extremophilic enzymes. Thermograms of DNA-ligases recorded by differential scanning microcalorimetry showing, from left to right, psychrophilic (*heavy line*), mesophilic, and thermophilic proteins. The cold-active enzyme is characterized by a lower T_m (top of the transition) and ΔH_{cal} (area under the transition), by a sharp and cooperative transition, and by the lack of stability domains (indicated by *thin lines* in stable proteins). Adapted from (Georlette et al. 2003)

temperatures as indicated by the temperature of half-denaturation T_m, given by the top of the transition. This property, known for decades, has been highlighted by various techniques. By contrast, the energetics of structure stability was essentially revealed by microcalorimetry (D'Amico et al. 2001; Collins et al. 2003; Georlette et al. 2003). The calorimetric enthalpy ΔH_{cal} (area under the curves in *Fig. 6.7.9*), corresponding to the total amount of heat absorbed during unfolding, reflects the enthalpy of disruption of bonds involved in maintaining the compact structure and is markedly lower for the psychrophilic enzymes. In addition, there is a clear trend for increasing ΔH_{cal} values in the order psychrophile $<$ mesophile $<$ thermophile. The transition for the psychrophilic enzymes is sharp and symmetric whereas other enzymes are characterized by a flattening of the thermograms. This indicates a pronounced cooperativity during unfolding of the psychrophilic enzymes: the structure is stabilized by fewer weak interactions and disruption of some of these interactions strongly influences the whole molecular edifice and promotes its unfolding. The psychrophilic enzymes unfold according to an all-or-none process, revealing a uniformly low stability of the architecture. By contrast, all other homologous enzymes display two to three transitions (indicated by deconvolution of the heat capacity function in *Fig. 6.7.9*). Therefore, the conformation of these mesophilic and thermophilic enzymes contains structural blocks or units of distinct stability that unfold independently. Finally, the unfolding of the psychrophilic proteins is frequently more reversible than that of other homologous enzymes that are irreversibly unfolded after heating. The weak hydrophobicity of the core clusters in cold-adapted enzymes and the low T_m at which hydrophobic interactions are restrained certainly account for this reversible character because, unlike mesophilic proteins, aggregation does not occur or occurs to a lower extent.

As a practical and useful consequence of the unfolding reversibility, it has been possible to calculate accurately the conformational stability of a psychrophilic α-amylase over a broad range of temperatures (Feller et al. 1999). The comparison of these data with those of other proteins reveals some unsuspected properties of cold-adapted proteins. The thermodynamic stability of a protein that unfolds reversibly according to a two-state mechanism

$$N \rightleftharpoons U \tag{6.7.3}$$

is described by its stability curve, i.e., the free energy of unfolding as a function of temperature (Fig. 6.7.10). By definition, this stability is nil at T_m (equilibrium constant $K = [U]/[N] = 1$ and $\Delta G = -RT\ln K$). At temperatures below T_m, the stability increases, as expected, but perhaps surprisingly for the non-specialist, the stability reaches a maximum close to room temperature then it decreases at lower temperatures (Fig. 6.7.10). In fact, this function predicts a temperature of cold unfolding, which is generally not observed because it occurs below 0°C. Nevertheless, cold unfolding has been well demonstrated under specific conditions (Privalov 1990). Increasing the stability of a protein is essentially obtained by lifting the curve toward higher free energy values (Kumar and Nussinov 2004). As far as extremophiles are concerned, one of the most puzzling observations of the last decade is that most proteins obey this pattern, i.e., whatever the microbial source, the maximal stability of their proteins is clustered around room temperature (for more details see Kumar and Nussinov 2004). Accordingly, the environmental temperatures for mesophiles and (hyper)thermophiles lie on the right limb of the bell-shaped stability curve and, obviously, the thermal dissipative force is used to promote molecular

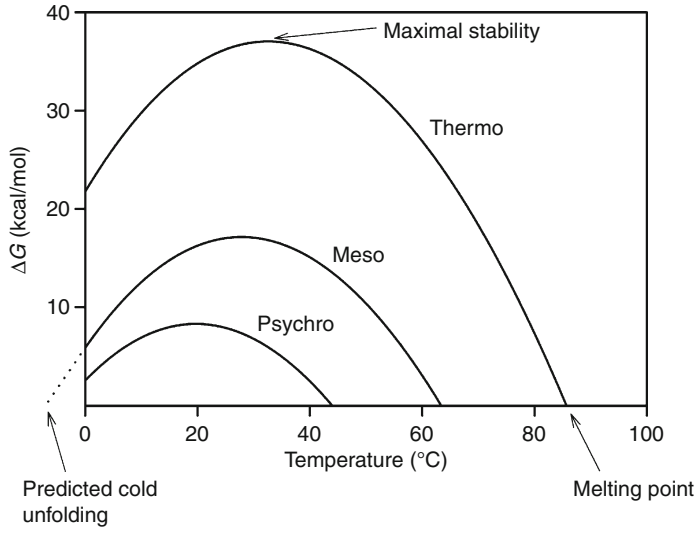

Fig. 6.7.10

Representative stability curves of homologous extremophilic proteins. The energy required to disrupt the native state (i.e., the conformational stability) is plotted as a function of temperature. At the melting point, this energy = 0 and in addition, the curves also predict cold unfolding and a maximal stability close to room temperature. A high stability in thermophiles is reached by lifting the curve toward higher free energy values, whereas the low stability in psychrophiles corresponds to a collapse of the bell-shaped stability curve. Adapted from (D'Amico et al. 2003b)

motions in these molecules. By contrast, the environmental temperatures for psychrophiles lie on the left limb of the stability curve. It follows that molecular motions in proteins at low temperatures are gained from the factors ultimately leading to cold unfolding (Feller et al. 1999), i.e., the hydration of polar and nonpolar groups (Makhatadze and Privalov 1995). The origin of flexibility in psychrophilic enzymes at low temperatures is therefore drastically different from mesophilic and thermophilic proteins, the latter taking advantage of the conformational entropy rise with temperature to gain in mobility.

A surprising consequence of the free energy function for the psychrophilic protein shown in *Fig. 6.7.10* is its weak stability at low temperatures when compared with mesophilic and thermophilic proteins, whereas it was intuitively expected that cold-active proteins should also be cold stable. This protein is in fact both heat and cold labile. Assuming constant properties of the solvent below 0°C (i.e., no freezing) and the absence of protective effects from cellular components, this α-amylase should unfold at −10°C. Therefore, cold denaturation of some key enzymes in psychrophiles can be an additional, though unsuspected factor fixing the lower limit of life at low temperatures. It has also been shown that the psychrophilic α-amylase has reached a state close to the lowest possible stability of the native state (D'Amico et al. 2001). If psychrophilic enzymes have indeed gained in flexibility at the expense of stability in the course of evolution, this implies that the actual native state precludes further adaptation toward a more mobile structure. This aspect can account for the imperfect adaptation of the catalytic function in some psychrophilic enzymes, mentioned at the beginning of this chapter and illustrated in *Fig. 6.7.1*.

Structural Basis of Low Stability

The number of X-ray crystal structures from psychrophilic enzymes has increased dramatically, demonstrating the growing interest for these peculiar proteins. However, the interpretation of these structural data is frequently difficult for two main reasons. First, the structural adaptations are extremely discrete and can easily escape the analysis. Second, these structural adaptations are very diverse, reflecting the complexity of factors involved in the stability of a macromolecule at the atomic level. For instance, it was found that all structural factors currently known to stabilize the protein molecule could be attenuated in strength and number in the structure of cold-active enzymes (Smalas et al. 2000; Russell 2000; Gianese et al. 2002). An exhaustive description of all these factors is beyond the scope of this chapter and only the essential features are summarized below. Two review articles can be consulted for a comprehensive discussion of this topic (Smalas et al. 2000; Siddiqui and Cavicchioli 2006).

The observable parameters related to protein stability include structural factors and mainly weak interactions between atoms of the protein structure. In psychrophilic proteins, this involves the clustering of glycine residues (providing local mobility), the disappearance of proline residues in loops (enhancing chain flexibility between secondary structures), a reduction in arginine residues which are capable of forming multiple salt bridges and H-bonds, as well as a lower number of ion pairs, aromatic interactions or H-bonds, compared to mesophilic enzymes. The size and relative hydrophobicity of nonpolar residue clusters forming the protein core are frequently smaller, lowering the compactness of the protein interior by weakening the hydrophobic effect on folding. The N and C-caps of α-helices are also altered (weakening the charge-dipole interaction) and loose or relaxed protein extremities appear to be preferential sites for unzipping. The binding of stabilizing ions, such as calcium, can be extremely weak, with binding constants

differing from mesophiles by several orders of magnitude. Insertions and deletions are sometimes responsible for specific properties such as the acquisition of extra-surface charges (insertion) or the weakening of subunit interactions (deletion).

Calculation of the solvent accessible area showed that some psychrophilic enzymes expose a higher proportion of nonpolar residues to the surrounding medium (Aghajari et al. 1998b; Russell et al. 1998). This is an entropy-driven destabilizing factor caused by the reorganization of water molecules around exposed hydrophobic side chains. Calculations of the electrostatic potential revealed in some instances an excess of negative charges at the surface of the protein and, indeed, the pI of cold-active enzymes is frequently more acidic than that of their mesophilic or thermophilic homologues. This has been related to improved interactions with the solvent, which could be of prime importance in the acquisition of flexibility near 0° (Feller et al. 1999). Besides the balance of charges, the number of salt bridges covering the protein surface is also reduced. There is a clear correlation between surface ion pairs and temperature adaptation, since these weak interactions significantly increase in number from psychrophiles to mesophiles, to thermophiles and hyperthermophiles, the latter showing arginine-mediated multiple ion pairs and interconnected salt bridge networks (Yip et al. 1995; Vetriani et al. 1998). Such an altered pattern of electrostatic interactions is thought to improve the dynamics or the "breathing" of the external shell of cold-active enzymes.

However, each enzyme adopts its own strategy by using one or a combination of these altered structural factors in order to improve the local or global mobility of the protein edifice. Comparative structural analyses of psychrophilic, mesophilic, and thermophilic enzymes indicate that each protein family displays different structural strategy to adapt to temperature. However, some common trends are observed: the number of ion pairs, the side-chain contribution to the exposed surface, and the apolar fraction of the buried surface show a consistent decrease with decreasing optimal temperatures (Gianese et al. 2002; Bell et al. 2002; Bae and Phillips 2004; Mandrich et al. 2004). As a result of the great diversity of factors involved in protein stability, the bias in the amino acid composition observed in individual psychrophilic protein (low proline or arginine content, etc.) is not found when analyzing the mean amino acid composition of the whole genome. On the contrary, the available genomic data have produced ambiguous results (Gerday and Glansdorff 2007; Margesin et al. 2008) and it is currently difficult to correlate the reported trends in genomic amino acid composition with adaptations to low temperatures or with species-specific differences.

Activity–Stability Relationships: Experimental Insights

In order to check the validity of the proposed relationships between the activity and the stability in cold-active enzymes, a psychrophilic α-amylase has been used as a model because the identical architecture of its active site, when compared with a close mesophilic homologue, indicates that structural adaptations affecting the active site properties occur outside from the catalytic cavity. Accordingly, the crystal structure (Aghajari et al. 1998a, b) has been closely inspected to identify structural factors involved in its weak stability, such as those described in the previous section. On this basis, 17 mutants of this enzyme were constructed, each of them bearing an engineered residue forming a weak interaction found in mesophilic α-amylases but absent in the cold-active α-amylase, or a combination of up to six stabilizing structural factors (D'Amico et al. 2001, 2002b, 2003a). As illustrated in *Fig. 6.7.11*, it was found that single amino acid side-chain substitutions can significantly modify the melting point T_m and the

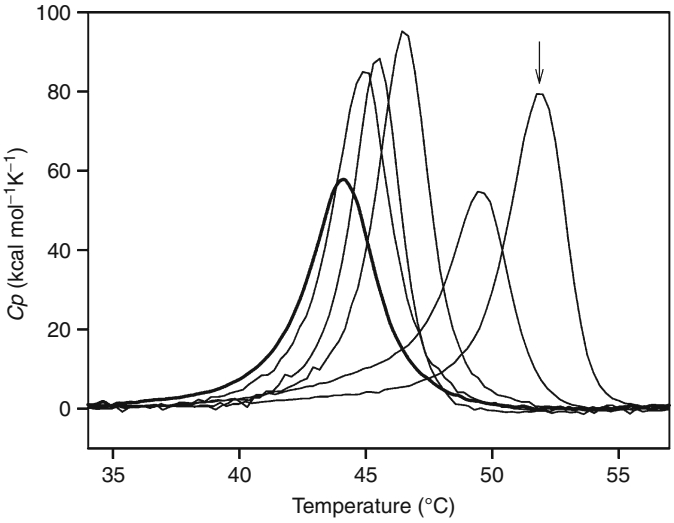

Fig. 6.7.11

Engineering mesophilic-like stability in mutants of the psychrophilic α-amylase. Structure-stabilizing interactions have been introduced in the heat-labile enzyme (*heavy line*). As shown by the microcalorimetric thermograms, the resulting mutants (*thin lines*) display increased melting points (top of the transitions) and calorimetric enthalpies (area below the curves). The most stable mutant (*arrow*) bears six additional interactions. Adapted from (D'Amico et al. 2001, 2003a)

calorimetric enthalpy ΔH_{cal} but also the cooperativity and reversibility of unfolding as well as the thermal inactivation rate constant. Therefore, these mutants of the psychrophilic α-amylase consistently approximate and reproduce the unfolding patterns of the heat-stable enzymes depicted in *Fig. 6.7.9*.

However, in the context of catalysis at low temperatures, the most significant observation was that these mutations tend to decrease both k_{cat} and K_m. As shown in *Fig. 6.7.12*, stabilizing the cold-active α-amylase tends to decrease the k_{cat} values and concomitantly the K_m values of the mutant enzymes, revealing the high correlation between both kinetic parameters (illustrated in *Fig. 6.7.8*). In fact, in addition to an engineered mesophilic-like stability, the multiple-mutant bearing six stabilizing structural factors also displays an engineered mesophilic-like activity in terms of alterations in k_{cat} and K_m values and even in thermodynamic parameters of activation (D'Amico et al. 2003a). Considering the various available data on the psychrophilic α-amylase, it can be concluded that the improved molecular motions of the side chains forming the active site (motions responsible for the high activity, the low affinity and heat-lability) originate from the lack of structure-stabilizing interactions in the vicinity or even far from the active site. This is another strong indication that structural flexibility is an essential feature related to catalysis at low temperatures in psychrophilic enzymes.

Psychrophilic Enzymes in Folding Funnels

The various properties of psychrophilic enzymes that have been presented in this chapter can be integrated in a model based on folding funnels (Dinner et al. 2000; Schultz 2000) to describe

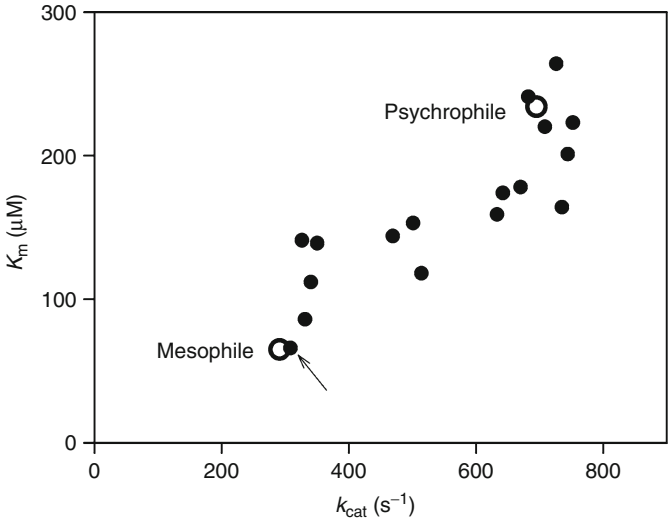

Fig. 6.7.12

Engineering mesophilic-like activity in mutants of the psychrophilic α-amylase. This plot of the kinetic parameters for the stabilized mutants (*filled symbols*) shows that the general trend is to decrease the activity and to increase the affinity for the substrate of the wild-type psychrophilic enzyme (*open symbol*). The most stable mutant bearing six additional interactions (*arrow*) displays kinetic parameters nearly identical to those of the mesophilic homologue (*open symbol*). Adapted from (D'Amico et al. 2001, 2003a)

the activity–stability relationships in extremophilic enzymes. *Figure 6.7.13* depicts the energy landscapes of psychrophilic and thermophilic enzymes. The top of the funnel is occupied by the unfolded state and having a high free energy (considering the spontaneous folding reaction), whereas the bottom of the funnel is occupied by the stable (low free energy) native state. The height of the funnel, i.e., the free energy of folding, also corresponding to the conformational stability, has been fixed here in a 1–5 ratio according to the stability curves shown in *Fig. 6.7.10*. The upper edge of the funnels is occupied by the unfolded state in random coil conformations but it should be noted that psychrophilic enzymes tend to have a lower proline content than mesophilic and thermophilic enzymes, a lower number of disulfide bonds and a higher occurrence of glycine clusters (Russell 2000; Smalas et al. 2000; Gianese et al. 2002; Siddiqui and Cavicchioli 2006). Accordingly, the edge of the funnel for the psychrophilic protein is slightly larger (broader distribution of the unfolded state) and is located at a higher energy level. When the polypeptide is allowed to fold, the free energy level decreases, as well as the conformational ensemble. However, thermophilic proteins pass through intermediate states corresponding to local minima of energy. These minima are responsible for the ruggedness of the funnel slopes and for the reduced cooperativity of the folding-unfolding reaction, as demonstrated by heat-induced unfolding (*Fig. 6.7.9*). By contrast, the structural elements of psychrophilic proteins generally unfold cooperatively without intermediates, as a result of fewer stabilizing interactions and stability domains (Feller et al. 1999; D'Amico et al. 2001; Georlette et al. 2003) and therefore the funnel slopes are steep and smooth. The bottom of the funnel depicts the stability of the native state ensemble.

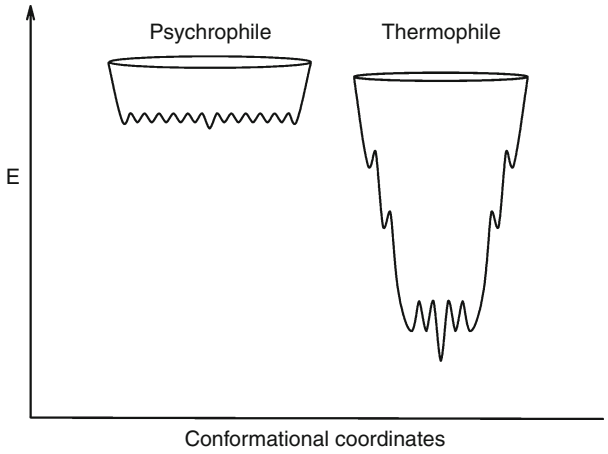

Fig. 6.7.13

Folding funnel model for extremophilic enzymes. In these schematic energy landscapes, the free energy of folding (E) is depicted as a function of the conformational diversity. The height of the funnels is deduced from the determination of the conformational stabilities. The top of the funnels is occupied by the unfolded states in the numerous random coil conformations, whereas the bottom of the funnels corresponds to native and catalytically active conformations. The ruggedness of the bottom depicts the energy barriers for interconversion, or structural fluctuations of the native state (D'Amico et al. 2003b)

The bottom for a very stable and rigid thermophilic protein can be depicted as a single global minimum or as having only a few minima with high energy barriers between them, whereas the bottom for an unstable and flexible psychrophilic protein is rugged and depicts a large population of conformers with low energy barriers to flip between them. Rigidity of the native state is therefore a direct function of the energy barrier height (Tsai et al. 1999; Kumar et al. 2000) and is drawn here according to the results of fluorescence quenching (*Fig. 6.7.2*) and neutron scattering experiments (Tehei et al. 2004). In this context, the activity–stability relationships in these extremophilic enzymes depend on the bottom properties. Indeed, it has been argued that upon substrate binding to the association-competent sub-population, the equilibrium between all conformers is shifted toward this sub-population, leading to the active conformational ensemble (Tsai et al. 1999; Kumar et al. 2000; Ma et al. 2000; Benkovic et al. 2008). In the case of the rugged bottom of psychrophilic enzymes, this equilibrium shift only requires a modest free energy change (low energy barriers), a low enthalpy change for interconversion of the conformations, but is accompanied by a large entropy change for fluctuations between the wide conformer ensemble. The converse picture holds for thermophilic enzymes, in agreement with the activation parameters shown in *Table 6.7.3* and with the proposed macroscopic interpretation. Such energy landscapes integrate nearly all biochemical and biophysical data currently available for extremophilic enzymes but they will certainly be refined by future investigations of other series of homologous proteins from psychrophiles, mesophiles and thermophiles. This model has nevertheless received support from independent studies (Bjelic et al. 2008; Xie et al. 2009).

Acknowledgments

Research at the author's laboratory was supported by the European Union, the Région wallonne (Belgium), the Fonds National de la Recherche Scientifique (Belgium), and the University of Liège. The facilities offered by the Institut Polaire Français are also acknowledged.

Cross-References

- 6.1 Ecology of Psychrophiles: Subglacial and Permafrost Environments
- 6.2 Taxonomy of Psychrophiles
- 6.3 Diversity of Psychrophilic Bacteria from Sea Ice - and Glacial Ice Communities
- 6.4 Adaptation Mechanisms of Psychrotolerant Bacterial Pathogens
- 6.5 Ecological Distribution of Microorganisms in Terrestrial, Psychrophilic Habitats
- 6.6 Genetics, Genomics, Evolution

References

Aghajari N, Feller G, Gerday C, Haser R (1998a) Crystal structures of the psychrophilic α-amylase from *Alteromonas haloplanctis* in its native form and complexed with an inhibitor. Protein Sci 7:564–572

Aghajari N, Feller G, Gerday C, Haser R (1998b) Structures of the psychrophilic *Alteromonas haloplanctis* α-amylase give insights into cold adaptation at a molecular level. Structure 6:1503–1516

Aghajari N, Roth M, Haser R (2002) Crystallographic evidence of a transglycosylation reaction: ternary complexes of a psychrophilic alpha-amylase. Biochemistry 41:4273–4280

Aghajari N, Van Petegem F, Villeret V, Chessa JP, Gerday C, Haser R, Van Beeumen J (2003) Crystal structures of a psychrophilic metalloprotease reveal new insights into catalysis by cold-adapted proteases. Proteins 50:636–647

Bae E, Phillips GN Jr (2004) Structures and analysis of highly homologous psychrophilic, mesophilic, and thermophilic adenylate kinases. J Biol Chem 279:28202–28208

Bae E, Phillips GN Jr (2006) Roles of static and dynamic domains in stability and catalysis of adenylate kinase. Proc Natl Acad Sci USA 103:2132–2137

Bell GS, Russell RJ, Connaris H, Hough DW, Danson MJ, Taylor GL (2002) Stepwise adaptations of citrate synthase to survival at life's extremes. From psychrophile to hyperthermophile. Eur J Biochem 269:6250–6260

Benkovic SJ, Hammes GG, Hammes-Schiffer S (2008) Free-energy landscape of enzyme catalysis. Biochemistry 47:3317–3321

Bjelic S, Brandsdal BO, Aqvist J (2008) Cold adaptation of enzyme reaction rates. Biochemistry 47:10049–10057

Brandsdal BO, Smalas AO, Aqvist J (2001) Electrostatic effects play a central role in cold adaptation of trypsin. FEBS Lett 499:171–175

Casanueva A, Tuffin M, Cary C, Cowan DA (2010) Molecular adaptations to psychrophily: the impact of 'omic' technologies. Trends Microbiol 18:374–381

Cherry JR, Lamsa MH, Schneider P, Vind J, Svendsen A, Jones A, Pedersen AH (1999) Directed evolution of a fungal peroxidase. Nat Biotechnol 17:379–384

Chiuri R, Maiorano G, Rizzello A, del Mercato LL, Cingolani R, Rinaldi R, Maffia M, Pompa PP (2009) Exploring local flexibility/rigidity in psychrophilic and mesophilic carbonic anhydrases. Biophys J 96:1586–1596

Claverie P, Vigano C, Ruysschaert JM, Gerday C, Feller G (2003) The precursor of a psychrophilic alpha-amylase: structural characterization and insights into cold adaptation. Biochim Biophys Acta 1649: 119–122

Collins T, Meuwis MA, Gerday C, Feller G (2003) Activity, stability and flexibility in glycosidases adapted to extreme thermal environments. J Mol Biol 328:419–428

D'Amico S, Gerday C, Feller G (2001) Structural determinants of cold adaptation and stability in a large protein. J Biol Chem 276:25791–25796

D'Amico S, Claverie P, Collins T, Georlette D, Gratia E, Hoyoux A, Meuwis MA, Feller G, Gerday C (2002a) Molecular basis of cold adaptation. Philos Trans R Soc Lond B Biol Sci 357:917–925

D'Amico S, Gerday C, Feller G (2002b) Dual effects of an extra disulfide bond on the activity and stability of

a cold-adapted alpha-amylase. J Biol Chem 277: 46110–46115

D'Amico S, Gerday C, Feller G (2003a) Temperature adaptation of proteins: engineering mesophilic-like activity and stability in a cold-adapted alpha-amylase. J Mol Biol 332:981–988

D'Amico S, Marx JC, Gerday C, Feller G (2003b) Activity-stability relationships in extremophilic enzymes. J Biol Chem 278:7891–7896

D'Amico S, Collins T, Marx JC, Feller G, Gerday C (2006a) Psychrophilic microorganisms: challenges for life. EMBO Rep 7:385–389

D'Amico S, Sohier JS, Feller G (2006b) Kinetics and energetics of ligand binding determined by microcalorimetry: insights into active site mobility in a psychrophilic alpha-amylase. J Mol Biol 358: 1296–1304

De Vos D, Collins T, Nerinckx W, Savvides SN, Claeyssens M, Gerday C, Feller G, Van Beeumen J (2006) Oligosaccharide binding in family 8 glycosidases: crystal structures of active-site mutants of the beta-1, 4-xylanase pXyl from Pseudoaltermonas haloplanktis TAH3a in complex with substrate and product. Biochemistry 45:4797–4807

Dinner AR, Sali A, Smith LJ, Dobson CM, Karplus M (2000) Understanding protein folding via free-energy surfaces from theory and experiment. Trends Biochem Sci 25:331–339

Feller G, Gerday C (2003) Psychrophilic enzymes: hot topics in cold adaptation. Nat Rev Microbiol 1: 200–208

Feller G, D'Amico D, Gerday C (1999) Thermodynamic stability of a cold-active α-amylase from the Antarctic bacterium *Alteromonas haloplanctis*. Biochemistry 38:4613–4619

Fields PA, Somero GN (1998) Hot spots in cold adaptation: localized increases in conformational flexibility in lactate dehydrogenase A(4) orthologs of Antarctic notothenioid fishes. Proc Natl Acad Sci USA 95:11476–11481

Garsoux G, Lamotte J, Gerday C, Feller G (2004) Kinetic and structural optimization to catalysis at low temperatures in a psychrophilic cellulase from the Antarctic bacterium *Pseudoalteromonas haloplanktis*. Biochem J 384:247–253

Georlette D, Damien B, Blaise V, Depiereux E, Uversky VN, Gerday C, Feller G (2003) Structural and functional adaptations to extreme temperatures in psychrophilic, mesophilic, and thermophilic DNA ligases. J Biol Chem 278:37015–37023

Gerday C, Glansdorff N (2007) Physiology and biochemistry of extremophiles. ASM Press, Washington

Gianese G, Bossa F, Pascarella S (2002) Comparative structural analysis of psychrophilic and meso- and thermophilic enzymes. Proteins 47:236–249

Giver L, Gershenson A, Freskgard PO, Arnold FH (1998) Directed evolution of a thermostable esterase. Proc Natl Acad Sci USA 95:12809–12813

Gorfe AA, Brandsdal BO, Leiros HK, Helland R, Smalas AO (2000) Electrostatics of mesophilic and psychrophilic trypsin isoenzymes: qualitative evaluation of electrostatic differences at the substrate binding site. Proteins 40:207–217

Kim SY, Hwang KY, Kim SH, Sung HC, Han YS, Cho YJ (1999) Structural basis for cold adaptation. Sequence, biochemical properties, and crystal structure of malate dehydrogenase from a psychrophile *Aquaspirillium arcticum*. J Biol Chem 274: 11761–11767

Kumar S, Nussinov R (2004) Experiment-guided thermodynamic simulations on reversible two-state proteins: implications for protein thermostability. Biophys Chem 111:235–246

Kumar S, Ma B, Tsai CJ, Sinha N, Nussinov R (2000) Folding and binding cascades: dynamic landscapes and population shifts. Protein Sci 9:10–19

Leiros I, Moe E, Lanes O, Smalas AO, Willassen NP (2003) The structure of uracil-DNA glycosylase from Atlantic cod (*Gadus morhua*) reveals cold-adaptation features. Acta Crystallogr D Biol Crystallogr 59:1357–1365

Lonhienne T, Gerday C, Feller G (2000) Psychrophilic enzymes: revisiting the thermodynamic parameters of activation may explain local flexibility. Biochim Biophys Acta 1543:1–10

Lonhienne T, Zoidakis J, Vorgias CE, Feller G, Gerday C, Bouriotis V (2001) Modular structure, local flexibility and cold-activity of a novel chitobiase from a psychrophilic Antarctic bacterium. J Mol Biol 310:291–297

Ma B, Kumar S, Tsai CJ, Hu Z, Nussinov R (2000) Transition-state ensemble in enzyme catalysis: possibility, reality, or necessity? J Theor Biol 203:383–397

Makhatadze GI, Privalov PL (1995) Energetics of protein structure. Adv Protein Chem 47:307–425

Mandrich L, Pezzullo M, Del Vecchio P, Barone G, Rossi M, Manco G (2004) Analysis of thermal adaptation in the HSL enzyme family. J Mol Biol 335:357–369

Margesin R, Schinner F, Marx JC, Gerday C (2008) Psychrophiles, from biodiversity to biotechnology. Springer, Berlin/Heidelberg

Privalov PL (1990) Cold denaturation of proteins. Crit Rev Biochem Mol Biol 25:281–305

Qian M, Haser R, Buisson G, Duee E, Payan F (1994) The active center of a mammalian alpha-amylase. Structure of the complex of a pancreatic alpha-amylase with a carbohydrate inhibitor refined to 2.2-Å resolution. Biochemistry 33:6284–6294

Russell NJ (2000) Toward a molecular understanding of cold activity of enzymes from psychrophiles. Extremophiles 4:83–90

Russell RJ, Gerike U, Danson MJ, Hough DW, Taylor GL (1998) Structural adaptations of the cold-active citrate synthase from an Antarctic bacterium. Structure 6:351–361

Schultz CP (2000) Illuminating folding intermediates. Nat Struct Biol 7:7–10

Siddiqui KS, Cavicchioli R (2006) Cold-adapted enzymes. Annu Rev Biochem 75:403–433

Siddiqui KS, Feller G, D'Amico S, Gerday C, Giaquinto L, Cavicchioli R (2005) The active site is the least stable structure in the unfolding pathway of a multidomain cold-adapted alpha-amylase. J Bacteriol 187: 6197–6205

Skalova T, Dohnalek J, Spiwok V, Lipovova P, Vondrackova E, Petrokova H, Duskova J, Strnad H, Kralova B, Hasek J (2005) Cold-active beta-galactosidase from *Arthrobacter* sp. C2-2 forms compact 660 kDa hexamers: crystal structure at 1.9Å resolution. J Mol Biol 353:282–294

Smalas AO, Leiros HK, Os V, Willassen NP (2000) Cold adapted enzymes. Biotechnol Annu Rev 6:1–57

Somero GN (1995) Proteins and temperature. Annu Rev Physiol 57:43–68

Suzuki Y, Takano K, Kanaya S (2005) Stabilities and activities of the N- and C-domains of FKBP22 from a psychrotrophic bacterium overproduced in *Escherichia coli*. FEBS J 272:632–642

Tehei M, Franzetti B, Madern D, Ginzburg M, Ginzburg BZ, Giudici-Orticoni MT, Bruschi M, Zaccai G (2004) Adaptation to extreme environments: macromolecular dynamics in bacteria compared in vivo by neutron scattering. EMBO Rep 5:66–70

Tsai CJ, Ma B, Nussinov R (1999) Folding and binding cascades: shifts in energy landscapes. Proc Natl Acad Sci USA 96:9970–9972

Tsigos I, Velonia K, Smonou I, Bouriotis V (1998) Purification and characterization of an alcohol dehydrogenase from the Antarctic psychrophile *Moraxella* sp. TAE123. Eur J Biochem 254:356–362

Vetriani C, Maeder DL, Tolliday N, Yip KS, Stillman TJ, Britton KL, Rice DW, Klump HH, Robb FT (1998) Protein thermostability above 100°C: a key role for ionic interactions. Proc Natl Acad Sci USA 95:12300–12305

Violot S, Aghajari N, Czjzek M, Feller G, Sonan GK, Gouet P, Gerday C, Haser R, Receveur-Brechot V (2005) Structure of a full length psychrophilic cellulase from *Pseudoalteromonas haloplanktis* revealed by X-ray diffraction and small angle X-ray scattering. J Mol Biol 348:1211–1224

Wintrode PL, Arnold FH (2000) Temperature adaptation of enzymes: lessons from laboratory evolution. Adv Protein Chem 55:161–225

Xie BB, Bian F, Chen XL, He HL, Guo J, Gao X, Zeng YX, Chen B, Zhou BC, Zhang YZ (2009) Cold adaptation of zinc metalloproteases in the thermolysin family from deep sea and arctic sea ice bacteria revealed by catalytic and structural properties and molecular dynamics: new insights into relationship between conformational flexibility and hydrogen bonding. J Biol Chem 284:9257–9269

Xu Y, Feller G, Gerday C, Glansdorff N (2003) Metabolic enzymes from psychrophilic bacteria: challenge of adaptation to low temperatures in ornithine carbamoyltransferase from *Moritella abyssi*. J Bacteriol 185:2161–2168

Yip KS, Stillman TJ, Britton KL, Artymiuk PJ, Baker PJ, Sedelnikova SE, Engel PC, Pasquo A, Chiaraluce R, Consalvi V (1995) The structure of *Pyrococcus furiosus* glutamate dehydrogenase reveals a key role for ion-pair networks in maintaining enzyme stability at extreme temperatures. Structure 3:1147–1158

I.I.1 State of the art in 2022

Since the publication of this book chapter, the concepts and models proposed have not been challenged but were the starting point for some new refinements. In particular, with the improvement of computing tools, molecular dynamic simulations (MDS) were applied in order to provide a more detailed definition of "flexibility" in extremophilic enzymes. This includes the location of regions with improved dynamics in psychrophilic enzymes, which can be close or at the active site or even global (Ferreira *et al.*, 2020; Zhang *et al.*, 2021; Sen & Sarkar, 2022) as well as the type of movements, vibrations and atomic fluctuations (Rapuano & Graziano, 2022). In many cases, such calculations allowed to describe the catalytic reaction path and its energetics with good agreements with experimental enzymatic data (Dong *et al.*, 2018; Socan *et al.*, 2019; Socan *et al.*, 2020; van der Ent *et al.*, 2022). An emerging concept is also worth mentioning, which involves local unfolding promoted by conformational entropy enhancing mutations (the destabilizing mutations in psychrophilic proteins). It has been shown that local unfolding modulates enzyme dynamics in determining affinity and turnover, mimicking the behavior of cold-active enzymes. In the investigated enzyme (adenylate kinase), affinity is controlled by one domain whereas the reaction rate is determined by another domain, both domains displaying dynamic allostery. These aspects have been convincingly probed by experiments such as NMR (Saavedra *et al.*, 2018).

I.II – Part A – Copper in biological systems and copper resistance in bacteria

I. II. A. 1 Copper and (human) life

Since its discovery in ~9000 BCE, metal copper (Cu) has been utilized for a number of applications including in the creation of jewelry, as a material for cooking and storage vessels, as a medication for disease used by the ancient Greeks, as a key component of fungicides such as Bordeaux mixture (used to protect vineyards in France since the late 1800s) and currently as a potent conductor of electricity (Koch *et al.*, 1997).

The essentiality of copper for animals and humans has been known for nearly a century. The human body contains around 100 mg of copper. It is a trace element (minerals required in amounts 1 to 100 mg/day by adults) found in high concentrations in the brain, liver, and kidney. These high concentrations are probably related to metabolic activity, because copper is a cofactor for cytochrome c oxidase, the terminal enzyme in the electron transport chain. Due to possible adverse consequences of high copper ingestion, an upper tolerable intake level of 10 mg/day has been established. Copper toxicity is rather rare in humans and animals, because mammals have evolved precise homeostatic control of copper due to the high reactivity of the free metal (Collins & Klevay, 2011). In human, the principal pathologies of copper are Menkes syndrome and Wilson's disease. These life-threatening genetic disorders are both due to defective intracellular copper transport. Menkes syndrome is an X-chromosome-linked disorder and Wilson's disease is an autosomal recessive disorder. The former is characterized by progressive cerebral degeneration, essentially due to insufficient copper absorption, and the latter is due to excessive copper accumulation in liver, accompanied by liver disease and haemolytic crises. Both the Menkes and Wilson's gene products are members of a family of ion-transporting integral membrane proteins called P-type ATPases (Crichton & Pierre, 2001; Koch *et al.*, 1997; Andrei *et al.*, 2020; Finney & O'Halloran, 2003).

The so-called Great Oxidation Event (GOE), which occurred between 2.4-2.7 billion years ago, refers to an increase in atmospheric oxygen that potentially changed the bioavailability of metals including Cu (Dupont *et al.*, 2011). During prebiotic times, water soluble ferrous iron (Fe^{2+} or Fe(II)) was present and was the form used in the first stage of life. The natural abundance and the redox properties of iron allowed the chemistry that was suited for life. At the same time, copper was in the water-insoluble Cu(I) state (cuprous copper or Cu^{+}), in the form of highly insoluble sulphides, and was not available for life. It can then be said that the early chemistry of life used iron (II) (Crichton & Pierre, 2001). Nowadays, copper is the second most abundant transition metal in biological systems, next to iron (Underwood, 1977). How could this notable evolution have happened? After the rise of photosynthetic organisms such as the cyanobacteria, oxygen accumulated in the atmosphere and oxygenated the oceans. This led to a decrease in the solubility of iron, oxidized and transformed into the insoluble Fe(III) state, and an expansion of the biological role of copper, now available as the oxidized and soluble Cu(II), suggesting there was a shift from the exclusive use of iron in biology to embrace similar, though not identical, roles for Cu (Festa & Thiele, 2011). The rise of O_2 altered the redox chemistry of the environment. In the absence of molecular oxygen, life had adapted to reaction systems in the lower portion of the redox potential spectrum, limited by the H_2S/S and H_2/H^+ potentials ranging 0.0 to -0.4 V at a pH of 7. The presence of O_2 increased the upper limit of the range to 0.8 V (Rubino & Franz, 2012). The high redox potential of the Cu(II)/Cu(I) pair (+160 mV) favors reactions with oxygen and oxygen containing molecules and it is generally assumed that Cu-dependent proteins have evolved concomitantly with the appearance of molecular oxygen (Giachino & Waldron, 2020).

In general, prokaryotic organisms have adopted a limited role for Cu in their biochemistry and physiology. Almost all anaerobic bacteria and all anaerobic archaea are limited Cu users, likely reflective of the limited availability of the metal under these conditions, and then thought to be representative of the majority of life in primordial, anaerobic Earth. The majority of the prokaryotes that use Cu express cytochrome c oxidase, the last enzyme in the respiratory electron transport chain. In bacteria, cytochrome c oxidase is located in the cell membrane and is the most common cuproenzyme (Festa & Thiele, 2011). On one hand, the advent of O_2 produced by cyanobacteria about 2.5 Ma ago was a catastrophic event at that time for most living organisms and can be considered as the first general irreversible pollution of the Earth. On the other hand, the oxidation of water-insoluble Cu(I) led to soluble and more bioavailable Cu(II), which was ideally suited to exploit the oxidizing power of dioxygen. Biological systems did not use copper before the advent of O_2 and after the GOE, copper has become an essential element for most living organisms. This event also coincides with the development towards multicellular organisms and so, the 'catastrophe' turned out to be a new step for the progress of life (Crichton & Pierre, 2001).

I. II. A. 2 Copper properties and binding

Cu is a first row transition-metal ion which can assume two oxidation states, Cu(I) (cuprous copper) or Cu(II) (cupric copper) (Koch *et al.*, 1997). Cu(I) is a strong soft metal whereas Cu(II) is borderline according to the Hard and Soft (Lewis) Acids and Bases (HSAB) classification (Pearson, 1963). Therefore, in biological systems, Cu binding sites are dominated by amino acids with soft (sulfur donor atoms) and borderline (nitrogen donor atoms) ligands (Dupont *et al.*, 2011). Within proteins, copper is thus coordinated predominantly by just three ligand types: the side chains of histidine, cysteine, and methionine, with of course some exceptions. The diversity provided by just these three ligands provides choices of nitrogen vs. sulfur, neutral vs. charged, hydrophilic vs. hydrophobic, susceptibility to oxidation, and degree of pH-sensitivity (Rubino & Franz, 2012).

In the Cu(II) oxidation state, the copper ion is a d^9 transition metal ion that contains one unpaired electron in its outer shell (Koch *et al.*, 1997). The $3d^9$ outer electronic configuration of Cu(II) lacks cubic symmetry and hence yields distorted forms of the basic stereochemistry. The coordination numbers 4 (square planar), 5 (trigonal bipyramid or square pyramid) or 6 (distorted octahedral) predominate (Crichton & Pierre, 2001). Cu(I) is a closed shell d^{10} transition metal ion and can be found coordinated by 2, 3 or 4 ligands and showing linear, trigonal planar, or tetrahedral geometries (Dupont *et al.*, 2011). As histidine is the only borderline ligand, it has the ability to effectively bind both Cu(I) and Cu(II), as opposed to the soft methionine and cysteine ligands that more effectively bind Cu(I). Cysteine exhibits the strongest affinity for copper as a result of the electrostatic character of the coordinate covalent bond that is lacking in histidine and methionine interactions with copper. Histidine and cysteine bind copper via protonatable side chains with pKa values for the free amino acids of 6 and 8, respectively, and thus exhibit pH-dependent binding affinity (Rubino & Franz, 2012). In addition to the imidazole nitrogen group, Cu(II) can also be coordinated to oxygen groups found in aspartic and glutamic acid (Festa & Thiele, 2011). Although to a lesser extent, tyrosine can also be involved in copper binding, notably as one of the coordinating ligand in the mononuclear type II (T2) center of the amyloid precursor protein (APP) (Rubino & Franz, 2012) and of galactose oxidase (Lu *et al.*, 2003).

The total number of ligands, their spatial arrangement and solvent accessibility, the various combinations of imidazole, thiolate, and thioether donors, all work together to provide binding sites that either enable copper to carry out a function, or safely transport it in a way that prevents toxic reactivity. Copper proteins can be separated into two broad classes: (i) proteins that utilize the metal as a cofactor to carry out a specific function and (ii) proteins that traffic the metal, i.e. transporting copper as a cargo (Figure I.II.1).

For the latter class, the metal cargo is usually conveyed as the more labile Cu(I) oxidation state. Primary functions of the members of the former class include electron transfer, catalyzing redox reactions of various biological substrates, and dioxygen transport (Rubino & Franz, 2012). The blue-pigmented oxygen carriers hemocyanins ensure the latter function. Hemocyanins are respiratory proteins occurring freely dissolved in the hemolymph of many arthropods and molluscs, they bind one dioxygen molecule between two copper atoms (Heinz *et al.*, 2007).

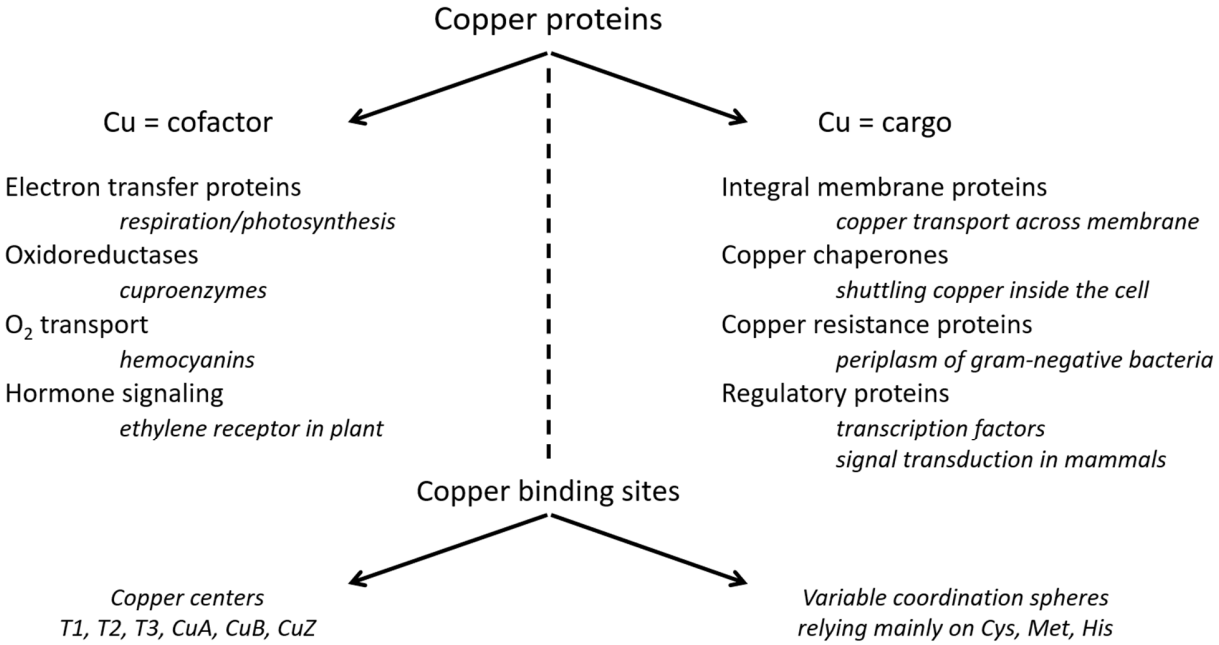

Fig. I.II.1 - Classification of copper proteins, including their roles and copper binding sites.

Almost all copper cofactor-containing proteins are extracellular; notable exceptions are cytochrome c oxidase, which is a large transmembrane protein complex (also called Complex IV) located in the inner mitochondrial membrane and the copper-zinc superoxide dismutase found in the cytosol of eukaryotic cells (Crichton & Pierre, 2001). Enzymes and proteins that utilize copper as a cofactor use high affinity sites of high coordination numbers of 4-5 that prevent loss of the metal during redox cycling. Copper trafficking proteins, on the other hand, promote metal transfer either by having low affinity binding sites with moderate coordination number ~4, or by having lower coordinate binding sites of 2-3 ligands that bind with high affinity. Both strategies retain the metal but allow transfer under appropriate conditions (Rubino & Franz, 2012). The composition and geometry of the Cu binding motif is also important for its reduction potential. While redox cycling is required for the catalytic activity of cuproenzymes, cuproproteins involved in Cu tracking need to avoid Cu(I)/Cu(II) redox cycling and therefore their Cu binding motifs require a more negative reduction potential that stabilizes the Cu(I) state (Andrei *et al.*, 2020). Proteins have evolved to utilize the principles of coordination to effectively fine tune the redox potential and stability of the bound Cu to produce the desired function of the protein (Koch & Thiele, 1997).

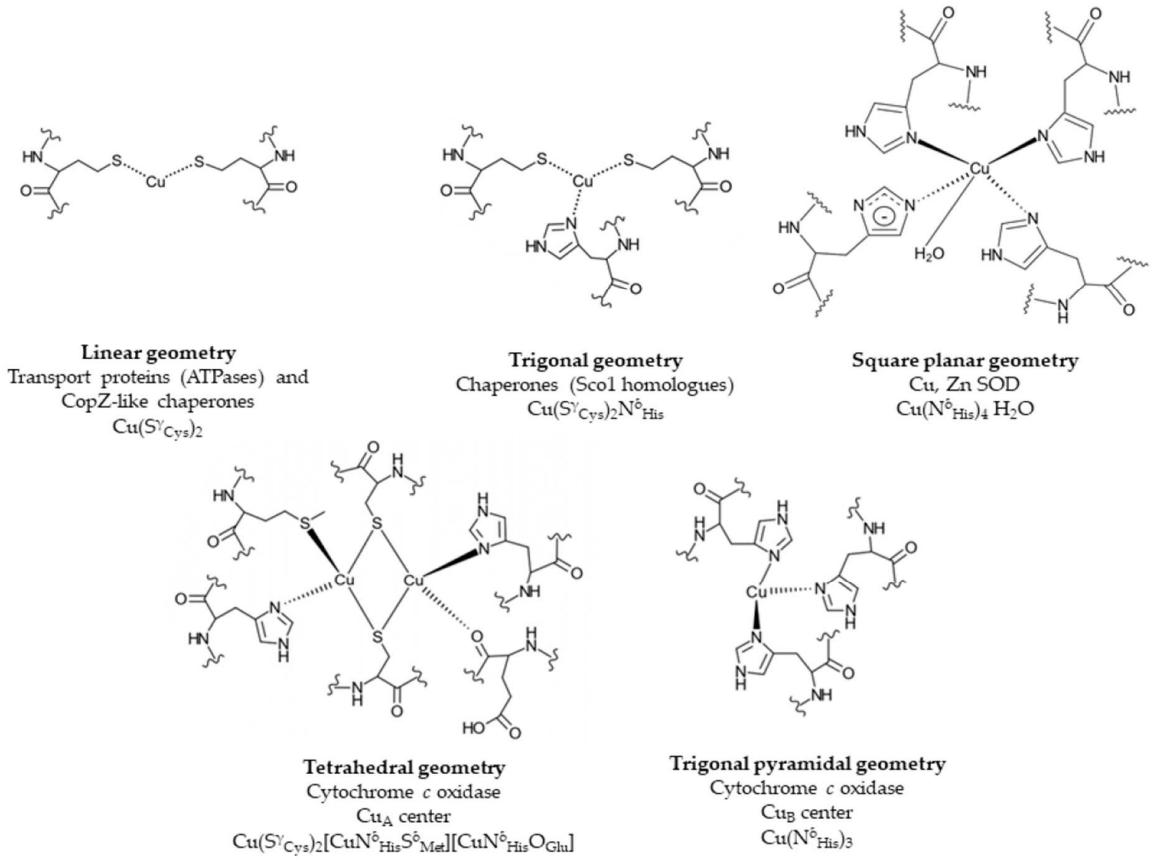

Fig. I.II.2 - Examples of Cu binding sites in Cu trafficking proteins and cuproenzymes.
(Figure from Andrei *et al.*, 2020).

Figure I.II.2 illustrates different examples of Cu binding sites in copper proteins. Copper tracking proteins coordinate Cu(I) via a CXC or CXXC motif (where X is any amino acid) with a linear geometry as in Cu(I)-transporting P1B-type ATPases or in CopZ-like Cu chaperones, or with a trigonal planar geometry as in Sco1-like chaperones. Here, two cysteine residues and a distal histidine residue provide the binding site for Cu(I). In cuproenzymes, such as Cu,Zn superoxide dismutase (SOD) or cytochrome oxidase, Cu is coordinated by histidine, cysteine and methionine residues (Andrei *et al.*, 2020).

Most of the cysteine-rich copper sites are found in reducing intracellular compartments, whereas an abundance of methionine-rich copper sites are found in the oxidizing compartments and the extracellular milieu. As a matter of fact, cysteine thiolate ligands have been shown to be critical to the Cu(I) binding chemistry of many cytosolic metallochaperone and metalloregulatory proteins involved in copper physiology. While the thioether group of methionine is an important Cu(I) ligand for trafficking proteins in more oxidizing cellular environments (Davis & O'Halloran, 2008). This cellular compartmentalization of copper binding motif can be related to the contrasting oxidation sensitivity of methionine compared to cysteine. Methionine-rich sites have emerged as a dominant motif for Cu binding in less redox-balanced spaces that are outside the protective cytosolic environment, including the periplasm of prokaryotic organisms and the cell-surface environment of eukaryotic cells. Methionine is certainly not immune to oxidative modification, but it is more difficult to oxidize than copper-binding CXXC motifs, which readily form disulfides (Davis & O'Halloran, 2008). Methionine as ligand is also less pH sensitive and more hydrophobic and provides often an additional weaker ligand for Cu (Andrei *et al.*, 2020). Moreover,

another important feature of the methionine-rich sites and motifs is their selectivity against the two most abundant intracellular transition metal ions: zinc and iron. Notably, the +2 ions of these metals are not favored for binding in the methionine-rich sites, but hundreds of examples of zinc and iron ions bound to CXXC motifs can be found in the metalloprotein literature (for example, in zinc finger proteins and iron-sulfur proteins) (Davis & O'Halloran, 2008). Therefore different coordination motifs seem to be tailored to different pathways and cellular environments in order to preserve copper-specific recognition within a robust metal-binding site (Davis & O'Halloran, 2008).

Proteins utilizing copper as a cofactor are classified according to ligand composition and geometry of the metal center. These copper centers exhibit very similar characteristics, including UV-visible and Electron Paramagnetic Resonance (EPR) signals, and reduction potentials, regardless of the protein within which they are found (Rubino & Franz, 2012) (Table I.II.1). The EPR signals differ according to the binding environment of the copper atom (Solomon *et al.*, 1996). The EPR is a technique very close to Nuclear Magnetic Resonance (NMR), with one important difference: while NMR is based on the nuclear spin, in EPR it is the electronic spin which is the basis of the measurements carried out. The EPR allows an investigation of paramagnetic systems, which have one or more unpaired electrons (non-zero electron spin). The measurements are made using a magnetic field which causes the degeneration of the electronic energy levels to rise (Zeeman effect), transitions between the two resulting energy levels can then be induced by supplying energy in the form of an electromagnetic wave perpendicular to the magnetic field. Generally, the energy supplied is constant (microwave source at a frequency of 9 to 10 GHz) and the scanning is done in a magnetic field (from 0 to 1 Tesla) to produce the Zeeman effect, when there is resonance the transition shows a line on the spectrum. This technique can thus provide valuable insight into the electronic environment of metal ions in metalloenzymes and into the catalytic process.

Center	*# Cu*	*Geometry*	*Common ligands*	*Examples*
Type I	1	Distorted tetrahedral	His, Cys, (Met)	Azurin, plastocyanin, nitrite reductase, laccase
Type II	1	Distorted tetragonal	His, H_2O, (Asp), (Tyr)	Cu,Zn superoxide dismutase, galactose oxidase, nitrite reductase, laccase
Type III	2	Tetragonal	His	Hemocyanin, tyrosinase, laccase
CuA	2	Trigonal planar	His, Cys, (Met)	Cytochrome c oxidase
CuB	1	Trigonal pyramidal	His	Cytochrome c oxidase
CuZ	4	Tetrahedron	His, S^{2-}	N_2O reductase

Table I.II.1 - Classification of copper centers.
The different types of copper centers in copper proteins, including the number of copper atoms, the metal center geometry and common ligands, along with example proteins.
(Adapted from Lu *et al.*, 2003; Rubino & Franz, 2012).

On the research aspect, the same property that makes copper a valuable biometal, namely the redox cycling between copper(I) and copper(II), also complicates experimental work. While free copper(II) ions are stable in neutral, aqueous solutions exposed to the atmosphere, free copper(I) ions can only be maintained at very acidic pH or in complexed form. Copper(I) complexes which are stable in air can be formed with acetonitrile, CN^-, Tris-buffer and other complexing agents. Another difficulty is the interaction of copper(I) or (II) with all biological molecules, buffer substances, standard reducing agents etc. (Magnani & Solioz, 2007). It is then of paramount importance to carefully consider these aspects when planning and performing experiments and obviously when drawing conclusions from them.

I. II. A. 3 Copper and electron transfer

Reduction potential (E^o) is defined as a tendency of a chemical species to be reduced by gaining an electron and is defined with electrochemical reference of hydrogen, which is globally given the reduction potential of zero (Gupta *et al.*, 2016).

Redox reactions play important roles in almost all biological processes, including photosynthesis and respiration, which are two essential energy processes that sustain all life on earth. Redox-active metal ions, as biological cofactors, play an important role in these processes. And even though most metal ions are redox active, biology employs only a limited number of them for electron transfer (ET) processes (Liu *et al.*, 2014). It exists three classes of metalloproteins known to carry out biological electron transfer:

1. Cytochromes. The redox center of these proteins found ubiquitously in biology consists of an heme prosthetic group. Heme is a coordination complex consisting of an iron ion (Fe) coordinated to a porphyrin acting as a tetradentate ligand, and to one or two axial ligands (Moss *et al.*, 1995).
2. Proteins with iron-sulfur redox centers. In these ET proteins, iron and sulfur atoms are organized as so-called Fe-S clusters. Most prominent members of this class are the small proteins ferredoxins (Liu *et al.*, 2014).
3. Proteins with copper redox centers. Cupredoxins form a group of copper proteins that share the same overall fold with the cupredoxin center always residing in a pocket between three loops connecting the strands, with two of the three loops providing ligands to the copper center made of a mononuclear type I (T1) Cu (Lu *et al.*, 2003)

Although each class spans a wide range of reduction potentials, none of them can cover the whole range needed for biological processes. Together, however, they can cover the whole range, with cytochromes in the middle, Fe-S centers toward the lower end, and the cupredoxins toward the higher end (Figure I.II.3) (Liu *et al.*, 2014).

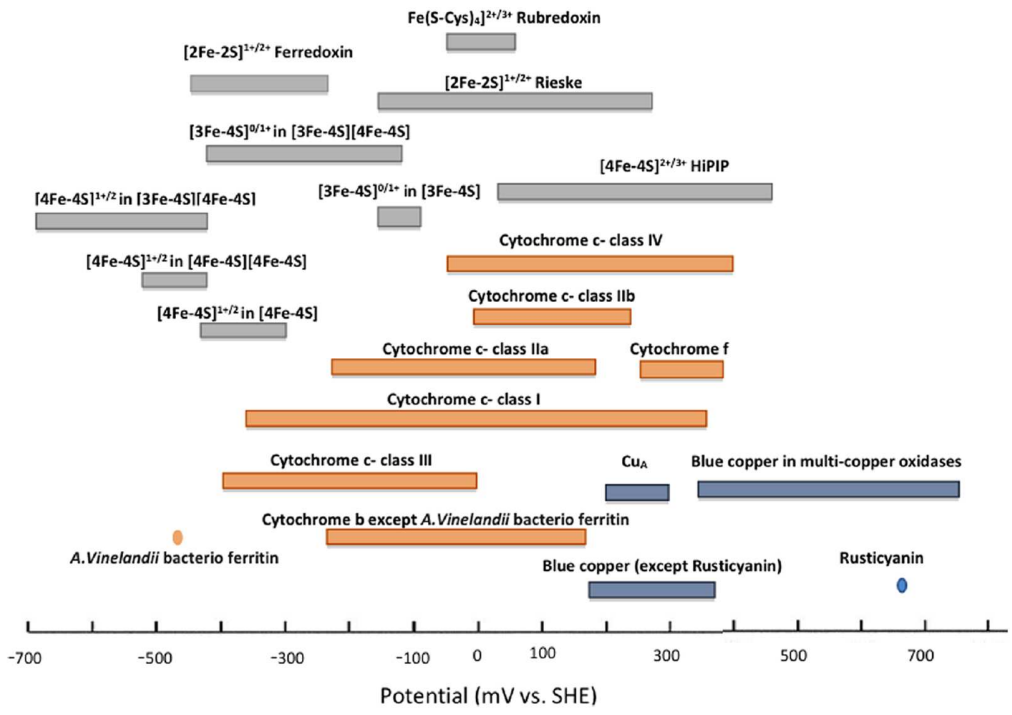

Figure I.II.3 - Reduction potential range of redox centers in electron transfer processes.
(Figure from Liu *et al.*, 2014).

Proteins using Cu as a cofactor have positive reduction potentials, as do some iron-containing proteins that evolved after the rise in oxygen and having an oxygen-related function (Dupont *et al.*, 2011; Rubino & Franz, 2012). While the proteins and enzymes involved in anaerobic metabolism were designed to act in the lower portion of the redox potential spectrum, the presence of dioxygen created the need of a new redox active metal with E_0 M^{n+1}/M^n from 0 to 0.8V. Copper, which became bioavailable after the GOE, was then quite ideally-suited (Crichton & Pierre, 2001). T1 copper proteins have reduction potentials spanning a wide range (>600 mV), nearly half the range of biologically relevant potentials (Liu *et al.*, 2014). Despite its proximity to the protein surface, the cupredoxin center is completely shielded from the solvent, a structural feature that is important for its electron transfer function because it contributes to lowering of the reorganization energy in ET (Lu, 2003). According to the semiclassical Marcus equation (Marcus & Sutin, 1985) the rate of biological electron transfer depends on three factors: driving force (or reduction potential differences between the donor and acceptor, ΔE°), reorganization energy (λ), and the donor-acceptor electronic coupling (H_{AB}) :

$$k_{ET} = \left(\frac{\pi}{\hbar^2 \lambda k_B T}\right)^{1/2} (H_{AB})^2 \exp\left[\frac{-(\Delta E^\circ + \lambda)^2}{4\lambda k_B T}\right]$$

Under the same driving force, the rate is maximized when H_{AB} is large and λ is small. In long-range ET, as it occurs in T1 copper proteins, there is little direct coupling between the donor and the acceptor. The coupling is mediated by intervening atoms via the superexchange mechanism. H_{AB} is determined by the distance between the donor and acceptor and the covalency of the metal-ligand bond (Lu, 2003).
The redox potential of Cu within a polypeptide can be altered substantially depending on the available coordinating ligands, how strongly the polypeptide chain controls the coordination geometry of the metal center, and the dielectric environment of the metal center. For example, an environment that has a tetrahedral coordination of Cu(II) would promote the transition to the Cu(I) oxidation state and consequently raise the redox potential of the metal (Koch *et al.*, 1997). Therefore the protein matrix plays a prominent role in enforcing the unique binding geometry of the redox center to maintain a low reorganization energy for the ET function. The geometry and the type of amino acid ligands in the primary coordination sphere, but also the local hydrophobicity and the H-bonding network in the secondary coordination sphere play a dominant role in controlling and fine-tuning the redox properties of the metal center (Liu *et al.*, 2014).

I. II. A. 4 Copper: essential but toxic

Copper is an essential trace element for a majority of life forms and used as cofactor in key enzymes of important biological processes. But copper can also be potentially toxic. Cu toxicity is intrinsically linked to its redox properties that favor the generation of reactive oxygen species via a Fenton-like reaction (Andrei *et al.*, 2020):

$$Cu^+ + H_2O_2 > Cu^{2+} + OH^- + {}^\circ OH$$

The hydroxyl radicals generated can damage proteins, nucleic acids, and lipids, and can interfere with the synthesis of iron-sulfur clusters that are essential for the activity of a number of important cellular enzymes (Festa & Thiele, 2011). In addition, metalloproteins *in vitro* coordinate metal ions with affinities largely reflective of the Irving-Williams series ($Mn^{2+} < Fe^{2+} < Co^{2+} < Ni^{2+} < Cu^{2+} > Zn^{2+}$), with Cu^{2+} being the most competitive (Rubino & Franz, 2012). Excess Cu could lead to significant mis-metalation of proteins naturally containing other metals, iron or zinc in particular, resulting in their inactivation or in inappropriate protein structures (Andrei *et al.,* 2020; Festa & Thiele, 2011). The consequence of the essential yet toxic nature of Cu is that all cells must have homeostatic mechanisms that maintain Cu at a level required for Cu-

dependent enzymes but that also prevent the accumulation of Cu to toxic levels (Koch *et al.*, 1997). Copper import and efflux pathways, copper chaperone networks, metal sensing transcription factors, metal compartmentalization for protein maturation and maintenance of differential cellular levels of competing metals are critical components of these mechanisms (Rubino & Franz, 2012).

Copper, as other transition metals such as zinc and iron, must be acquired to reach intracellular concentration quotas of tens to hundreds of micromolar; however, few if any of these ions are 'free' or readily accessible in terms of their thermodynamic availability or reaction chemistry (Davis & O'Halloran, 2008). In the periplasm of Gram-negative bacteria, copper concentration is also maintained at micromolar levels (Giachino & Waldron, 2020). The level of copper toxicity for *E. coli* was found to be at 6 mM $CuSO_4$ in the culture medium (Gupta *et al.*, 1995; Grey & Steck, 2001). A study on the effect of copper on growth of various yeasts showed that the half inhibitory concentration (copper concentration representing 50% of maximum growth in basal medium) was comprised between 0.3 and 4.8 mM $CuSO_4$ (Imahara *et al.*, 1978). In contrast to most other nutrients, the concentration of many metals in natural environments usually exceeds cellular needs and hence multiple mechanisms that prevent metal-induced damage are encountered in bacteria (Andrei *et al.*, 2020).

I. II. A. 5 Copper resistance mechanisms in bacteria

As an essential cofactor for redox-active cuproenzymes, copper is an important micronutrient for bacteria (Xiao & Wedd, 2011). For most of them, copper enters the cell via passive diffusion along its chemical gradient. The mechanisms of intracellular copper handling, which regulate its acquisition, storage, detoxification and delivery to maturing cuproenzymes, have been extensively studied in the model organism *Escherichia coli* (Figure I.II.4) (Giachino & Waldron, 2020). In *E. coli*, copper bioavailability in the cytoplasm is buffered to an exquisitely low concentration, equivalent to less than one atom per cell (Outten *et al.*, 2000).

The Cue system (Copper Efflux) was first discovered in *E. coli* and consists of a copper responsive element, CueR, that can activate the expression of P-type ATPase CopA, a transmembrane transporter which pumps Cu(I) from the cytoplasm into the periplasm, CueO, a periplasmic multicopper oxidase which converts Cu(I) into less toxic Cu(II) (see below I.II Part B), and the cuprochaperone CopZ. The core *cue* regulon is functionally conserved in all proteobacteria (Giachino & Waldron, 2020).

Like in the cytosol, free Cu is virtually absent in the bacterial periplasm and CopA does not just release Cu into the periplasm, but it rather transfers it to periplasmic Cu chaperones, such as CusF which is part of the CusCBA system that translocates Cu across the outer membrane. Expression of the *cusFCBA* operon is regulated by the two-component CusRS system. The CusCBA complex can receive Cu from CusF but can also transport Cu from the cytoplasm into the extracellular space (Andrei *et al.*, 2020).

Many Gram-negative bacteria contain a third line of defense against high Cu concentrations, the *pco* cluster (plasmid-borne copper resistance) which is often encoded on a transferable plasmid and found in strains experiencing high Cu concentrations in their environment. In *E. coli*, the *pcoABCDE* genes code for several inner, outer and periplasmic proteins, while *pcoRS* codes for a Cu-responsive two-component regulatory system regulating *pcoABCDE* expression in response to Cu (Andrei *et al.*, 2020). PcoA is the major determinant of the *pcoABCDE* induced Cu-resistance. It belongs to the family of periplasmic multicopper oxidases and can replace CueO in *E. coli*. The exact function of PcoB is uncertain, but it might be required for exporting Cu(II) from the periplasm to the extracellular environment. PcoD is a predicted

inner membrane copper permease and PcoC and PcoE are predicted periplasmic Cu chaperones (Andrei *et al.*, 2020).

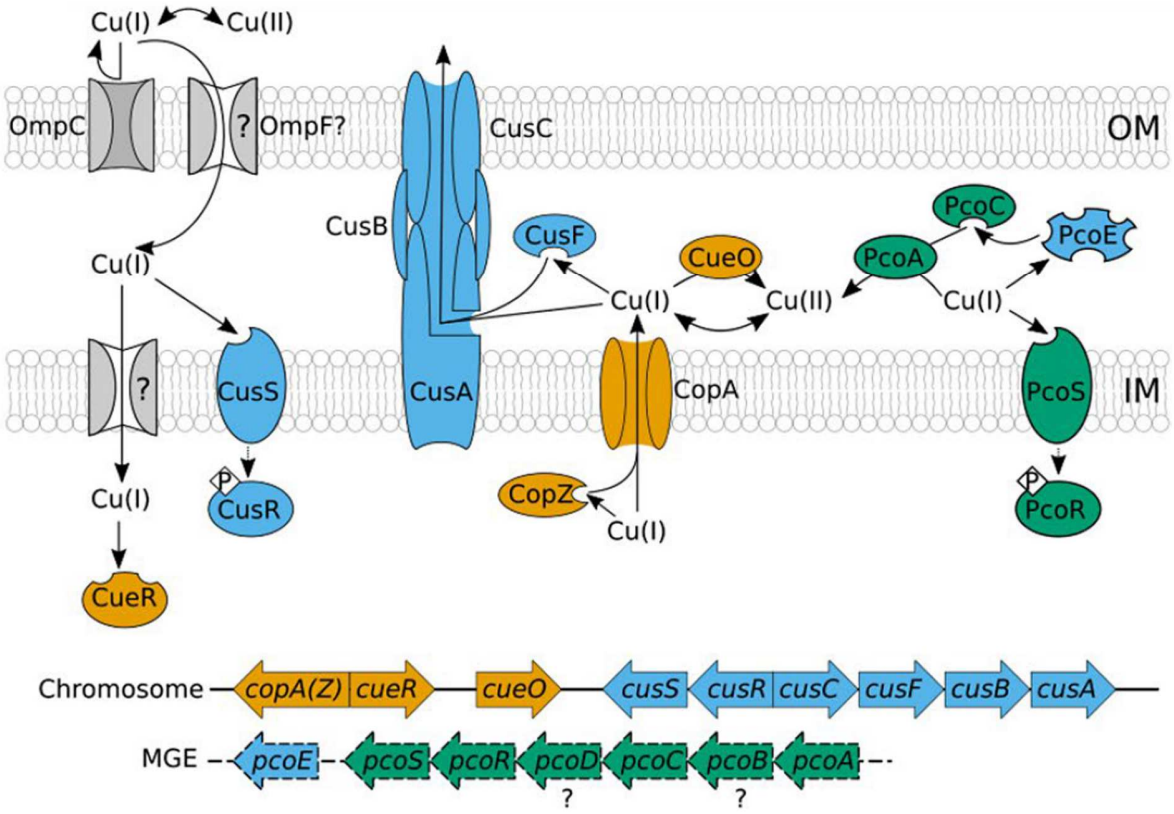

Figure I.II.4 - Copper homeostasis in *Escherichia coli*.
In *Escherichia coli*, three sensory systems, CueR,l CusSR, and the plasmid-borne PcoSR, monitor Cu(I) concentration in the two cellular compartments (cytoplasm and periplasm). Two efflux pumps, CopA and CusCBA, actively secrete copper from the cytoplasm and periplasm, respectively. Each ATPase is associated with one high-affinity cuprochaperone that scavenges copper in the respective compartment (CopZ in the cytoplasm; CusF in the periplasm). A multicopper oxidase, CueO, carries out copper detoxification in the periplasm. The plasmid-borne Pco system provides two additional periplasmic chelators, PcoC and PcoE, and one additional multicopper oxidase, PcoA. Although the copper entry route across biological membranes is unknown, the outer membrane porin, OmpC, may contribute to copper resistance by selecting against copper. MGE = Mobile Genetic Element. Color codes correspond to different regulons: orange = CueR, blue = CusRS, green = PcoRS. The function of PcoB and PcoD are only putative.
(Adapted from Giachino & Waldron, 2020).

I.II – Part B – Multicopper oxidases

MultiCopper Oxidases (MCOs) are typically monomeric proteins that consist of three cupredoxin-like domains. MCOs catalyze the reduction of molecular oxygen to water by oxidation of an electron donor substrate. This process takes place via the transfer of 4 electrons, each electron coming from one substrate molecule, so as to reduce one oxygen molecule according to the equations:

$$(\text{Reducing substrate} \rightarrow \text{Oxidized substrate} + 1\ e^-) \times 4$$
$$O_2 + 4\ e^- + 4\ H^+ \rightarrow 2\ H_2O$$

The mechanism of action of MCOs is based on an active site composed of 4 copper atoms coordinated in total by 10 histidine residues and 1 cysteine residue which are strictly conserved in all MCOs. Figure I.II.5 shows an alignment of the 4 regions involved in the formation of copper clusters of different MCOs with different specificities. Among these 4 copper atoms, there is a type I copper (T1) or "blue" copper, and three copper atoms forming a trinuclear cluster (TNC) consisting of a type II (T2) or "normal" copper and two type III (T3) or “binuclear” coppers.

Figure I.II.5 - Sequence alignment of amino acids involved in the formation of the Cu binding sites in different multicopper oxidases.
CueO (*Escherichia coli* cuproxidase), (BO) *Myrothecium verrucaria* bilirubin oxidase, RvLc (*Rhus vernicifera* laccase), AO (zucchini ascorbate oxidase), TvLc (*Trametes versicolor* laccase), CcLc (*Coprinus cinereus* laccase), Fet3p (*Sacharomyces cerevisiae* ferroxidase), CumA (*Pseudomonas putida* manganese oxidase), CotA (*Bacillus subtilis* endospore oxidase), SLAC (*Streptomyces coelicolor* small laccase), and hCp (human ceruloplasmin). Numbers indicate the amino acids as ligands for each type of Cu. Amino acids coordinating the trinuclear cluster, made of the T2 and the two T3 Cu, are highlighted in light grey and amino acids coordinating the T1 Cu are highlighted in black in the sequences. Asterisk indicate a potential proton donor for the reaction intermediates, the acidic amino acid is framed in grey in the sequences.
(Figure from Sakurai & Kataoka, 2007).

The type I Cu is coordinated by two histidine residues and one cysteine residue (and usually a fourth methionine residue). The charge transfer in the Cu(II)-S(Cys) bond of this copper atom is responsible for the (very beautiful) deep blue color characteristic of MCOs, which is why they are also called “blue oxidases”. This type I copper gives a peak in UV-visible absorption centered around 600-610 nm (ε ~5000 $M^{-1}cm^{-1}$), it also gives a special signal in EPR. The T1 center does not play a role in the binding and activation of O_2, it only plays a role in the transfer of the electron between the substrate and the trinuclear cluster (Rosenzweig & Sazinsky, 2006). There is a distance of 12-13 Å separating T1 from the TNC and electron transfer happens through the conserved HCH motif where the cysteine residue is a ligand of T1 copper and the two histidine residues are ligands of the trinuclear cluster (Solano *et al.*, 2001).

The type II Cu does not contribute significantly to the UV-visible spectrum of MCOs but shows EPR characteristics typical of so-called "normal" copper sites. It is coordinated by two histidine residues and a water molecule (Ueki *et al.*, 2006).

The two type III Cu, each coordinated by three histidine residues and forming the binuclear center, show an absorption band at 330 nm and are said to be silent in EPR due to the antiferromagnetic coupling between the two copper atoms mediated by a bridging ligand (hydroxide, dioxygen or peroxide, see below) (Galli *et al.*, 2004).

In the general catalytic scheme of an MCO, the electron of the donor substrate is first transferred to the T1 center and then, via the path formed by the HCH motif, passes to the trinuclear cluster (Bento *et al.*, 2005). It has been established that all MCOs require a fully reduced TNC to initiate the O_2 reduction process (Figure I.II.6). When a fully reduced MCO reacts with O_2, two key intermediates are formed in the reductive cleavage of the O−O bond by the TNC: the two-electron-reduced peroxy intermediate (PI, also called intermediate I) and the four-electron-reduced native intermediate (NI, also called intermediate II) (Tian *et al.*, 2020). Acidic amino acids in the direct vicinity of the trinuclear center play an essential role in the efficacy of enzyme catalysis by supplying the protons (Sakurai *et al.*, 2017). Spectroscopic studies defined PI as a species with two Cu atoms oxidized and antiferromagnetically coupled, one Cu atom-reduced, and peroxide bridging all three Cu of the TNC. The NI has all Cu oxidized with a μ_3-oxo in the center of the TNC and a μ_2-hydroxo ligand between the two T3 Cu. In the presence of excess amounts of a reductant, NI is rapidly reduced to the fully reduced (FR) form. In the absence of a reductant, NI slowly decays to the resting oxidized (RO) form (Tian *et al.*, 2020).

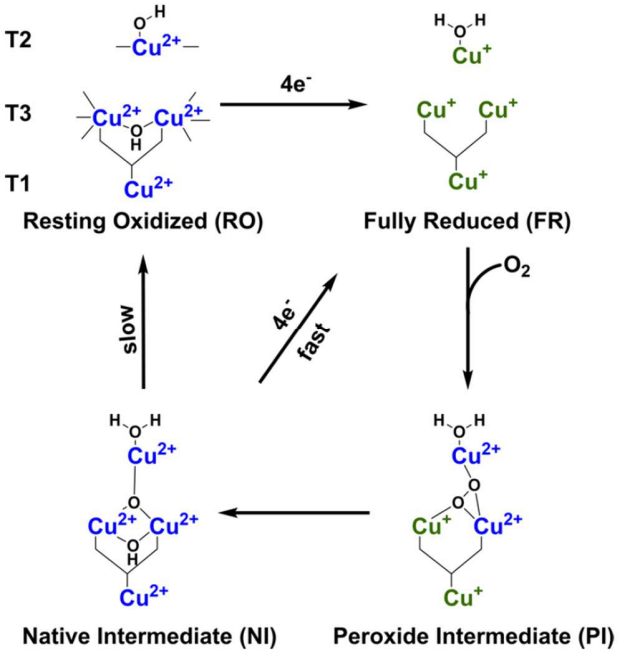

Figure I.II.6 - Reaction mechanism of multicopper oxidases.
Cu^{2+} and Cu^{+} ions are shown in blue and green, respectively.
(Figure from Tian *et al.*, 2020).

The different MCOs are distinguished by their substrate specificity which is related to their role fulfilled *in vivo*. Here is a list of MCOs sorted in ascending EC (Enzyme Commission) number:

- Bilirubin oxidase (EC 1.3.3.5): this enzyme found in fungi catalyze the oxidation of bilirubin, a breakdown product of heme, to biliverdin (Solomon *et al.*, 1996).

- Laccase (EC 1.10.3.2): this blue oxidase represent the largest group of MCOs. They show a polyphenol oxidase activity, which means that they have the ability to oxidize a fairly wide range of phenolic compounds such as *ortho*- or *para*-quinols, aminophenols, phenylenediamines, anilines, benzenethiols, aryldiamines and lignins. Substituted phenols with methoxy groups (guaiacol, dimethoxyphenol) and synthetic substrates with large molar extinction coefficients such as *ortho*-dianisidine, 2,2'-azino-bis(3-ethylbenzothiazoline-6-sulfonic acid (ABTS) and syringaldazine are furthermore preferred for detecting laccase activity (Solano *et al.*, 2001). The laccase was one of the first enzymes to be studied and was first described in 1883 by Yoshida who discovered it in the sap of the Japanese lacquer tree (*Rhus vernicifera*), hence its name (Baldrian, 2006). Laccases are found mainly in plants and fungi. In higher plants, the laccases are involved in the lignification process of the cell walls while in fungi they play a role in the morphogenesis and delignification of the wood. They have also been shown to be a virulence factor in many diseases caused by fungi. Laccases have also been found in a few insects where they are thought to be involved in cuticle formation (Mayer & Staples 2002). They are also found in some bacteria, such as CotA, a thermostable laccase involved in spore formation in *Bacillus subtilis* (Enguita *et al.*, 2003). It should be noted that tyrosinases (catecholase and cresolase activities) are also polyphenol oxidases but are not MCOs because they only have the type III pair of coppers (Sanchez-Amat & Solano, 1997). Laccases are also useful "green" catalysts in the treatment of effluents for decolorization-detoxification, in the field of paper production (bleaching) or in the baking industry.

- Ascorbate oxidase (EC 1.10.3.3): these enzymes, which are found mainly in plants as homodimers, specifically oxidize ascorbate to dehydroascorbate. They play a role in the rate of plant growth through cell elongation (Shleev *et al.*, 2005).

- Phenoxazinone synthase (EC 1.10.3.4): this o-aminophenol oxidase is involved in antibiotic biosynthesis in *Streptomyces* strains and its 3D structure has been determined (Smith *et al.*, 2006).

- Ferroxidase (EC 1.16.3.1): ferrous oxidases or ferroxidases oxidize ferrous iron (Fe^{2+}) to ferric iron (Fe^{3+}). In mammals, the ceruloplasmin, a plasma MCO protein, displays this essential ferroxidase activity required for the assimilation of iron by cells which can only import it into their cytoplasm in the form of a ferric ion, the transmembrane transporter being specific to this form. Human ceruloplasmin is the subject of extensive research as it is linked to several diseases (Hellman & Gitlin, 2002). In yeast, the highly studied protein Fet3p performs the same function in the periplasm (Stoj *et al.*, 2006).

- Manganese oxidases (EC 1.16.3.3): this enzyme is found in many bacterial strains. It oxidizes soluble manganese(II) to insoluble manganese(IV) oxides. The enzyme is localized to the outer surface of the cell and its activity usually results in encrustation of the cells by the oxides. The physiological function of bacterial manganese(II) oxidation remains unclear (Dick *et al.*, 2008).

- Cuproxidase (EC 1.16.3.4): cuprous oxidases or cuproxidases oxidize cuprous copper (Cu^{1+}) to cupric copper (Cu^{2+}). This type of MCO related to copper homeostasis was first discovered in *Escherichia coli* and named Cu efflux oxidase (CueO). In contrast to the other MCOs listed above, where the residues close to the T1 copper form a depression allowing to accommodate the substrate, it features an additional Met-

and His-rich insert that includes a helix that blocks physical access to the T1 center and a flexible surface loop that is frequently not resolved in the crystal structures (Figure I.II.7). The insert provides three Cu(I) binding sites for rapid oxidation of bound Cu(I) to Cu(II) ensuring a robust cuprous oxidase function of CueO (Cortes *et al.*, 2015).

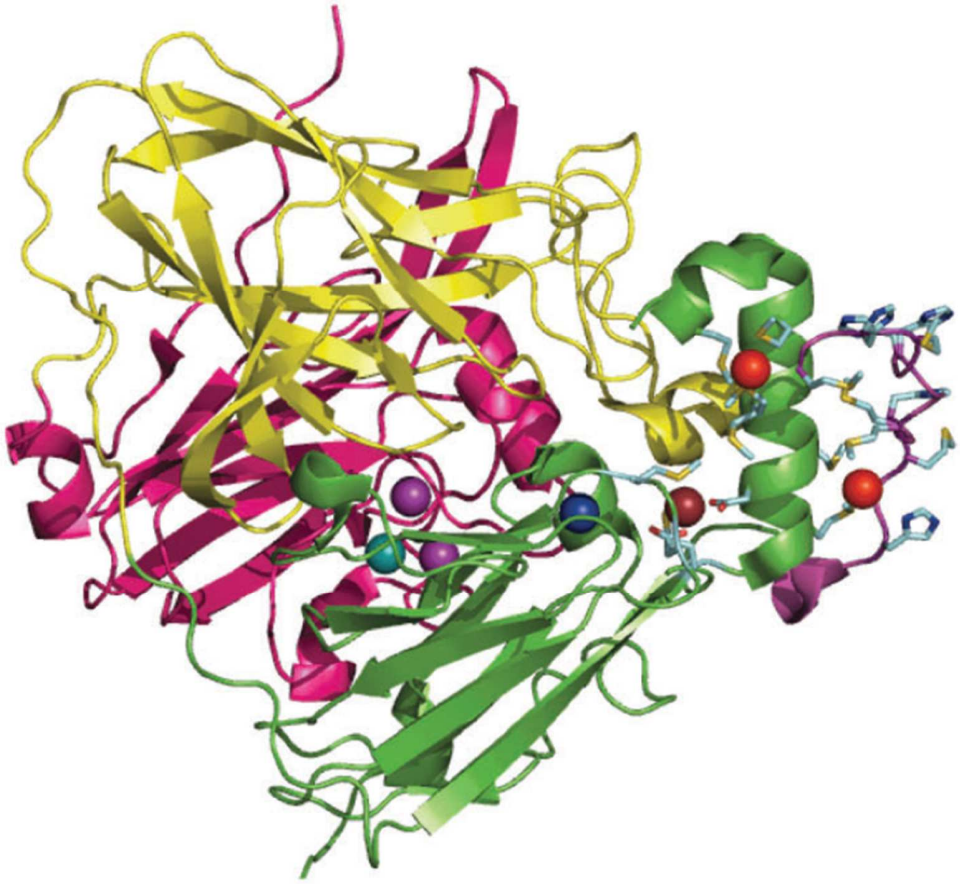

Figure I.II.7 - Ribbon model of fully copper-loaded CueO variant C500S (PDB: 3NT0).
The overall structure is highlighting the three structural cupredoxin domains (D1, red; D2, gold; D3, green), the copper centers associated with MCO activity (T1, blue; T2, teal; T3 (binuclear), purple) and the additional Cu(I) centers associated with the methionine-rich insert (Cu5, chocolate; Cu6 & Cu7, red). Note: (i) T1 Cu is not present in the C500S structure but is added to the figure for illustration; (ii) the disordered Met- and His-rich loop (383-400; shown in purple) was not resolved but is added to the figure by superimposing the wild type CueO structure (PDB: 3OD3) to show potential alternative ligands for Cu6 and Cu7, especially in the Cu(II) form; (iii) Cu5 is also labelled as sCu by other authors to emphasize its role as a site for binding of substrate Cu(I), it is buried underneath the protein surface and H-bonded to the T1 site, suggesting an electron transfer pathway from sCu to the T1 site and then to the trinuclear cluster where oxygen is reduced to water. The Cu6 and Cu7 binding sites in the Met-rich region can be described as substrate-docking-oxidation sites, and the sCu site connects those surface-exposed Cu sites to the catalytic T1 site.
(Figure from Cortes *et al.*, 2015).

It is important to note that the different MCOs mentioned above are categorized based on information on their substrate preferences *in vitro* combined with information coming from studies on their regulation and physiological function. Indeed, and this is what sometimes makes it difficult to assign their “true”

substrate *in vivo*, they are also generally able to oxidize the substrates of other categories, especially phenolic substrates, to a certain extent and with restrictions that differ depending on the enzyme and/or the organism from which they originate (Solomon *et al.*, 1996). As a matter of fact, for CueO, structural and functional studies have shown that removal of the methionine-rich helical region significantly decreases cuprous oxidase activity of the enzyme, but increases its phenol oxidase activity (Wang *et al.*, 2018).

CueO catalyzes both cuprous oxidation and phenol oxidation but via different mechanisms. As a cuprous oxidase, the reactivity relies on the reaction sites Cu6 and Cu7 for high-affinity Cu(I) binding and oxidation via an inner sphere mechanism and on the subsequent release of the product Cu(II) from the reaction sites (Figure I.II.8). As a phenol oxidase, the reactivity depends on occupation of the reaction sites by Cu(II) ions that provide necessary oxidation and electron transfer sites for the phenolic substrate via an outer sphere mechanism. The internal Cu5 (sCu) site is part of the essential electron transfer pathway connecting surface-exposed sites Cu6 and Cu7 to site T1. In both cuprous oxidase function and phenol oxidase function, the same facile electron transfer route is utilized. The reaction sites Cu6 and Cu7 possess higher affinities for Cu(I) (~0.13 pM) than for Cu(II) (~5.5 nM) and in physiologically relevant condition of limiting copper levels, CueO is acting only as a robust cuprous oxidase. While *in vitro*, addition of excess Cu(II) brings about the phenol oxidase or "laccase-like" activity of CueO (Cortes *et al.*, 2015).

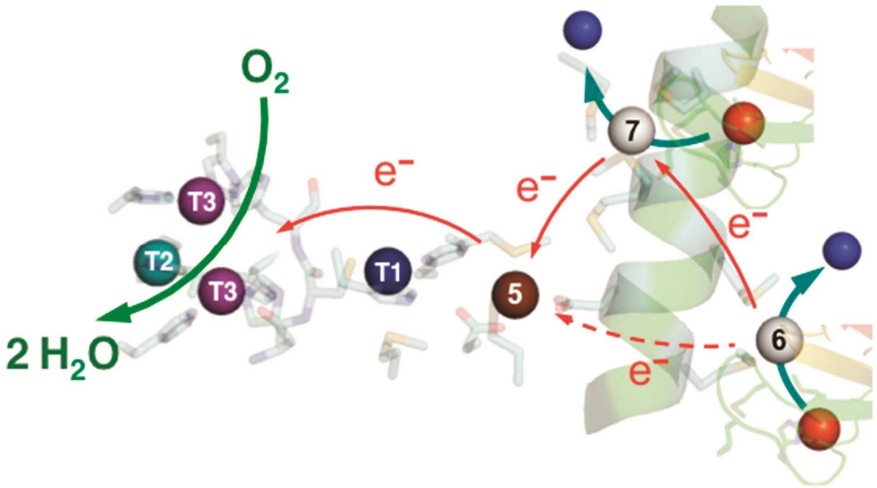

Figure I.II.8 - Proposed reaction mechanism for CueO as a cuprous oxidase.
The Cu5 site (brown sphere 5), also called the sCu site, is an essential electron-transfer mediator, not a substrate reaction site. Cu6 and Cu7 (grey spheres 6 and 7, respectively) are the two reaction sites for Cu(I) (red spheres) loading and oxidation to Cu(II) (blue spheres). The function of Cu6 depends primarily on electron transfer to Cu7. Electrons are transferred from the Cu5 site to the blue T1 copper (blue sphere T1) and then to the trinuclear center, composed of the T2 copper (teal sphere T2) and of the binuclear T3 copper (purple spheres), where dioxygen is reduced to water.
(Figure from Cortes *et al.*, 2015).

To date, the 3D structures of four different cuproxidases are available (Figure I.II.9). They all display a very different Met-rich region, whether by their size, or by their location or by their structure. In *Tth*-MCO, the cuproxidase from *Thermus thermophilus* HB27, a unique 16-residue methionine-rich β-hairpin motif found in the cupredoxin domain 2 is located over the T1 Cu and it appears very probable to be involved in extra copper(I)-binding sites in a way reminiscent to the Met-rich region of CueO (Serrano-Posada *et al.*, 2015).

Extra Cu(I) binding in their Met-rich region can also be expected for McoC from the human pathogen *Campylobacter jejuni* CGUG11284 (Silva *et al.*, 2012) and McoP from the hyperthermophilic archaeon *Pyrobaculum aerophilum* (Sakuraba *et al.*, 2011). Experiments have demonstrated a strong cuprous oxidase activity for both enzymes, although they display a shorter Met-rich region compared to CueO.

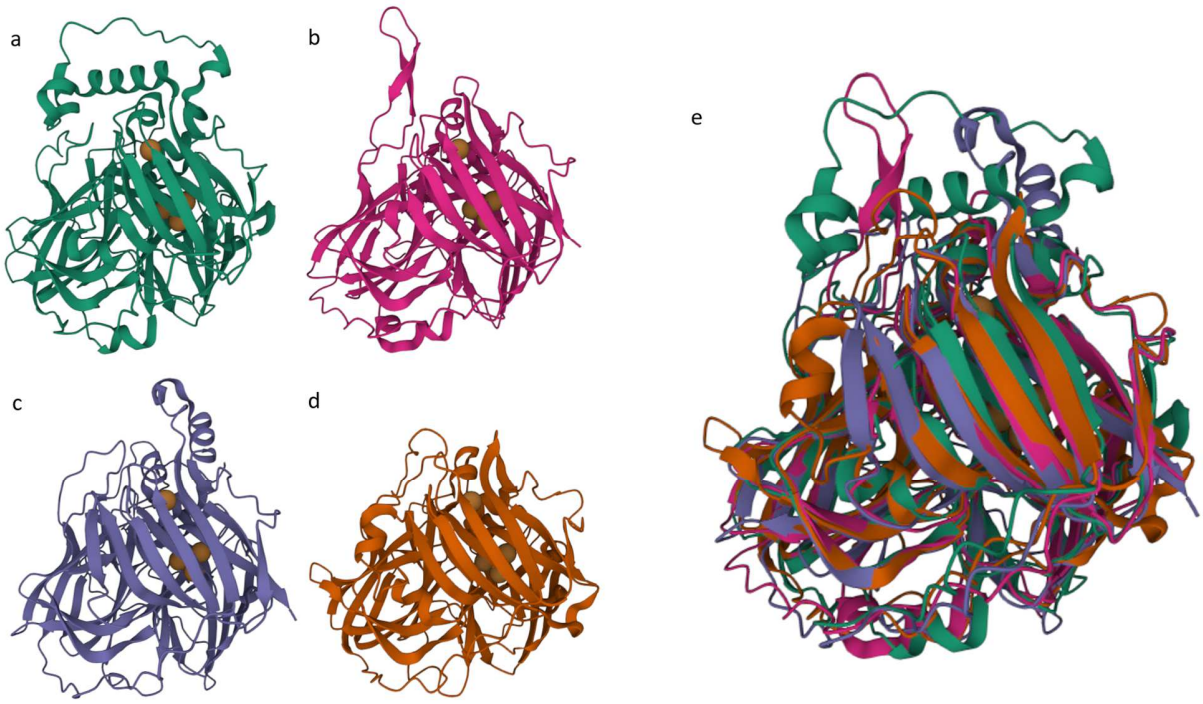

Figure I.II.9 - Ribbon models of the four cuproxidases with a known 3D structure.
(a) CueO from *E. coli* (PDB: 3OD3), (b) *Tth*-MCO from *T. Thermophilus* (PDB: 2XU9), (c) McoC from *C. jejuni* (PDB: 3ZX1), (d) McoP from *P. aerophilum* (PDB: 3AW5) and (e) superposition of the four structures. The four catalytic copper are depicted in brown spheres. All the structures are represented in the exact same orientation. The variable extension observed at the top of each structure is the Met-rich region covering the T1 Cu (the highest brown sphere).
Images created using Mol* (Sehnal *et al.*, 2021).

Chapter II – Objective

This work is part of a broader effort conducted for several years at the Laboratory of Biochemistry, Center for Protein Engineering, University of Liège, to understand the adaptation of enzymes to temperature. Within this context, many different enzymes have been extensively studied to generate a knowledge that has greatly contributed to establish the activity-stability-flexibility tradeoff hypothesis for temperature adaptation. However, a comparative study of extremophilic enzymes catalyzing electron transfer was still lacking. The first aim of the present work was to investigate this aspect using psychrophilic, mesophilic and thermophilic blue multicopper oxidases (MCOs) as models.
The three enzymes selected for the study are homologous periplasmic cuproxidases involved in copper resistance mechanisms of bacteria and they display a methionine-rich (Met-rich) region with high diversity in both the length and composition. The second aim of this study was to examine the role of this peculiar region.

The model enzymes chosen to conduct the investigations of thermal adaptation in bacterial MCOs were CueO from the mesophilic bacterium *Escherichia coli*, because this enzyme has been extensively studied and its 3D-structure determined, the thermophilic *Tth*-MCO, the corresponding MCO from *Thermus thermophilus* HB27, and PhaMOx, the corresponding psychrophilic enzyme from the Antarctic bacterium *Pseudoalteromonas haloplanktis* TAC125.
Moreover, the large loop length differences in the three model cuproxidases allowed to conduct investigations on the Met-rich regions, notably by the construction of deletion mutants of PhaMOx, in order to provide precise structural and functional information.
Extensive biochemical and biophysical characterization combined to protein sequence analysis approaches helped to gather new knowledge on how enzymes adaptation is at work.

Chapter III – Results

Activity-stability relationships revisited in blue oxidases catalyzing electron transfer at extreme temperatures

Roulling F, Godin A, Cipolla A, Collins T, Miyazaki K, Feller G. Activity-stability relationships revisited in blue oxidases catalyzing electron transfer at extreme temperatures. Extremophiles 2016;20(5):621-629.

Extremophiles (2016) 20:621–629
DOI 10.1007/s00792-016-0851-9

ORIGINAL PAPER

Activity–stability relationships revisited in blue oxidases catalyzing electron transfer at extreme temperatures

Frédéric Roulling[1] · Amandine Godin[1] · Alexandre Cipolla[1] · Tony Collins[2] · Kentaro Miyazaki[3] · Georges Feller[1]

Received: 21 March 2016 / Accepted: 31 May 2016 / Published online: 17 June 2016

Abstract Cuproxidases are a subset of the blue multicopper oxidases that catalyze the oxidation of toxic Cu(I) ions into less harmful Cu(II) in the bacterial periplasm. Cuproxidases from psychrophilic, mesophilic, and thermophilic bacteria display the canonical features of temperature adaptation, such as increases in structural stability and apparent optimal temperature for activity with environmental temperature as well as increases in the binding affinity for catalytic and substrate copper ions. In contrast, the oxidative activities at 25 °C for both the psychrophilic and thermophilic enzymes are similar, suggesting that the nearly temperature-independent electron transfer rate does not require peculiar adjustments. Furthermore, the structural flexibilities of both the psychrophilic and thermophilic enzymes are also similar, indicating that the firm and precise bindings of the four catalytic copper ions are essential for the oxidase function. These results show that the requirements for enzymatic electron transfer, in the absence of the selective pressure of temperature on electron transfer rates, produce a specific adaptive pattern, which is distinct from that observed in enzymes possessing a well-defined active site and relying on conformational changes such as for the induced fit mechanism.

Keywords Multicopper oxidase · Cuproxidase · Psychrophiles · Thermophiles · Electron transfer

Communicated by S. Albers.

Electronic supplementary material The online version of this article (doi:10.1007/s00792-016-0851-9) contains supplementary material, which is available to authorized users.

✉ Georges Feller
gfeller@ulg.ac.be

[1] Laboratory of Biochemistry, Center for Protein Engineering, University of Liège, Liège, Belgium

[2] Department of Biology, Center of Molecular and Environmental Biology, University of Minho, Braga, Portugal

[3] Department of Life Science and Biotechnology, Bioproduction Research Institute, National Institute of Advanced Industrial Science and Technology (AIST), Tsukuba, Ibaraki, Japan

Introduction

In recent years, the range of biological temperatures has been expanded with the discovery of new strains inhabiting extreme biotopes. Psychrophiles have been found in the brine veins between polar sea ice crystals at −20 °C (Deming 2002). More recently, the bacterium *Planococcus halocryophilus* isolated from Arctic permafrost was found to divide at −15 °C and to be metabolically active at −25 °C (Mykytczuk et al. 2013), which possibly represents the lowest temperature for sustained life before dormancy. On the other hand, the archaeon *Methanopyrus kandleri* has been isolated from a hydrothermal vent at 122 °C and was shown to resist exposure to 130 °C (Takai et al. 2008).

Among the numerous cellular adaptations required to thrive at these extreme temperatures, the enzymatic function has attracted much attention for both fundamental research and biotechnological applications. To compensate for the reduction of chemical reaction rates inherent to low temperature, psychrophiles synthesize highly active enzymes. In most cases, such activity improvements arise from a flexible, heat-labile protein structure and a dynamic active site that loosely bind its substrate to decrease the free energy barrier of activation (Feller and Gerday 2003; Siddiqui and Cavicchioli 2006; Struvay and

Feller 2012). In contrast, thermophilic enzymes have to maintain a functional native state at elevated temperatures. Their robust protein structure resists unfolding but, as a consequence of the compact and rigid conformation, thermophilic enzymes are generally inactive at room temperature (Kohen et al. 1999; Kumar and Nussinov 2001; Vieille and Zeikus 2001). These adaptations have been explained in terms of activity–stability–flexibility relationships or tradeoffs (Feller and Gerday 2003; Feller 2010). Interestingly, the same types of weak interactions and structural factors are reduced in number and/or strength to provide the dynamic structure in psychrophilic proteins, or are increased to provide the heat-stable structure in thermophilic proteins.

However, noticeable exceptions to the activity–stability–flexibility tradeoff hypothesis for temperature adaptation have been reported. Phosphoribosyl anthranilate isomerase from the hyperthermophile *Thermotoga maritima* is extremely stable but also much more active than its mesophilic counterpart from *E. coli*. This has been related to the requirement for a very fast turnover of its heat-labile substrate at high temperature (Sterner et al. 1996). The chaperonin GroEL from the Antarctic bacterium *Pseudoalteromonas haloplanktis* is not cold adapted and displays similar stability and activity than that of its mesophilic homolog from *E. coli*. This has been tentatively related to the requirement for a heat-stable structure and activity of the psychrophilic chaperonin during heat stress of the Antarctic bacterium (Tosco et al. 2003). These examples suggest that different adaptive strategies can be used, depending on the type of reaction catalyzed or on the cellular context. In this respect, the rate of electron transfer in macromolecules is expected to be almost unaffected in the range of biological temperatures. However, a comparative study of extremophilic enzymes catalyzing electron transfer is currently lacking. This aspect has been investigated here using psychrophilic, mesophilic, and thermophilic blue oxidases as models.

Cuproxidases (cuprous oxidases) are members of the blue multicopper oxidase (MCO) family. In the bacterial periplasm, they catalyze the one-electron oxidation of toxic Cu(I) ions into much less harmful Cu(II) with concomitant four-electron reduction of dioxygen to water (Fig. 1). Cuproxidases display the general fold of MCOs consisting of three repeated cupredoxin domains, with an additional methionine-rich region that confers specificity for Cu(I) (Djoko et al. 2010). Oxidation is mediated via four catalytic copper ions arranged in two centers and designated according to their spectroscopic properties (Solomon et al. 1996). The T1 copper has an absorption peak around 600 nm and gives rise to the blue color typical of MCOs. The T2 and two T3 copper atoms form a trinuclear center (TNC) and

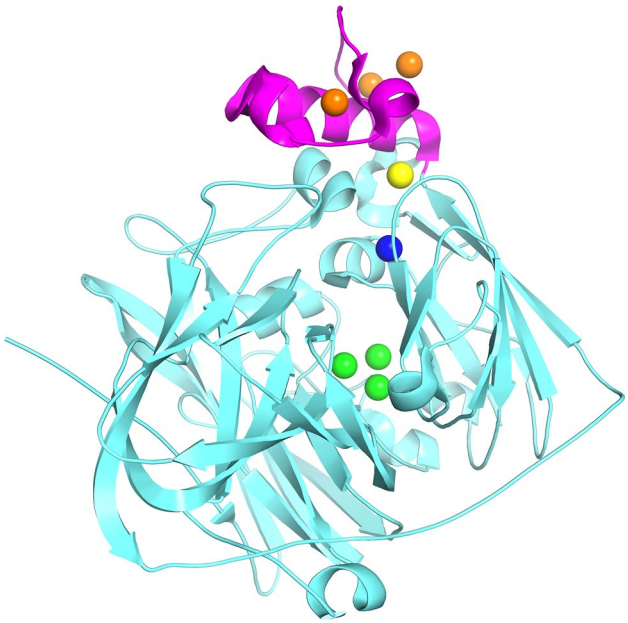

Fig. 1 Ribbon diagram of the cuproxidase CueO from *E. coli*. In *magenta*, the Met-rich insert binding three Cu(I) ions (*orange spheres*). According to the proposed mechanism, electrons are transferred from the sCu site (*yellow*) to the blue T1 copper (*blue*) and then to the trinuclear center (*green*) where dioxygen is reduced to water. Figure based on PDB entries 3OD3 and 3NT0 [limited to Cu(I) ions] from Singh et al. 2011

give rise to a peak in the region of 330 nm. These catalytic coppers are coordinated by strictly conserved histidine, cysteine, and methionine side chains. According to the reaction mechanism proposed for the cuproxidase CueO (Cu efflux oxidase) from *E. coli*, Cu(I) ions are gathered via a methionine-rich region, mainly a disordered loop, and an adjacent substrate binding site (sCu). The latter is buried underneath the protein surface and H-bonded to the T1 site, suggesting an electron transfer pathway from sCu to the T1 site, and then to the TNC where oxygen is reduced to water (Solomon et al. 2008; Singh et al. 2011; Cortes et al. 2015). Cuproxidases also display a laccase-like activity (phenol oxidase) which is dependent on a single Cu(II) binding to the sCu site, the latter becoming a mediator of electron transfer between reducing organic substrates and the T1 site (Djoko et al. 2010). This oxidation has been used here for activity measurements.

To conduct investigations of thermal adaptation in bacterial MCOs, three model enzymes were chosen: CueO from the mesophilic bacterium *E. coli* (Djoko et al. 2010), because this enzyme has been extensively studied, and its 3D-structure was determined (Roberts et al. 2002; Singh et al. 2011), the thermophilic *Tth*-MCO, the corresponding MCO from *Thermus thermophilus* (Miyazaki 2005; Bello et al. 2012) and *Pha*MOx, a new psychrophilic

(cold-adapted) MCO encoded in the genome of the Antarctic bacterium *Pseudoalteromonas haloplanktis* (Medigue et al. 2005). The three enzymes are homologous periplasmic cuproxidases with laccase-like activity. This study was undertaken to analyze the adaptive strategy of enzymes involving electron transfer in catalysis. We show here that a specific, non-canonical adaptive pattern is observed for these enzymes.

Materials and methods

Expression and purification

Cuproxidases from *P. haloplanktis* TAC125, *E. coli* JM109, and *T. thermophilus* HB27 were produced and purified as described elsewhere. Briefly, the coding sequences were PCR-amplified from genomic DNA without the native Tat signal peptide and cloned into the pET28a expression vector for intracellular production in *E. coli* BL21(DE3). The psychrophilic *Pha*MOx was purified by a combination of Q-Sepharose FF, S-Sepharose, and hydroxyapatite column chromatographies. CueO was purified as described (Kim et al. 2001), except that all steps were carried out at 4 °C and *Tth*-MCO was purified as previously described (Miyazaki 2005). Fully copper-loaded holoenzymes were obtained by addition of a 15-fold excess of Cu(I) from a stock solution of $[Cu(I)MeCN)_4]^+$ in acetonitrile, and the excess was removed by gel filtration on PD10 columns eluted with the appropriate buffer. Holoenzymes were used in all experiments, except differential scanning calorimetry (see below).

Differential scanning calorimetry

The PD10 elution buffer for holoenzymes contained 30 mM MOPS and 1 M 3-(1-pyridinio)-1-propanesulfonate (NDSB, a nondetergent sulfobetaine) at pH 7.0. Apoenzymes (Sedlak et al. 2008) were prepared by overnight incubation at 4 °C in the presence of 50 mM ascorbic acid, 50 mM NaCN, and 10 mM EDTA in 30 mM MOPS, 1 M NDSB, pH 7.0. The PD10 elution buffer for apoenzymes contained 30 mM MOPS and 1 M NDSB, pH 7.0. Measurements were performed using a MicroCal VP-DSC instrument at a scan rate of 90 K h^{-1} and under ~25 psi positive cell pressure with samples at ~1 mg/ml concentration. After cell loading, the protein concentration was determined for the remaining sample by the Bradford method (Pierce). Thermograms were analyzed using the MicroCal Origin software (version 7) to determine the melting point T_m, the temperature corresponding to the transition peak, and the calorimetric enthalpy ΔH_{cal} as the area under the transition.

Analytical procedures

The acrylamide-induced quenching of intrinsic fluorescence was measured as described (D'Amico et al. 2003) on an SML-AMINCO Model 8100 spectrofluorimeter (Spectronic Instruments) at an excitation wavelength of 280 nm (1 nm bandpass) and an emission wavelength of 340 nm (2 nm bandpass). Holoenzymes were diluted in 50 mM Tris, pH 7.5 to reach an absorbance at 280 nm of about 0.1. The Cu(II)-dependence of phenol oxidase activity was determined at 25 °C in 50 mM Na-acetate, 10 mM 2,6-dimethoxyphenol, pH 5.0 in the presence of increasing concentrations of $CuSO_4$. The reaction was initiated by substrate addition and monitored by the linear absorbance variation at 477 nm with time. One unit corresponds to 1 µmol of 2,6-dimethoxyphenol oxidized per min, and the $K_{d,app}$ for Cu(II) binding to the sCu site is defined as the concentration of $CuSO_4$ providing half-maximal activity. The temperature dependence of laccase-like activity was recorded in 50 mM Na-acetate, 5 mM 2,2′-azino bis(3-ethylbenzothiazoline-6-sulfonate) (ABTS), 1 mM $CuSO_4$, pH 5.0 in test tubes incubated in a water bath. The reaction was initiated by enzyme addition and absorbance was monitored after 2 min at 415 nm. All activity measurements were performed in triplicates, using a UVIKON XS spectrophotometer (Bio-Tek Instruments).

Results

Primary structure analysis of the homologous cuproxidases

The primary structure of the investigated enzymes displays the typical patterns of cuproxidases, i.e., the strictly conserved ligands of the four catalytic coppers and a Met-rich region involved in Cu(I) binding (Supplementary Fig. S1). When compared with the protein sequence of CueO from *E. coli*, the psychrophilic *Pha*MOx shows 53.5 % sequence similarity (24.6 % identity), and the thermophilic *Tth*-MCO exhibits 59.9 % similarity (30.5 % identity). Tables 1 and 2 show general features of the three MCOs and some peculiarities possibly related to protein adaptation to different thermal environments. The Tat signal sequence gets shorter on going from the psychrophilic to the thermophilic enzyme. Signal peptides of Tat-dependent precursor proteins are optimally adapted to their cognate export apparatus (Blaudeck et al. 2001), and here, the latter has apparently evolved differently in the three bacterial species, possibly as a consequence of their different thermal regimes and membrane compositions. The size of the mature MCOs also decreases on going from the psychrophilic to the thermophilic enzyme. These differences

Table 1 General properties of the investigated cuproxidases

Oxidase	Source	T^{a}_{env} (°C)	Tat peptide (*n* aa)	Mature form (*n* aa)	M_w (kDa)	p*I* calculated	p*I* experimental
*Pha*MOx	*P. haloplanktis* TAC 125	<0	36	576	64.2	5.47	~6.0
CueO	*E. coli* JM109	37	28	488	53.4	6.07	~7.5
Tth-MCO	*T. thermophilus* HB27	~80	21	440	48.8	7.09	~9.5

[a] Estimated average environmental temperature

Table 2 Amino acid content (in mol%) and aliphatic index in relation to temperature adaptation

Oxidase	Pro	Asn	Gln	Arg	Asp	Glu	Met	Met_{core}	Aliphatic index
*Pha*MOx	5.4	4.5	3.6	5.2	8.0	4.5	6.4	4.0	75.31
CueO	6.8	4.3	4.5	3.5	6.1	4.3	5.7	2.9	83.14
Tth-MCO	10.0	2.3	3.2	7.3	4.1	6.8	3.0	1.6	96.61

Met_{core} Met content without Met residues involved in Cu(I) binding

in polypeptide lengths mainly arise from longer and additional loops in the sequence of the psychrophilic *Pha*MOx and from shorter loops in the 3D structure of the thermophilic *Tth*-MCO. Thermophilic proteins tend to decrease the size of unstructured regions, as these often destabilize the native state and are preferential sites for unfolding (Kumar and Nussinov 2001). Conversely, long loops in psychrophilic proteins exert a structural constraint on the protein core, possibly enhancing their dynamic conformation (Feller 2013).

The number of proline residues (Table 2) increases from the psychrophilic to the thermophilic enzymes despite the sequence length decreases. This reflects the constraints imposed by this imino acid on the dihedral angles in the polypeptide chain, leading to a better stability of the native state in thermostable proteins. In the case of *Tth*-MCO, the lower number of Asn and Gln can be related to selection for heat-stable side chains as both residues are prone to thermal deamination (Vieille and Zeikus 2001). Furthermore, its Arg content is higher, reflecting the stabilizing properties of this side chain which is able to perform multiple H-bonds or salt bridges (Mrabet et al. 1992). As a result, the thermophilic enzyme also displays a high p*I* (even higher than the theoretical value, Table 1) compared with its counterparts that could arise from a high density of positively charged residues at the surface of the protein, possibly contributing to an electrostatic network enhancing thermal stability. As a matter of fact, a large number of salt bridges, composed of 34 ion pairs, have been reported in the 3D structure of *Tth*-MCO (Bello et al. 2012). Conversely, the more acidic p*I* of *Pha*MOx, arising from a high Asp content (Table 2), has been frequently reported in psychrophilic proteins and has been related to free acidic surface side chains destabilizing the outer protein shell via interactions with the solvent (Schiffer and Dotsch 1996). The Glu content of *Tth*-MCO is high, as also observed in thermophilic genomes (Suhre and Claverie 2003), and is believed to be important in structural stability. Although the prevalence of Glu over Asp in stabilization has been experimentally demonstrated, the molecular origin remains poorly understood (Lee et al. 2004). The Met content decreases with increasing environmental temperature for the three MCOs, and this trend remains identical after removing the number of Met residues involved in Cu(I) binding, (Met_{core}, Table 2, Supplementary Fig. S1). Methionine provides a less rigid packing of the hydrophobic core (Gassner et al. 1996) and is expected to improve the dynamics of the cold-adapted enzyme, whereas the low Met content in *Tth*-MCO could contribute to its thermal stability. Finally, the aliphatic index increases from *Pha*MOx to *Tth*-MCO, suggesting an increasing involvement of non-polar side chains to stability via improvement of the hydrophobic effect (Kumar and Nussinov 2001).

Structural stability recorded by microcalorimetry

Thermal stability of the cuproxidases in their holo and apo forms was studied by differential scanning calorimetry (DSC). Thermograms obtained for holoenzymes were distorted by a downward drift of the microcalorimetric signal after the transition due to protein aggregation, possibly promoted by the copper ions released during unfolding. Addition of NDSB, a non-detergent sulfobetaine that delays protein aggregation (Collins et al. 2006; D'Amico and Feller 2009), improved the microcalorimetric signals to a certain extent but still only allowed for estimations of the apparent T_m (Table 3). In contrast, apoenzymes displayed clear microcalorimetric signals in presence of NDSB (Fig. 2) and allowed determination of the microcalorimetric parameters (Table 3). Denaturation was irreversible in all cases and, therefore, prevented a thermodynamic analysis of unfolding. *Pha*MOx is the least stable

Table 3 Microcalorimetric parameters for cuproxidase unfolding

Oxidase	Apoenzyme			Holoenzyme T_m (°C)	ΔT_m (holo–apo) (°C)
	T_m (°C)	ΔH_{cal} (kcal mol^{-1})	$\Sigma\ \Delta H_{cal}$ (kcal mol^{-1})		
*Pha*MOx	54.2	178	178	58.2	4.0
CueO	61.8	355	355	79.4	17.6
Tth-MCO	83.4	183	436	111.8	28.4
	96.7	115			
	111.8	138			

Errors are ±0.2 °C on T_m and ±5 % on ΔH_{cal}

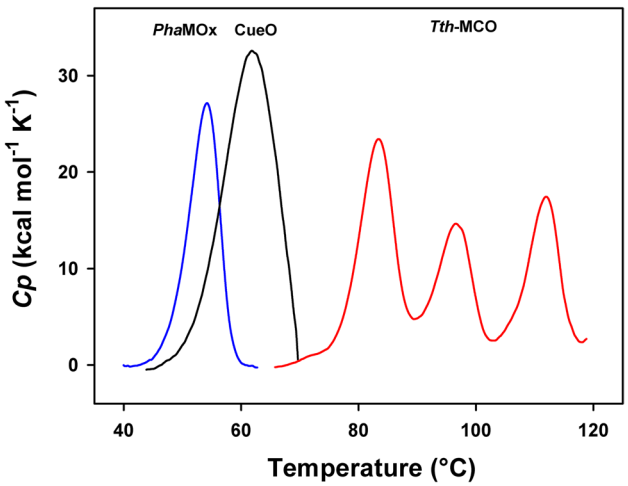

Fig. 2 Differential scanning calorimetry of the homologous cuproxidase apoenzymes in 30 mM MOPS, 1 M NDSB, pH 7.0

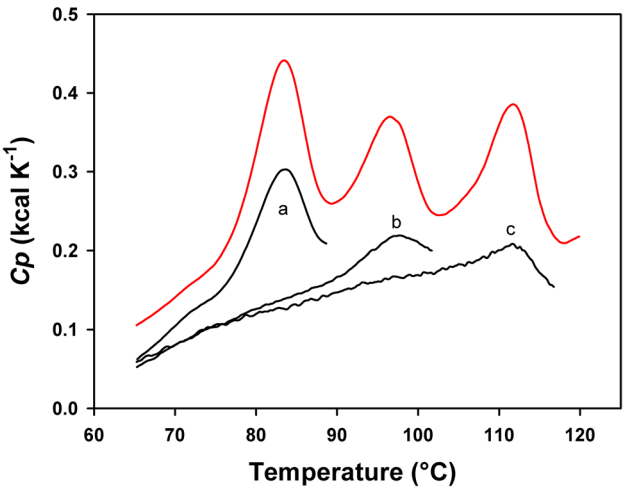

Fig. 3 Sequential unfolding of *Tth*-MCO domains. Upper trace: raw DSC thermogram of Apo *Tth*-MCO full unfolding. **a** Thermogram interrupted after the first transition and cooled to 15 °C. **b** Rescan of the same sample interrupted after the second transition and cooled. **c** Rescan of the same sample

protein followed by CueO and *Tth*-MCO, as both T_m and the calorimetric enthalpy (ΔH_{cal}) increase on going from the cold-adapted protein to the heat-stable homolog. The parameter ΔH_{cal} (calculated from the area under the transition) records the total amount of heat required to disrupt all enthalpy-driven interactions during unfolding. Surprisingly, the *Tth*-MCO apoenzyme displays three well-resolved transitions. These three completely independent stability domains are reminiscent of the three cupredoxin structural domains forming an MCO. This is further supported by the possibility of sequentially unfolding these domains by cooling the sample after each transition, before a new up-scan (Fig. 3). This is in line with previous reports showing a gain in unfolding cooperativity mediated by copper cofactors at the interface of the cupredoxin domains in MCOs (Koroleva et al. 2001; Sedlak et al. 2008). Table 3 also shows the gain in stability (ΔT_m holo–apo) induced by binding of the copper cofactors. These differences in melting point temperatures basically reflect the copper binding strength (Brandts and Lin 1990), which increases on going from the psychrophilic to the thermophilic enzyme. Such increases in the binding affinity with the environmental temperature are frequently observed in extremophilic proteins (Feller et al. 1999; Feller 2010).

Structural flexibility probed by fluorescence quenching

Fluorescence quenching by acrylamide has been successfully used to probe the molecular permeability or "breathability" of homologous protein structures. As the position of the Trp residues is not strictly conserved in the tertiary structures of the homologous cuproxidases, the variation of quenching with temperature becomes the relevant parameter (Fig. 4). In all extremozymes investigated so far, psychrophilic proteins demonstrated a large quenching effect arising from the deep penetration of the quencher into their flexible structures, whereas thermophilic proteins displayed a weaker quenching effect resulting from their rigid conformation near room temperature (Collins et al. 2003; D'Amico et al. 2003; Georlette et al. 2003; Huston et al. 2008; Xie et al. 2009). However, this pattern is not observed when comparing *Pha*MOx,

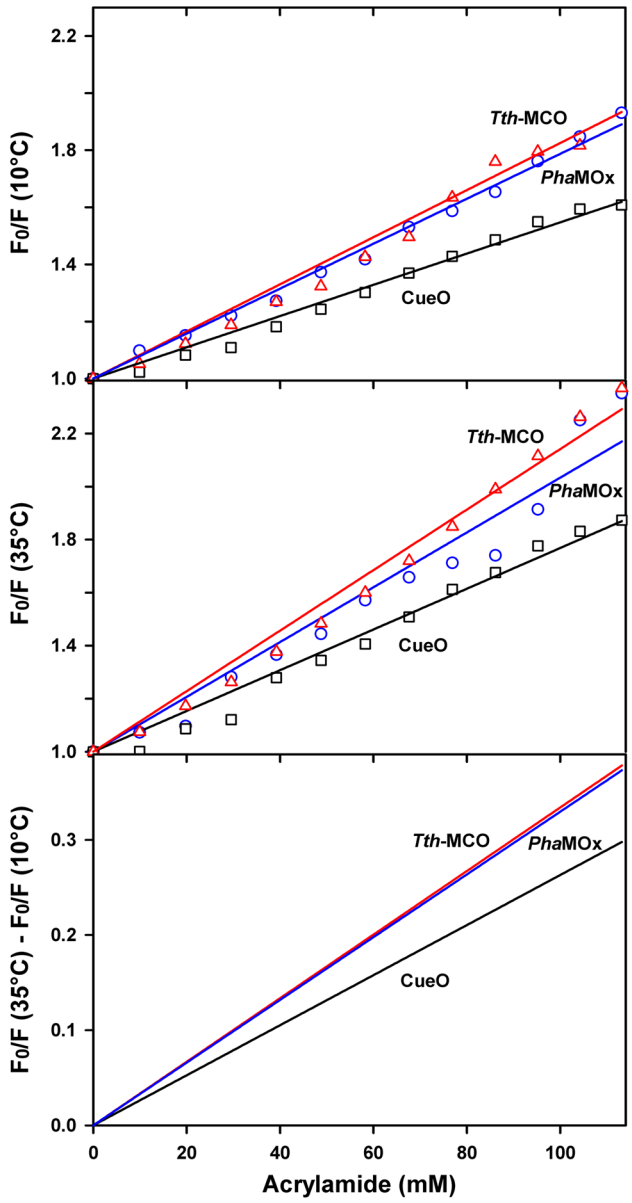

Fig. 4 Stern–Volmer plots of fluorescence quenching by acrylamide. Fluorescence quenching values at 10 °C (*upper panel*) and at 35 °C (*middle panel*) for *Pha*MOx (*circles*), CueO (*squares*), and *Tth*-MCO (*triangles*). *Lower panel* variation of fluorescence quenching between 10 and 35 °C obtained by subtracting the regression lines of the Stern–Volmer plots at individual temperatures

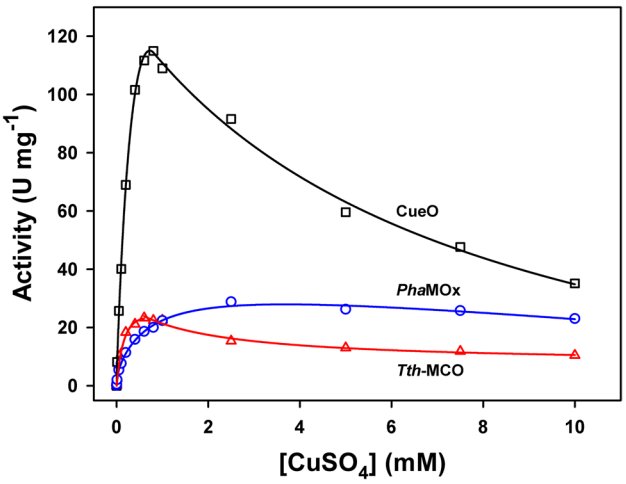

Fig. 5 Specific activity of *Pha*MOx (*circles*), CueO (*squares*), and *Tth*-MCO (*triangles*) on 2,6-dimethoxyphenol as a function of Cu(II) concentration at 25 °C

CueO, and *Tth*-MCO (Fig. 4) as both the cold-adapted and the thermophilic cuproxidases demonstrate an identical quenching effect and a higher flexibility as compared with the mesophilic enzyme. In the case of these MCOs, structural stability (Fig. 2) is not correlated with structural flexibility (Fig. 4) using dynamic quenching of fluorescence, although Trp residues are evenly distributed in the sequences, mostly at conserved positions (Supplementary Fig. S1).

Laccase-like activity of the homologous cuproxidases

Laccase or phenol oxidase activity of cuproxidases is dependent on the presence of a single extra Cu(II) ion which binds in the substrate binding site sCu. The phenol oxidase activity of the three cuproxidases as a function of Cu(II) concentrations was measured in the same conditions, in acetate buffer pH 5.0 at 25 °C with 10 mM 2,6-dimethoxyphenol (2,6-DMP) as substrate (Fig. 5; Table 4). Typically, cold-adapted enzymes are characterized by a high catalytic activity, whereas most thermophilic enzymes are nearly inactive at room temperature. However, in this case, the maximal activity of both the psychrophilic and thermophilic MCOs is similar and lower than that of the mesophilic CueO (Fig. 5). In contrast, the apparent K_d for Cu(II) binding to the sCu site (Table 4) follows the generally observed trend for extremophilic proteins: a weak binding for the cold-adapted protein, intermediate for the mesophilic CueO, and a stronger binding for the thermophilic protein. Finally, Cu(II) inhibition at high, non-physiological concentrations (Fig. 5), also indicates different interactions between the cupric ion, the substrate, and the cuproxidases, as shown by the strong inhibition of CueO and the moderate inhibition of *Pha*MOx and *Tth*-MCO.

Temperature dependence of activity

The temperature dependence of laccase-like activity with ABTS as substrate (which is less prone to oxidation and precipitation at high temperatures than 2,6-DMP) and in the presence of 1 mM Cu(II) was recorded for the three enzymes (Fig. 6). *Pha*MOx is active at low to moderate temperatures, CueO displays a maximal activity around 80 °C, whereas the maximum is not yet attained for

Table 4 Phenol oxidase activity on 2,6-dimethoxyphenol and apparent dissociation constants for Cu(II) binding to the sCu site at 25 °C

Oxidase	V_{max} (U mg^{-1})	$K_{d,app}$ (μM)
*Pha*MOx	28.8 ± 0.8	334
CueO	117.9 ± 6.2	165
Tth-MCO	23.3 ± 1.2	108

Errors are ±5 % on $K_{d,app}$

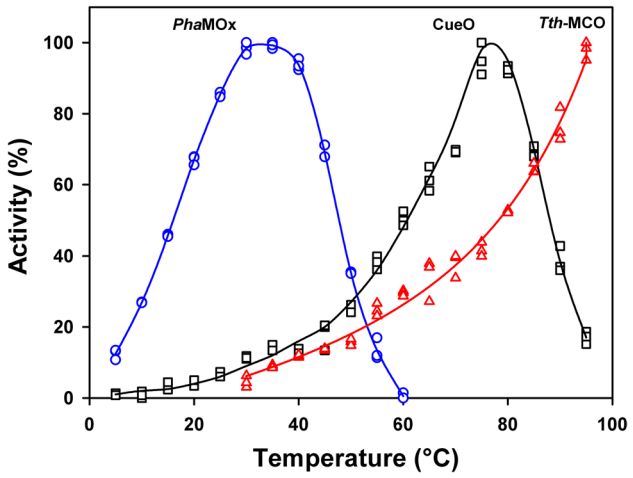

Fig. 6 Temperature dependence of laccase-like activity with ABTS as substrate and 1 mM Cu(II) for *Pha*MOx (*circles*), CueO (*squares*), and *Tth*-MCO (*triangles*)

Tth-MCO below the buffer boiling point. It should be mentioned that the recorded temperature dependence of activity does not reflect the temperature dependence of intrinsic electron transfer in the core enzyme, but rather the effect of temperature on the rate limiting step (electron transfer from the non-natural substrate to the sCu site) and possibly on dioxygen reduction to water. When comparing the temperature dependence of activity (Fig. 6) with the thermal unfolding of holoenzymes (T_m in Table 3), it can be seen that CueO loss of activity is concomitant with unfolding (T_m is close to maximal activity). In contrast, *Pha*MOx thermo-inactivation occurs before any detectable unfolding event is recorded by DSC. This can be related to the above-mentioned weaker copper binding in the redox centers (T1 and TNC) and sCu site in the laccase-like reaction ($K_{d,app}$ in Table 4): around 30 °C slight alterations in the copper chelation geometry impair the electron transfer process.

Discussion

Historically, the very weak temperature dependence of electron transfer in biological systems was discovered by the observation that electron transfer between a cytochrome *c* and a bacteriochlorophyll occurred even at 80 K (Chance and Nishimura 1960). Later, it was proposed that the reaction proceed through quantum mechanical tunneling, which is temperature-independent (DeVault and Chance 1966). According to the Marcus theory (Marcus and Sutin 1985), the rate equation of electron transfer contains an exponential term including *T*, as for any chemical rate constant, but the various parameters involved render this term negligible. Furthermore, in many bacterial redox centers, the rates actually increase slightly as the temperature is lowered, underlining the complexity of such systems. In the case of the extremophilic blue oxidases, it can be postulated that the rate of electron transfer in the core enzyme is also independent of the environmental temperatures, but it should be kept in mind that this assumption is currently not supported by experimental evidences.

In contrast with many previous studies on extremozymes, we have shown here that the stability of the extremophilic cuproxidases examined is correlated with neither activity, nor flexibility. The primary structures display several insights of adaptations linked to thermal stability (Tables 1, 2). As a matter of fact, the microcalorimetric parameters of stability T_m and ΔH_{cal} increase with environmental temperatures (Fig. 2), indicative of an increasing number of stabilizing interactions in the folded structures. Furthermore, the binding affinity of the catalytic coppers also increases from the psychrophilic to the thermophilic MCOs, as inferred from ΔT_m (holo–apo) in Table 3. As all copper ligands are strictly conserved in the three cuproxidases (Supplementary Fig. S1), the structures bearing the redox centers should be responsible for these differences in affinity. In the cold-adapted *Pha*MOx, weaker interactions chelating copper ions in their rigid binding sites would allow lower reorganization energy upon redox changes, still maintaining fast electron transfer reactions at low temperature, whereas strong copper binding by *Tth*-MCO is required for proper functioning at elevated temperatures. The binding affinity of Cu(II) to the substrate site sCu also increases with environmental temperatures (Table 4): a weak binding for the cold-adapted protein that could be related to improved binding site dynamics as shown in other psychrophilic proteins, and a stronger binding for the thermophilic protein arising from the compact conformation of these proteins. Finally, the temperature dependence of activity (Fig. 6) follows the same trend. The above-mentioned parameters are obviously related to the differences in structural stability between the three cuproxidases and follow the canonical pattern generally reported for extremophilic proteins.

All previous studies using acrylamide-induced fluorescence quenching as a probe for flexibility have invariably correlated this parameter with structural stability (Collins

et al. 2003; D'Amico et al. 2003; Georlette et al. 2003; Huston et al. 2008; Xie et al. 2009). In sharp contrast, such correlation is not found in the cuproxidases as flexibility of the cold-adapted *Pha*MOx and of the thermophilic *Tth*-MCO is identical, despite large differences in stability. Two explanations can be proposed for this uncommon observation. First, MCOs catalyze oxidation of reducing substrates by an outer-sphere electron transfer mechanism, and hence, large conformational changes linked to substrate binding, and oxidation is not required. Second, MCOs possess an active site containing accurately bound copper cofactors to exert the oxido-reduction function, substrate oxidation by the T1 site and oxygen reduction to water by the trinuclear cluster. The four conserved copper binding motifs are distributed along the amino acid sequence, and the strict maintenance of the copper ions in their specific binding configurations by a rigid conformation of the coordination sphere (and by extension of the protein matrix) allows low reorganization energy. Therefore, increased global flexibility of the cold-adapted enzyme structure to counterbalance the slowdown of molecular motions at low temperatures seems to be both unnecessary and incompatible with electron transfer catalysis. In this respect, whether the low stability of the psychrophilic cuproxidase originates from the lack of selective pressure or is an essential component for its function remains to be clarified. Furthermore, the phenol oxidase activity is also not correlated with stability as both psychrophilic and thermophilic cuproxidases display similar specific activities at 25 °C (Fig. 5; Table 4). The outer-sphere electron transfer process involved in oxidation of reducing substrates is expected to be unaffected at extreme biological temperatures, therefore explaining that activity of MCOs escape the canonical pattern of extremozymes. However, one cannot exclude that activity on the non-natural phenolic substrate is governed by other factors, such as the accessibility of the sCu site.

These results show that the requirements for enzymatic electron transfer produce a specific adaptive pattern, distinct from that observed in enzymes possessing a well-defined active site and relying on conformational changes such as for the induced fit mechanism. This aspect can potentially explain the non-conventional pattern also reported for other proteins involving electron transfer: the uncoupling between stability and flexibility in a psychrophilic ferricytochrome C_{552} (Oswald et al. 2014); the higher stability of a psychrophilic cytochrome c_5 as compared with its mesophilic homologue (Takenaka et al. 2010); the exceptional heat resistance of a psychrophilic thioredoxin reductase (Falasca et al. 2012); the similar thermal stability of psychrophilic and mesophilic superoxide dismutases (Merlino et al. 2010). In these examples and in the investigated cuproxidases, the strict maintenance of optimal distances between donors and acceptors (amongst other essential parameters for electron transfer) may have driven evolution toward such activity–stability patterns, in the absence of the selective pressure of temperature on electron transfer rates.

Acknowledgments This work was supported by the F.R.S-FNRS, Belgium (Fonds de la Recherche Fondamentale et Collective, contract numbers 2.4535.08, 2.4523.11 and U.N009.13 to G.F.) and by the Belgian program of Interuniversity Attraction Poles (iPros P7/44) initiated by the Federal Office for Scientific, Technical and Cultural Affairs. T.C. thanks the FCT and FEDER (POFC-COMPETE) for funding through the Investigador FCT Programme (IF/01635/2014) and project EngXyl (EXPL/BBB-BIO/1772/2013- FCOMP-01-0124-FEDER-041595) as well as strategic funding via UID/BIA/04050/2013. F.R., A.G. and A.C. were FRIA research fellows.

References

Bello M, Valderrama B, Serrano-Posada H, Rudino-Pinera E (2012) Molecular dynamics of a thermostable multicopper oxidase from *Thermus thermophilus* HB27: structural differences between the apo and holo forms. PLoS One 7:e40700

Blaudeck N, Sprenger GA, Freudl R, Wiegert T (2001) Specificity of signal peptide recognition in Tat-dependent bacterial protein translocation. J Bacteriol 183:604–610

Brandts JF, Lin LN (1990) Study of strong to ultratight protein interactions using differential scanning calorimetry. Biochemistry 29:6927–6940

Chance B, Nishimura M (1960) On the mechanism of chlorophyll-cytochrome interaction: the temperature insensitivity of light-induced cytochrome oxidation in chromatium. Proc Natl Acad Sci USA 46:19–24

Collins T, Meuwis MA, Gerday C, Feller G (2003) Activity, stability and flexibility in glycosidases adapted to extreme thermal environments. J Mol Biol 328:419–428

Collins T, D'Amico S, Georlette D, Marx JC, Huston AL, Feller G (2006) A nondetergent sulfobetaine prevents protein aggregation in microcalorimetric studies. Anal Biochem 352:299–301

Cortes L, Wedd AG, Xiao Z (2015) The functional roles of the three copper sites associated with the methionine-rich insert in the multicopper oxidase CueO from *E. coli*. Metallomics 7:776–785

D'Amico S, Feller G (2009) A nondetergent sulfobetaine improves protein unfolding reversibility in microcalorimetric studies. Anal Biochem 385:389–391

D'Amico S, Marx JC, Gerday C, Feller G (2003) Activity-stability relationships in extremophilic enzymes. J Biol Chem 278:7891–7896

Deming JW (2002) Psychrophiles and polar regions. Curr Opin Microbiol 5:301–309

DeVault D, Chance B (1966) Studies of photosynthesis using a pulsed laser. I. Temperature dependence of cytochrome oxidation rate in chromatium. Evidence for tunneling. Biophys J 6:825–847

Djoko KY, Chong LX, Wedd AG, Xiao Z (2010) Reaction mechanisms of the multicopper oxidase CueO from *Escherichia coli* support its functional role as a cuprous oxidase. J Am Chem Soc 132:2005–2015

Falasca P, Evangelista G, Cotugno R, Marco S, Masullo M, De Vendittis E, Raimo G (2012) Properties of the endogenous components of the thioredoxin system in the psychrophilic eubacterium *Pseudoalteromonas haloplanktis* TAC 125. Extremophiles 16:539–552

Feller G (2010) Protein stability and enzyme activity at extreme biological temperatures. J Phys-Condens Mat 22:323101. doi:10.1088/0953-8984/1022/1032/323101

Feller G (2013) Psychrophilic enzymes: from folding to function and biotechnology. Scientifica 2013:512840. doi:10.1155/2013/512840

Feller G, Gerday C (2003) Psychrophilic enzymes: hot topics in cold adaptation. Nat Rev Microbiol 1:200–208

Feller G, d'Amico D, Gerday C (1999) Thermodynamic stability of a cold-active α-amylase from the Antarctic bacterium *Alteromonas haloplanctis*. Biochemistry 38:4613–4619

Gassner NC, Baase WA, Matthews BW (1996) A test of the "jigsaw puzzle" model for protein folding by multiple methionine substitutions within the core of T4 lysozyme. Proc Natl Acad Sci USA 93:12155–12158

Georlette D, Damien B, Blaise V, Depiereux E, Uversky VN, Gerday C, Feller G (2003) Structural and functional adaptations to extreme temperatures in psychrophilic, mesophilic, and thermophilic DNA ligases. J Biol Chem 278:37015–37023

Huston AL, Haeggstrom JZ, Feller G (2008) Cold adaptation of enzymes: structural, kinetic and microcalorimetric characterizations of an aminopeptidase from the Arctic psychrophile *Colwellia psychrerythraea* and of human leukotriene A(4) hydrolase. Biochim Biophys Acta 1784:1865–1872

Kim C, Lorenz WW, Hoopes JT, Dean JF (2001) Oxidation of phenolate siderophores by the multicopper oxidase encoded by the *Escherichia coli yacK* gene. J Bacteriol 183:4866–4875

Kohen A, Cannio R, Bartolucci S, Klinman JP (1999) Enzyme dynamics and hydrogen tunnelling in a thermophilic alcohol dehydrogenase. Nature 399:496–499

Koroleva OV, Stepanova EV, Binukov VI, Timofeev VP, Pfeil W (2001) Temperature-induced changes in copper centers and protein conformation of two fungal laccases from *Coriolus hirsutus* and *Coriolus zonatus*. Biochim Biophys Acta 1547:397–407

Kumar S, Nussinov R (2001) How do thermophilic proteins deal with heat? Cell Mol Life Sci 58:1216–1233

Lee DY, Kim KA, Yu YG, Kim KS (2004) Substitution of aspartic acid with glutamic acid increases the unfolding transition temperature of a protein. Biochem Biophys Res Commun 320:900–906

Marcus RA, Sutin N (1985) Electron transfers in chemistry and biology. Biochim Biophys Acta 811:265–322

Medigue C, Krin E, Pascal G, Barbe V, Bernsel A, Bertin PN, Cheung F, Cruveiller S, D'Amico S, Duilio A, Fang G, Feller G, Ho C, Mangenot S, Marino G, Nilsson J, Parrilli E, Rocha EP, Rouy Z, Sekowska A, Tutino ML, Vallenet D, von Heijne G, Danchin A (2005) Coping with cold: the genome of the versatile marine Antarctica bacterium *Pseudoalteromonas haloplanktis* TAC125. Genome Res 15:1325–1335

Merlino A, Russo Krauss I, Castellano I, De Vendittis E, Rossi B, Conte M, Vergara A, Sica F (2010) Structure and flexibility in cold-adapted iron superoxide dismutases: the case of the enzyme isolated from *Pseudoalteromonas haloplanktis*. J Struct Biol 172:343–352

Miyazaki K (2005) A hyperthermophilic laccase from *Thermus thermophilus* HB27. Extremophiles 9:415–425

Mrabet NT, Van den Broeck A, Van den Brande I, Stanssens P, Laroche Y, Lambeir AM, Matthijssens G, Jenkins J, Chiadmi M, van Tilbeurgh H et al (1992) Arginine residues as stabilizing elements in proteins. Biochemistry 31:2239–2253

Mykytczuk NC, Foote SJ, Omelon CR, Southam G, Greer CW, Whyte LG (2013) Bacterial growth at −15 degrees C; molecular insights from the permafrost bacterium *Planococcus halocryophilus* Or1. ISME J 7:1211–1226

Oswald VF, Chen W, Harvilla PB, Magyar JS (2014) Overexpression, purification, and enthalpy of unfolding of ferricytochrome c_{552} from a psychrophilic microorganism. J Inorg Biochem 131:76–78

Roberts SA, Weichsel A, Grass G, Thakali K, Hazzard JT, Tollin G, Rensing C, Montfort WR (2002) Crystal structure and electron transfer kinetics of CueO, a multicopper oxidase required for copper homeostasis in *Escherichia coli*. Proc Natl Acad Sci USA 99:2766–2771

Schiffer CA, Dotsch V (1996) The role of protein-solvent interactions in protein unfolding. Curr Opin Biotechnol 7:428–432

Sedlak E, Ziegler L, Kosman DJ, Wittung-Stafshede P (2008) In vitro unfolding of yeast multicopper oxidase Fet3p variants reveals unique role of each metal site. Proc Natl Acad Sci USA 105:19258–19263

Siddiqui KS, Cavicchioli R (2006) Cold-adapted enzymes. Annu Rev Biochem 75:403–433

Singh SK, Roberts SA, McDevitt SF, Weichsel A, Wildner GF, Grass GB, Rensing C, Montfort WR (2011) Crystal structures of multicopper oxidase CueO bound to copper(I) and silver(I): functional role of a methionine-rich sequence. J Biol Chem 286:37849–37857

Solomon EI, Sundaram UM, Machonkin TE (1996) Multicopper oxidases and oxygenases. Chem Rev 96:2563–2606

Solomon EI, Augustine AJ, Yoon J (2008) O_2 reduction to H_2O by the multicopper oxidases. Dalton Trans 30:3921–3932

Sterner R, Kleemann GR, Szadkowski H, Lustig A, Hennig M, Kirschner K (1996) Phosphoribosyl anthranilate isomerase from *Thermotoga maritima* is an extremely stable and active homodimer. Protein Sci 5:2000–2008

Struvay C, Feller G (2012) Optimization to low temperature activity in psychrophilic enzymes. Int J Mol Sci 13:11643–11665

Suhre K, Claverie JM (2003) Genomic correlates of hyperthermostability, an update. J Biol Chem 278:17198–17202

Takai K, Nakamura K, Toki T, Tsunogai U, Miyazaki M, Miyazaki J, Hirayama H, Nakagawa S, Nunoura T, Horikoshi K (2008) Cell proliferation at 122 degrees C and isotopically heavy CH_4 production by a hyperthermophilic methanogen under high-pressure cultivation. Proc Natl Acad Sci USA 105:10949–10954

Takenaka S, Wakai S, Tamegai H, Uchiyama S, Sambongi Y (2010) Comparative analysis of highly homologous *Shewanella* cytochromes c_5 for stability and function. Biosci Biotechnol Biochem 74:1079–1083

Tosco A, Birolo L, Madonna S, Lolli G, Sannia G, Marino G (2003) GroEL from the psychrophilic bacterium *Pseudoalteromonas haloplanktis* TAC 125: molecular characterization and gene cloning. Extremophiles 7:17–28

Vieille C, Zeikus GJ (2001) Hyperthermophilic enzymes: sources, uses, and molecular mechanisms for thermostability. Microbiol Mol Biol Rev 65:1–43

Xie BB, Bian F, Chen XL, He HL, Guo J, Gao X, Zeng YX, Chen B, Zhou BC, Zhang YZ (2009) Cold adaptation of zinc metalloproteases in the thermolysin family from deep sea and arctic sea ice bacteria revealed by catalytic and structural properties and molecular dynamics: new insights into relationship between conformational flexibility and hydrogen bonding. J Biol Chem 284:9257–9269

Supplementary Material to

Activity-stability relationships revisited in blue oxidases catalyzing electron transfer at extreme temperatures

Frédéric Roulling[1], Amandine Godin[1], Alexandre Cipolla[1], Tony Collins[2], Kentaro Miyazaki[3] and Georges Feller[1*]

[1]Laboratory of Biochemistry, Center for Protein Engineering, University of Liège, Liège, Belgium

[2]Centre of Molecular and Environmental Biology, Department of Biology, University of Minho, Braga, Portugal

[3]Department of Life Science and Biotechnology, Bioproduction Research Institute, National Institute of Advanced Industrial Science and Technology (AIST), Tsukuba, Ibaraki, Japan

* For correspondence E-mail gfeller@ulg.ac.be; Tel. +32 4 366 33 43; Fax +32 4 366 33 64

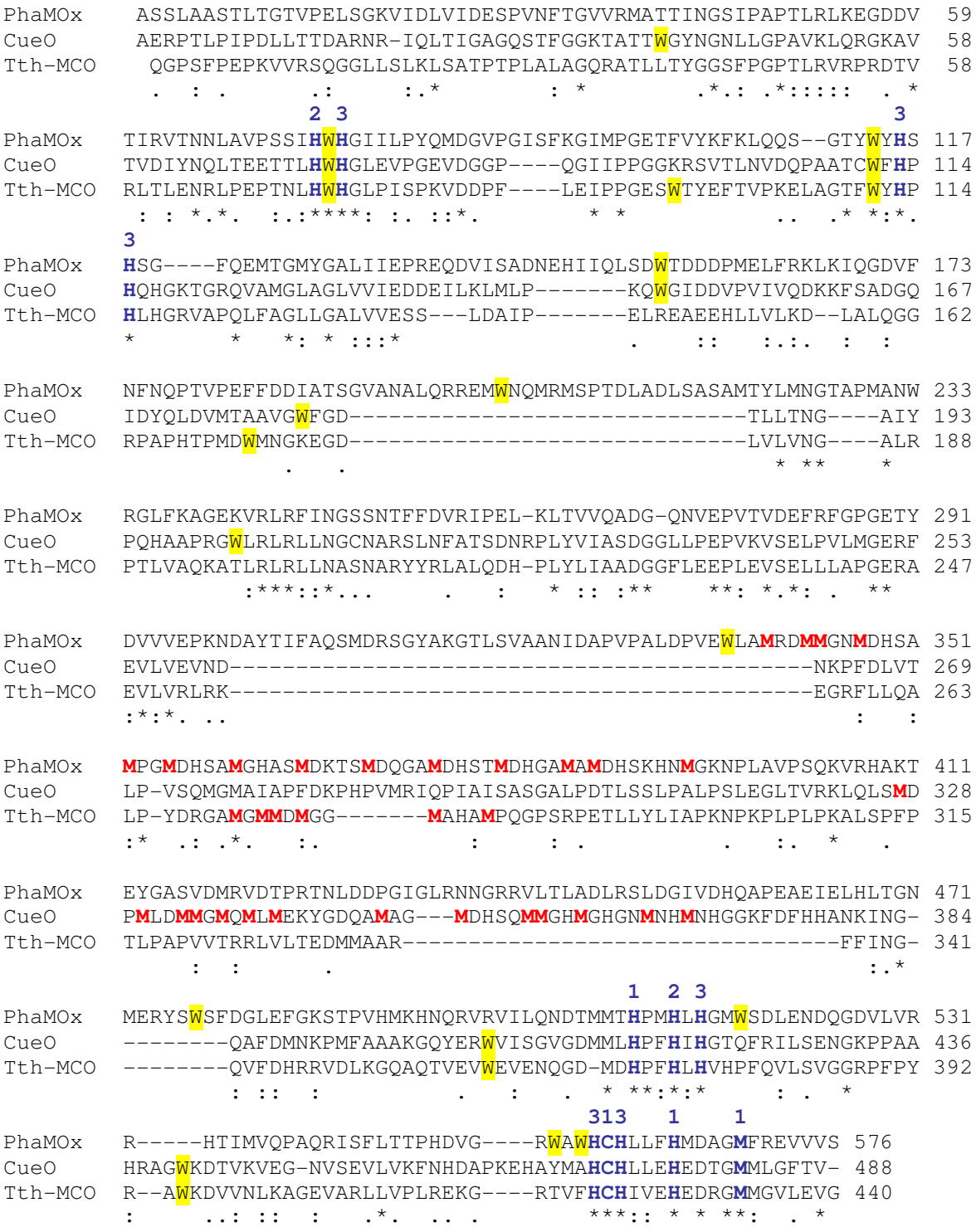

Supplementary Figure S1: Amino acid sequence alignment of the blue oxidase mature forms. Ligands of the four catalytic coppers and spectroscopic copper types are indicated in blue. Methionine residues in the Met-rich loops are indicated in red and tryptophan residues probed by fluorescence quenching are in yellow.

Chapter IV – Results

Function and versatile location of Met-rich inserts in blue oxidases involved in bacterial copper resistance

Roulling F, Godin A, Feller G. Function and versatile location of Met-rich inserts in blue oxidases involved in bacterial copper resistance. Biochimie 2022;194:118-126.

Biochimie 194 (2022) 118–126

Contents lists available at ScienceDirect

Biochimie

journal homepage: www.elsevier.com/locate/biochi

Function and versatile location of Met-rich inserts in blue oxidases involved in bacterial copper resistance

Frédéric Roulling, Amandine Godin, Georges Feller*

Laboratory of Biochemistry, Center for Protein Engineering - InBioS, University of Liège, Belgium

ARTICLE INFO

Article history:
Received 11 August 2021
Received in revised form
7 December 2021
Accepted 29 December 2021
Available online 1 January 2022

Keywords:
Multicopper oxidase
Cuproxidases
CueO
Copper resistance
Laccase
Extremophiles

ABSTRACT

Cuproxidases form a subgroup of the blue multicopper oxidase family. They display disordered methionine-rich loops, not observable in most available crystal structures, which have been suggested to bind toxic Cu(I) ions before oxidation into less harmful Cu(II) by the core enzyme. We found that the location of the Met-rich regions is highly variable in bacterial cuproxidases, but always inserted in solvent exposed surface loops, at close proximity of the conserved T1 copper binding site. We took advantage of the large differences in loop length between cold-adapted, mesophilic and thermophilic oxidase homologs to unravel the function of the methionine-rich regions involved in copper detoxification. Using a newly developed anaerobic assay for cuprous ions, it is shown that the number of Cu(I) bound is nearly proportional to the loop lengths in these cuproxidases and to the number of potential Cu(I) ligands in these loops. In order to substantiate this relation, the longest loop in the cold-adapted oxidase was deleted, lowering bound extra Cu(I) from 9 in the wild-type enzyme to 2–3 Cu(I) in deletion mutants. These results demonstrate that methionine-rich loops behave as molecular octopus scavenging toxic cuprous ions in the periplasm and that these regions are essential components of bacterial copper resistance.

1. Introduction

Since the advent of dioxygen produced by cyanobacteria about 10^9 years ago, copper has become an essential element for most living organisms. Indeed, oxidation of water-insoluble Cu(I), mainly in the form of sulfides, has provided soluble and more bioavailable Cu(II), which was ideally suited to exploit the oxidizing power of dioxygen [1,2]. The redox properties of the Cu(I)/Cu(II) couple make it an invaluable cofactor in proteins for electronic transfer process or redox transformation but are also responsible for severe hazards to the cell, for example by generating highly toxic hydroxyl radical in a Fenton-like reaction [3]. Moreover, copper can bind non-specifically to proteins or replace other metallic cofactors therefore impairing protein function [4,5]. Organisms have evolved several systems to finely control cellular copper levels and to resist to elevated concentrations in their environment mainly by the use of pumps and metallochaperones [2]. One of them, the Cue system (Cu efflux) was first discovered in *Escherichia coli* and, with the high number of genome sequences now available, it is considered widespread in aerobic Gram-negative bacteria [6]. This system consists of a copper responsive element, CueR, that can activate the expression of CopA, a transmembrane P-type ATPase which pumps Cu(I) from the cytoplasm into the periplasm, and of CueO (Cu efflux oxidase), a periplasmic multicopper oxidase which converts Cu(I) into the less toxic Cu(II) [7].

Multicopper oxidases (MCOs) are blue enzymes that catalyze the one-electron oxidation of various substrates and the concomitant four-electron reduction of dioxygen to water, the latter activity being only shared with terminal oxidases [8]. Their mechanism of action is based on an active site of four copper ions classified into three main copper spectroscopic types (Figs. 1 and 2). Substrates bind near the T1 site, responsible for the blue color, which transfers electrons to the trinuclear center (TNC), unique to MCOs and formed by a binuclear T3 site and a T2 copper, where oxygen is reduced to water [8]. Metallo-oxidases are a subset of the

Abbreviations: CueO, cuproxidase from *E. coli*; *Tth*-MCO, cuproxidase from the thermophile *Thermus thermophilus*; *Pha*MOx, cuproxidase from the psychrophile *Pseudoalteromonas haloplanktis*; DSC, differential scanning calorimetry.

* Corresponding author. Laboratory of Biochemistry, Institute of Chemistry B6a, B-4000, Liège-Sart Tilman, Belgium.
E-mail address: gfeller@uliege.be (G. Feller).

https://doi.org/10.1016/j.biochi.2021.12.015
0300-9084/

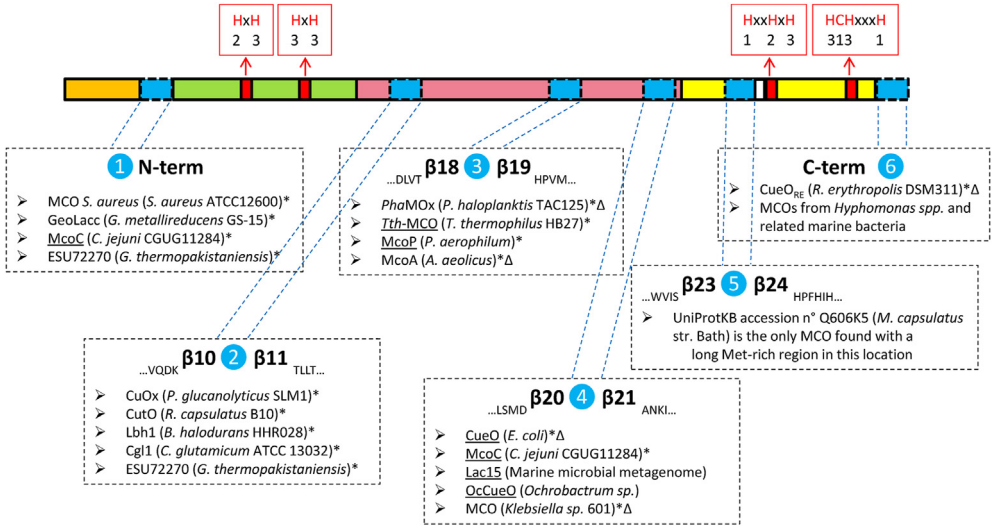

Fig. 1. Primary structure organization in cuproxidases. The six possible locations (in blue) for insertion of Met-rich loops depicted in a schematic view of CueO primary structure. Signal peptide in orange. Cupredoxin domains 1, 2 and 3 in green, pink and yellow, respectively. The four ultra-conserved catalytic copper binding sites are located in red. Red boxes indicate the copper chelating residues in red and the numbers refer to the spectroscopic copper types. The sequence directly preceding the third conserved catalytic copper binding site and consisting of D and/or M and/or H residues specific to cuproxidases and forming the inner part of the sCu binding site is in white. Blue boxes and numbers in blue circles indicate the six loop locations where a Met-rich region can be found in different cuproxidases. The numbering of β-sheets is based on CueO structure 3OD3 and the four residues of each extremity of β-sheets in CueO framing the insertion loops are indicated in subscript for clarity (see Figs. S1 and S2). Selected examples of cuproxidases are indicated for each location. The asterisk * indicates that this MCO has been characterized and at least one publication is available. The delta symbol Δ indicates that a mutant where the Met-rich region has been (partially) deleted or mutated was constructed and characterized. The six cuproxidases for which a crystal structure is available are underlined.

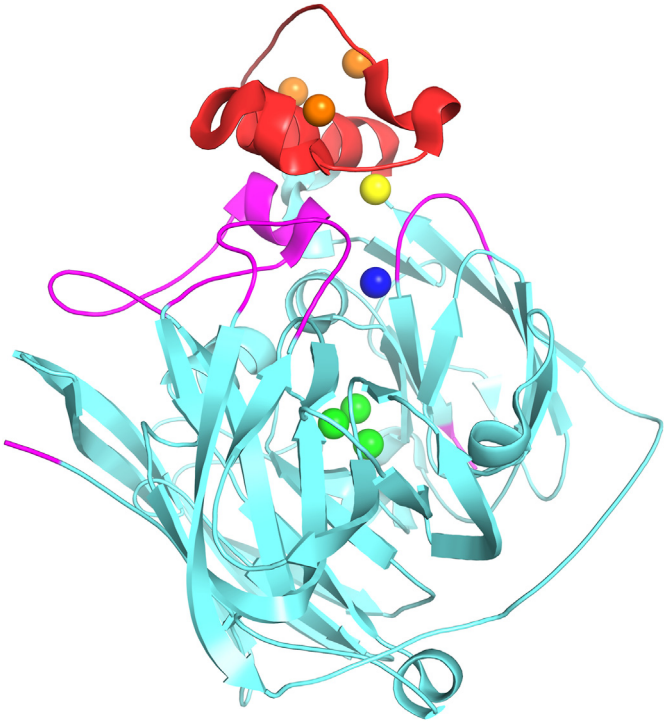

Fig. 2. Ribbon diagram of CueO from *E. coli*. In red, the Met-rich insert in CueO and in magenta, the solvent-exposed loops in which the Met-rich insert has been found in other bacterial cuproxidases. Note the proximity with the blue T1 site. Spheres represent bound copper ions with color code: blue, the T1 Cu; green, the trinuclear center; yellow, the sCu and orange, Cu(I) on the Met-rich region. The N-terminus (magenta) is in front, left and the C-terminus (magenta) is behind the structure. Figure based on PDB entries 3OD3 and 3NT0.

MCO family in which substrates are low-valent first-row transition metal ions such as Fe(II), Cu(I) and/or Mn(II) [9–11]. This subset includes cuproxidases (cuprous oxidases) and the well-studied ferroxidases (ferrous oxidases) Fet3p from yeast and human ceruloplasmin that illustrate the biological connection of copper to iron, making the former metal mandatory to aerobic metabolism of the latter in eukaryotes [12].

The structure of CueO (the cuproxidase from *E. coli*) displays the general fold of MCOs, consisting of three repeated beta-stranded cupredoxin domains, with an additional methionine-rich (Met-rich) region (Fig. 2) that restricts accessibility to the T1 site and confers specificity for Cu(I) [13]. This striking feature contrasts with other MCOs such as laccase or ascorbate oxidase where a depression near the T1 site creates a substrate specific site for phenolic compounds or ascorbic acid, respectively [14]. Met-rich regions are associated with several proteins involved in copper management and homeostasis, notably the high affinity copper transporters (Ctr) widely conserved from yeast to human. Recent structural and functional analysis of CueO showed that its Met-rich region provides additional Cu(I) binding sites, one of which is the sCu site (s standing for substrate). According to the reaction mechanism proposed for CueO, Cu(I) ions are gathered via the methionine-rich region, mainly a disordered loop, and the adjacent substrate binding site (sCu). The latter is buried underneath the protein surface and H-bonded to the T1 site, suggesting an electron transfer pathway from sCu to the T1 site and then to the TNC where oxygen is reduced to water [8,14,15]. The Cu(I) binding sites in the Met-rich region have been described as substrate-docking-oxidation sites, whereas the sCu site connects surface-exposed sites to the catalytic T1 site [15]. However, both the length and composition of the Met-rich insert are highly variable in other bacterial cuproxidases [16,17] but this aspect has not been investigated so far.

We report here the characterization of blue multicopper oxidases produced by bacteria living in different temperature niches. To conduct investigations on the function of Met-rich regions in bacterial MCOs, three model enzymes were chosen: CueO from the mesophilic bacterium *Escherichia coli* [13] because this enzyme has been extensively studied and its 3D-structure determined [14,18],

the thermophilic *Tth*-MCO, the corresponding MCO from *Thermus thermophilus* HB27 [19,20] and *Pha*MOx, a new psychrophilic (cold-adapted) MCO encoded in the genome of the Antarctic bacterium *Pseudoalteromonas haloplanktis* TAC125 [21,22]. The three enzymes are homologous periplasmic cuproxidases with laccase-like activity. Taking advantage of the large loop length differences in extremophilic cuproxidases and by mutagenesis of *Pha*MOx, we show here that the number of Cu(I) bound is nearly proportional to the size of the Met-rich loops and to the number of potential Cu(I) ligands (Met, His, Asp) and propose that these flexible loops behave as molecular octopus, scavenging toxic cuprous ions in the periplasm.

2. Materials and methods

2.1. Construction of expression plasmids and mutagenesis

Genomic DNA was extracted from a batch culture of *P. haloplanktis* TAC125 or *E. coli* JM109 using the Promega wizard genomic DNA purification kit. The coding sequences were PCR-amplified using Vent$_R$ Thermopol Polymerase (New England Biolabs), with the forward primers containing a *Nco*I site and the reverse primers containing a *Xho*I site and the stop codon (Table S1). The PCR products were cloned into the pSP73 cloning vector (Stratagene), excised with *Nco*I and *Xho*I and ligated into the pET28a (+) vector (Novagen). Mutants of *Pha*MOx were obtained using inverse PCR with the pET28a plasmid harboring the *Pha*MOx coding sequence as template and primers listed in Table S1. The resulting recombinant plasmids were transformed into *E. coli* BL21 (DE3) cells (Stratagene). Plasmid pTL1 harboring the *Tth*-MCO coding sequence was obtained as previously described [19].

2.2. Production and purification of recombinant PhaMOx, CueO, Tth-MCO and mutants of PhaMOx

Single colonies of *E. coli* BL21 (DE3) cells transformed with the pET28a vector carrying the MCO gene were used to inoculate a 30 ml preculture in LB containing 50 μg ml^{-1} kanamycin at 37 °C. This preculture was used to inoculate 330 ml of Terrific broth (12 g l^{-1} Bacto tryptone (Difco), 24 g l^{-1} yeast extract (Difco), 4 ml l^{-1} glycerol, 12.54 g l^{-1} K_2HPO_4, 2.31 g l^{-1} KH_2PO_4, pH 7.2) containing 50 μg ml^{-1} kanamycin in 2-L flasks. The cultures were incubated at 37 °C and 250 rpm until an absorbance at 600 nm reached about 5. Expression of the enzymes was induced with 0.1 mM isopropyl-1-thio-β-galactopyranoside. Following a further 20-h incubation at 18 °C, the cells were harvested by centrifugation at 10,000×*g* for 30 min at 4 °C, resuspended in 50 mM Tris, pH 8.0 supplemented with protease inhibitors (Complete EDTA-free, Roche) and disrupted in a prechilled high-pressure cell disrupter (EmulsiFlex-C3, Avestin). Cell debris were removed by centrifugation at 40,000×*g* for 30 min at 4 °C. Supernatants were supplemented with Benzonase and $MgCl_2$ and dialyzed overnight against 50 mM Tris, 1 mM $CuSO_4$, 1 mM PMSF, pH 8.0. The dialysate, which had turned blue, was then loaded on a Q-Sepharose Fast Flow (GE Healthcare) column equilibrated in 50 mM Tris, 1 mM PMSF, pH 8.0 and eluted using a linear gradient from 0 to 300 mM NaCl in the buffer. Active fractions were pooled and dialyzed against 50 mM acetate, 1 mM PMSF, pH 5.0. After centrifugation, the sample was loaded on a S-Sepharose Fast Flow (GE Healthcare) column equilibrated in the same buffer and eluted with a linear gradient (0–300 mM NaCl). Active fractions were dialyzed against 10 mM K_2HPO_4, 1 mM PMSF, pH 7.0 and further purified on a Hydroxyapatite column (Bio-Rad) using a linear gradient from 10 to 300 mM K_2HPO_4. Active fractions were pooled, dialyzed against 50 mM Tris, pH 8.0 and concentrated using an Amicon ultrafiltration device with a 10 kDa cut-off membrane (Millipore). CueO was purified as described [36], except that all steps were carried out at 4 °C and *Tth*-MCO was purified as previously described [19]. Protein concentration was determined by the Bradford assay using bovine serum albumin as a standard.

2.3. Copper loading

All enzymes preparations were loaded with a 15-fold excess of Cu(I) and excess was removed with PD10 columns (Amersham). Cu(I) was added from a 20 mM stock solution of [Cu(I) $(MeCN)_4$]PF_6 complex in acetonitrile. Holoenzymes were used in all experiments, except differential scanning calorimetry (see below). Copper content of enzymes samples was determined by the 2,2′-biquinoline method [32]. Hydroxylamine was added in the detection reagent for the determination of total copper, while it was omitted for the determination of copper present as cuprous state in the sample, referred to as “Cu total” and “Cu(I)”, respectively, in the measurements results.

2.4. Copper binding assay

Cu(I) binding capacity of the holoenzymes was determined in a similar manner as for the preparation of the holoenzymes but in fully anaerobic conditions. The experiment was carried out under N_2 atmosphere in an inflatable glove bag (Cole-Parmer). Aqueous solutions were degassed by bubbling with N_2 gas overnight prior transfer to the inflatable glove bag. Holoenzymes were diluted at 15 μM in 50 mM Tris, pH 8 and Cu(I) was added at a final concentration of 225 μM from a 20 mM stock solution of [Cu(I) $(MeCN)_4$] PF_6 complex in acetonitrile. The enzyme solution was incubated for 1 min and then applied to a PD10 column previously equilibrated in freshly prepared 50 mM Tris, 5 mM ascorbic acid, pH 8. Ascorbic acid was added in the degassed buffer solution just prior use from a freshly prepared 500 mM stock solution made inside the glove bag using degassed water. The column was directly eluted with the same strongly-reducing buffer and the elution was collected in several fractions in order to separate the late-eluting protein-containing fractions from the early-eluting excess-copper-containing fractions. Protein-containing fractions were then directly subjected to copper content determination.

2.5. Analytical procedures

N-terminal amino acid sequence of the recombinant enzymes was determined by automated Edman degradation using a pulsed-liquid-phase protein sequencer Procise 494 (Applied Biosystems). Mass determination was performed on an ESI-Q-TOF instrument (Waters, Micromass) in positive ion mode. Samples (10 μM) were analyzed in 30% acetonitrile, 0.5% formic acid, 25 mM ammonium acetate. Spectra deconvolution technique of calculation was the maximum entropy (Max ent1). Circular dichroism spectra of the holoenzymes were recorded using a Jasco J-810 spectropolarimeter under constant nitrogen flow. Spectra in the far UV were recorded at 20 °C in a 0.1 cm quartz cell at a protein concentration of ~100 μg ml^{-1} in 50 mM Tris, pH 7.5. For near UV spectra, 1 mg ml^{-1} concentration and 1 cm optical path length were used. Spectra were averaged over five scans and corrected for the buffer signal. Differential scanning calorimetry experiments carried out with apoenzymes and laccase-like activity tests using 2,6-dimethoxyphenol as substrate were performed as described previously [22].

3. Results

3.1. Location of the Met-rich region in bacterial cuproxidases

In order to compare the three investigated cuproxidases *Pha*-MOx, CueO and *Tth*-MCO with previously characterized bacterial homologs, a search was performed in the literature for MCOs displaying a Met-rich region, or involved in copper resistance, or experimentally confirmed as having a cuproxidase activity. This subset of 34 homologs included 6 cuproxidases for which a 3D structure has been solved (Table S2). They belong to both Gram negative and positive bacteria and are mainly secreted via the Tat (Twin-arginine translocation) export machinery specialized in the transport of folded and cofactor-containing proteins across the cytoplasmic membrane of prokaryotes [23]. However, some are Sec-dependently translocated according to the SignalP-5.0 analysis (Table S2) and as already reported [24]. The multiple sequence alignment of these homologs (Fig. S1) combined with the structural alignment of the 6 crystal structures (Fig. S2) allowed to locate the Met-rich regions within the secondary structures. The most interesting result was the position of the Met-rich region in these bacterial MCOs, which is highly variable in the sequence and frequently differs from the canonical position in CueO. In total, 5 different Met-rich region locations were identified (Fig. 1). To further reinforce this result, additional BLAST searches were performed with the purpose of exploring the vast amount of bacterial MCOs sequences available, particularly those displaying a long Met-rich region in their primary structure. Consequently, a new sequence alignment made of the 34 MCOs enriched with a selection of additional sequences discovered from the BLAST searches allowed to confirm the different possible locations - and also to highlight the variable amino acid composition - of the Met-rich region in 93 homologs (Fig. S3). Interestingly, a sixth Met-rich region location was found in this alignment, but in a single MCO sequence from the obligate methanotroph *Methylococcus capsulatus* str. Bath (Fig. S3). As shown in Fig. 2, based on crystal structures of CueO, the identified Met-rich regions are inserted at positions corresponding to 6 different solvent exposed surface loops in CueO, 4 framed by beta-sheets, and 2 as tails at the N-terminus and at the C-terminus, all being located at close proximity of the strictly conserved T1 copper binding site. In contrast to CueO depicted in Fig. 2, the long N-terminus loop of McoC, which contains the Met-rich region, extends toward the T1 site in the crystal structure [25]. In *R. erythropolis* and various actinobacteria, the Met-rich region is a C-terminal tail which was modelled and was found to point towards the T1 site [26].

Several MCOs possess two Met-rich-regions, such as in McoC [25] with one at the N-terminus and one in the Met-rich region 4. Various MCO sequences from marine bacteria (*Hyphomonas* spp., *Hirschia maritima*, *Henriciella marina*, *Oceanicaulis alexandrii*, *Maricaulis maris*) were found to have a long C-terminal Met-rich region, but also a long Met-rich region in position 3 or 4 (Fig. S3). A common observation on the Met-rich inserts was that they are composed by a conserved or semi-conserved motif repeated several times. As an example, the Met-rich region of *S. aureus* P0218 is formed by 5 repeats of the motif MMDMK separated by semi-conserved residues. The Met-rich regions found in CueO, *Tth*-MCO, *Pha*MOx and some cuproxidases are flanked by an N-terminal M(X)DM(X)G sequence (with X standing for any residue or none), forming the solvent-exposed outer part of the sCu site in CueO [27] and a D(X) (X)MX sequence immediately upstream from the motif consisting of the three strictly conserved copper-binding histidines, forming the buried inner part of the sCu site (Fig. S4). The size of the Met-rich region is also highly variable, ranging from its absence with only the sCu sequences like for *M. tuberculosis* MCO (Table S2) to about 130 residues, for instance in *P. putida* MCO Pp-CopA (Fig. S1). The size of the Met-rich region is apparently not related to temperature adaptation in contrast to what is frequently reported for non-functional loops in extremophiles [28]. For instance, the cuproxidase *Pha*MOx from the Antarctic *P. haloplanktis* displays a long 55 residue insert whereas both cuproxidases from the Arctic *Psychrobacter arcticus* 273-4 and *Psychrobacter cryohalolentis* K5 from Siberian permafrost are devoid of the Met-rich region and only display both conserved motifs of the sCu site in their cuproxidases (Fig. S5), although the three enzymes share 55% identity (82% similarity) in the core enzyme. Finally, the occurrence of a cuproxidase in bacteria is unpredictable: whereas the investigated *Tth*-MCO was isolated from *T. thermophilus* HB27, the genome of *T. thermophilus* HB8 is devoid of a cuproxidase coding sequence.

3.2. Genomic context and primary structure of the investigated blue oxidases

The multicopper oxidase *Pha*MOx encoded by the PSHAb0011 gene in the genome of the Antarctic bacterium *Pseudoalteromonas haloplanktis* TAC125 [21] is homologous to the cuproxidases CueO from the mesophile *E. coli* and to *Tth*-MCO from the thermophile *T. thermophilus* HB27. Like its two counterparts and despite genome annotation as a “putative laccase” [29], the function of the psychrophilic enzyme is clearly linked to copper resistance of the bacterium. Indeed, in the three bacteria, the gene encoding the MCO belongs to an operon also comprising a copper-responsive factor and a copper efflux P-type ATPase. General information on the investigated MCO is provided in Table 1. The three enzymes possess four ultra-conserved copper binding motifs typical of the MCO family and the Met-rich region specific to cuproxidases (Fig. 1, Fig. S4). They also display a signal peptide for periplasmic targeting by the Tat export pathway. The Met-rich regions specific to the cuproxidase sub-family are also very different in length and composition among the three MCOs and, with the regions surrounding them, are responsible for the differences in polypeptide size (Tables 1 and 2). In CueO, the Met-rich region is inserted at location 4, whereas the insertion is in location 3 for both *Tth*-MCO (Fig. 1) and *Pha*MOx, although for the latter insertion at location 4 cannot be ruled out (Fig. S1). In contrast to CueO and *Tth*-MCO, the 3D structure of *Pha*MOx is not known and its Met-rich insert has been delineated using the outer sCu consensus sequence and the Met and His abundance.

3.3. Cloning and production of the psychrophilic blue oxidase and of its homologs

The full-length coding sequence of the psychrophilic oxidase was cloned in a pET vector and expressed in *E. coli* BL21 (DE3). Laccase-like activity of the heterologously expressed enzyme was detected in the cytoplasmic fraction and to a much lower extent in the periplasmic fraction (data not shown). N-terminal sequencing of the new protein band observed by SDS-PAGE of the periplasmic fraction of induced cells confirmed both its identity and the cleavage site predicted by the SignalP server [30]. The heterologous Tat-signal is therefore recognized by the *E. coli* export machinery but the latter is apparently overloaded by the huge amounts of enzyme produced (estimated to ~0.5 g l^{-1} of culture). Indeed, most of the enzyme production was not processed and remained in the cytoplasm where different proteolytic cleavages occurred, leading to N-terminal heterogeneity in the Tat-signal peptide as deduced from N-terminal sequencing. Consequently, only the nucleotide sequence of the gene encoding the enzyme mature region was inserted in a pET vector and expressed. Purification of the recombinant psychrophilic mature enzyme *Pha*MOx was achieved by a

Table 1
General properties of the investigated multicopper oxidases.

Oxidase	Source	T_{env}[a] °C	TAT peptide aa	mature form aa	Mw kDa	UniProtKB acc n°
Tth-MCO	*T. thermophilus* HB27	~80	21	440	48.8	Q72HW2
CueO	*E. coli* JM109	37	28	488	53.4	P36649
*Pha*MOx	*P. haloplanktis* TAC 125	<0	36	576	64.2	Q3ICN9

[a] Estimated average environmental temperature.

Table 2
Properties of the Met-rich insert in the homologous blue oxidases.

Oxidase	Length aa	Met	His	Asp	∑ ligands
Tth-MCO	16	6	1	1	8
CueO	45	14	5	4	23
*Pha*MOx	55	14	7	8	29

combination of ion-exchangers. Both the Tat-processed (periplasmic) and the cytoplasmic-produced oxidases were found identical in terms of activity and stability. Accordingly, similar gene cloning and cytoplasmic production strategies were applied for CueO and *Tth*-MCO. Integrity of the purified proteins was confirmed by automated Edman N-terminal sequencing and ESI-Q-TOF mass spectrometry. The three recombinant MCOs appeared homogenous on SDS-PAGE and displayed laccase and ferroxidase activities (Fig. S6).

3.4. Circular dichroism spectra

As expected for MCOs formed by three cupredoxin domains, circular dichroism spectra in the far UV of holoenzymes showed that the secondary structures of the three cuproxidases essentially consist of beta-sheets (Fig. 3A). No alteration of these spectra were observed following addition of $CuSO_4$ or of the reducing agent hydroxylamine, showing that the copper redox state does not induce detectable secondary structure variations. CD spectra in the visible region displayed signals typical to T1 and T3 copper binding sites but clear differences were noted (Fig. 3B). As amino acids forming the copper binding motifs are strictly conserved among the three cuproxidases, these discrepancies should arise from slight differences in the lengths and angles between the bound copper and nitrogen or sulfur atoms from histidine or cysteine/methionine residues, respectively. In both UV regions, the CD spectra of the cold-adapted and thermophilic oxidases were similar and differed from the mesophilic CueO. Interestingly, this similarity pattern was also observed when comparing the flexibility of the 3 enzymes [22].

3.5. Copper binding by the homologous blue oxidases

The three cuproxidases were produced without supplemented copper ions in the culture medium in order to avoid induction of the endogenous chromosome-borne, copper-inducible cuproxidase of *E. coli* BL21 (DE3) and to increase the growth yield. The three purified enzymes displayed a blue color typical of MCOs but were not fully loaded with their cofactors. Indeed, addition of Cu(II) led to a very slow increase in color intensity, whereas addition of Cu(I) rendered the preparations instantly colorless due to reduction of the T1 copper and then rapidly more blue with increased absorbance at ~600 nm (T1 copper site) but also at ~340 nm (T3 copper site) (Fig. S7C). It has been shown that many apo-MCOs can only be completely loaded with copper in its cuprous Cu(I) and not cupric Cu(II) state [31] as Cu(I) is more exchange labile and is the

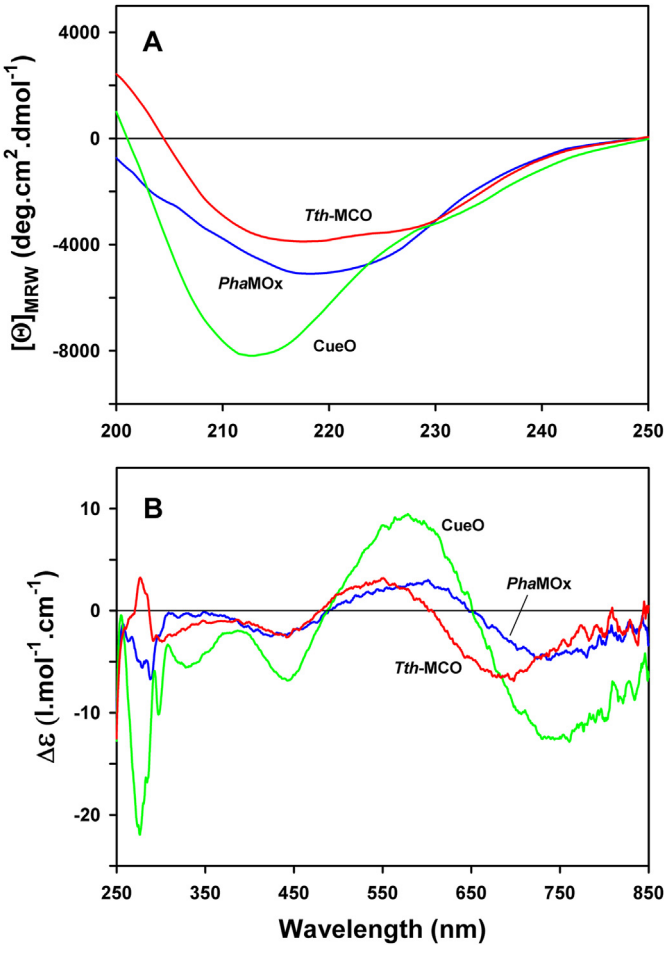

Fig. 3. Circular dichroism spectra of the cuproxidases *Pha*MOx (blue), CueO (green) and *Tth*-MCO (red). A: CD spectra in the far-UV region induced mainly by the secondary structures. B: CD spectra in the near-UV region induced mainly by aromatic side chains (250–300 nm) and by copper ions (>300 nm).

physiological form available in the cell. Accordingly, full holoenzymes were prepared by adding excess Cu(I) in the form of an acetonitrile delivery complex $[Cu(I)(MeCN)_4]^+$. Cu(I) ions added were incorporated into the copper centers and the excess was then a substrate of the enzyme, which was rapidly oxidized. This excess was removed by gel filtration and the holoenzymes were used for all subsequent experiments unless otherwise stated.

Copper content of the purified enzymes was determined by the 2,2′-biquinoline method [32] before and after the treatment described above. Increase in copper content was observed for all MCOs (Table 3). After Cu(I) loading, one should expect a total of 4 copper atoms per holoenzyme molecule under aerobic conditions. Deviations from this stoichiometry in Table 3 arises mainly from

Table 3
Copper binding by the homologous multicopper oxidases and by *Pha*MOx mutants (molar ratios).

	Purified enzymes	+ excess Cu(I) in aerobic conditions		+ excess Cu(I) in anaerobic conditions		Extra Cu(I) binding in anaerobic conditions
	Cu total	Experimental Cu total	Normalized Cu total	Cu(I)	Cu total	
Tth-MCO	1.5 ± 0.1	5.6 ± 0.1	4.0 ± 0.1	5.4 ± 0.1	5.4 ± 0.1	1.4 ± 0.1
CueO	7.6 ± 0.2	8.6 ± 0.1	4.0 ± 0.1	7.5 ± 0.1	7.4 ± 0.1	3.5 ± 0.1
*Pha*MOx	3.7 ± 0.2	5.1 ± 0.1	4.0 ± 0.1	13.2 ± 0.1	13.0 ± 0.1	9.2 ± 0.2
*Pha*MOx Δ1	3.5 ± 0.1	5.3 ± 0.1	4.0 ± 0.1	12.5 ± 0.2	12.5 ± 0.2	8.5 ± 0.2
*Pha*MOx Δ3	3.1 ± 0.1	4.8 ± 0.1	4.0 ± 0.1	5.7 ± 0.1	5.7 ± 0.1	1.7 ± 0.2
*Pha*MOx Δ23	3.4 ± 0.3	4.7 ± 0.1	4.0 ± 0.1	7.4 ± 0.1	7.4 ± 0.1	3.4 ± 0.1

cumulative errors on protein concentration. Accordingly, the copper content of holoenzymes was normalized to 4 Cu atoms per enzyme molecule for further calculations (see below).

To analyze the Cu(I) binding capacity of the homologous blue oxidases, the main issue was to resolve the instability of Cu(I) ion due to its fast oxidation to Cu(II) either directly by O_2 or by the enzyme. We have developed a new methodology for copper loading and for the determination of copper content using an excess of reductant and under strict N_2 atmosphere in order to block the catalytic turnover and oxidation of Cu(I) to Cu(II) (see *2.4.* for details). As shown in Table 3, the Cu(I) content of holoenzymes under anaerobic conditions was identical to the total copper content. This demonstrates that all copper atoms bound to the enzyme and quantified have been maintained in the cuprous state along the manipulation. Accordingly, subtracting the 4 copper atoms belonging to the active site from the copper content under anaerobic conditions provided the number of extra Cu(I) ions bound to the enzymes: *Tth*-MCO binds only ~1 extra Cu(I), ~3 extra Cu(I) ions are found for CueO and *Pha*MOx binds ~9 extra Cu(I) ions. It is worth mentioning that the result obtained for CueO is in excellent agreement with the 3 Cu(I) ions bound to the Met-rich insert in its high resolution crystal structure [14,15] and tends to validate our approach. Furthermore, the number of extra Cu(I) appears to be almost correlated with the length of the Met-rich loops and to the number of potential Cu(I) ligands (Table 2). The latter hypothesis was addressed by mutagenesis of the psychrophilic *Pha*MOx because of its high Cu(I) binding capacity and specific loop properties as detailed below.

3.6. Design of PhaMOx mutants

Based on sequence alignment comparison (Fig. S4) and on the crystal structures of CueO [14] and *Tth*-MCO [20], we have identified regions at the surface of *Pha*MOx near the T1 site potentially involved in its cuproxidase function. These regions are predicted to be disordered by algorithms such as PSIPRED [33]. In order to explore the role of these regions in *Pha*MOx, three different mutants have been constructed (Fig. 4).

(i) The mutant Δ1 in which a putative surface loop close to the T1 site and formed by residues 181 to 212 (native form numbering, 217–248 in the precursor) has been deleted. This loop is much longer as compared to CueO and *Tth*-MCO and is inserted at location 2 of other cuproxidases. Although it does not display the canonical Met and His-rich signature, the proximity to the T1 site might confer a specific function to this loop.
(ii) The mutant Δ3 in which the Met-rich region has been deleted (residues 347 to 394 deleted, 383–430 in the precursor), but keeping the outer sCu consensus sequence intact with Met340 and Asp342 as candidates for sCu coordination by the outer part of the binding site.
(iii) The mutant Δ23 in which both the entire Met-rich region and the outer sCu consensus sequence MRDMMG were removed (residues 340 to 394, 376–430 in the precursor). Both latter mutants could validate our consensus sequence for the sCu site.

3.7. Characterization of PhaMOx mutants

The three mutant enzymes were produced and purified according to the wild-type procedure and the copper content was similar both at the end of the purification and after treatment with the acetonitrile delivery complex $[Cu(I)(MeCN)_4]^+$ to obtain full holoenzymes (Table 3). The CD spectra in the far UV region of the mutants as compared to *Pha*MOx (Fig. 5A) indicated that no significant changes in secondary structures have occurred upon deletion of the loops, in agreement with their predicted disordered conformation. Spectra in the near UV region (Fig. 5B) also indicated that the tertiary structures and the copper centers remained unaffected by these loop deletions. Structural stability analyzed by DSC was performed on apoenzymes because copper release during thermal unfolding of the holoenzymes induced aggregation and precluded reliable thermogram records. The normalized DSC thermograms (Fig. 6A) and stability parameters (Table 4) of the mutants were similar to the parent *Pha*MOx, demonstrating that the Met-rich region has no influence on the cuproxidase stability.

By contrast, the effect of Cu(II) concentration on the laccase-like activity of the mutants with 2,6-dimethoxyphenol as substrate revealed distinct features (Fig. 6B and Table 4). Deletion of both the postulated outer part of the sCu site and of the Met-rich loop in mutant Δ23 resulted in 93% loss of activity, highlighting the importance of this region for phenol-oxidase activity, with however an improved apparent affinity for Cu(II). The severe activity decrease of mutant Δ23 arises from deletion of the MRDMMG sequence as evidenced by mutant Δ3. Indeed, the latter contains this sCu consensus sequence and retains 76% of the wild-type *Pha*MOx activity with similar apparent affinity for Cu(II). This also strongly suggests that the outer sCu consensus sequence in the Met-rich region, determined from our multiple sequence alignment, actually corresponds to the outer part of the sCu binding site. Unexpectedly, mutant Δ1 only retained 20% of activity with almost unaffected apparent affinity for Cu(II).

The Cu(I) binding ability of the mutants was assayed under anaerobic conditions (Table 3). The mutant Δ1 displayed an almost unaffected Cu(I) binding capacity as compared with *Pha*MOx. This shows that the loop 181–212 specific to *Pha*MOx is not involved in Cu(I) chelation. This mutant can also be regarded as a positive control, as deletion of the loop devoid of the Met-rich signature does not affect the Cu(I) binding ability. In contrast, removal of the Met-rich region decreases the number of extra Cu(I) bound from ~9 in *Pha*MOx to ~2 or ~3 in Δ3 and Δ23, respectively. The residual Cu(I) bound to the mutants can be regarded as non-specific binding

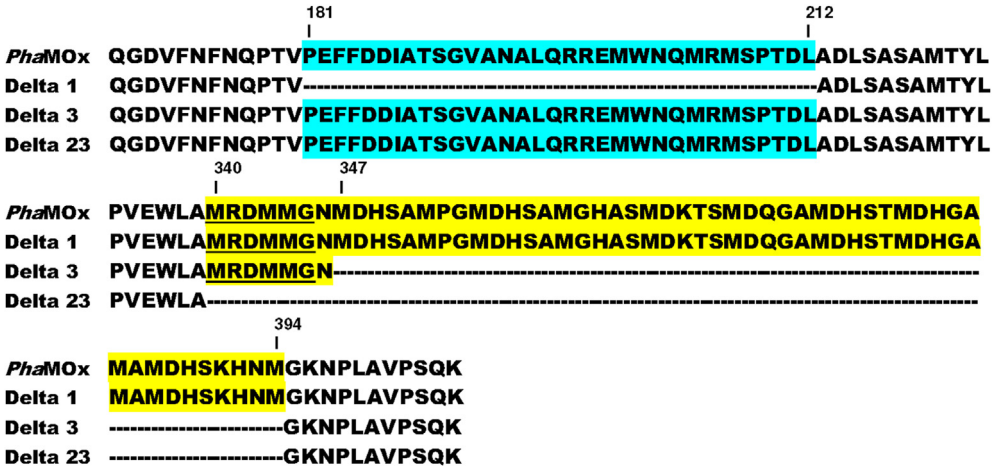

Fig. 4. Partial amino acid sequences of *Pha*MOx and of its deletion mutants. Numbering refers to the *Pha*MOx native form. The consensus sequence of the outer part of the sCu site is underlined.

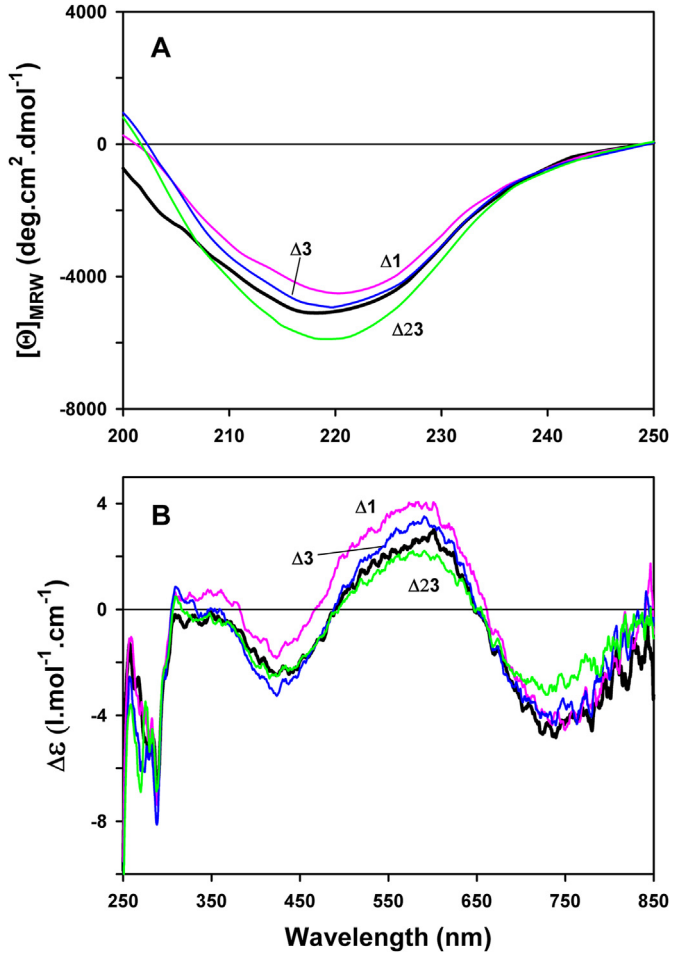

Fig. 5. Circular dichroism spectra of *Pha*MOx and of its mutants. A: CD spectra in the far-UV region (*Pha*MOx spectrum in heavy black trace). B: CD spectra in the near-UV region (*Pha*MOx spectrum in heavy black trace).

or they might also reflect distinct Cu(I) binding ability of the core enzyme.

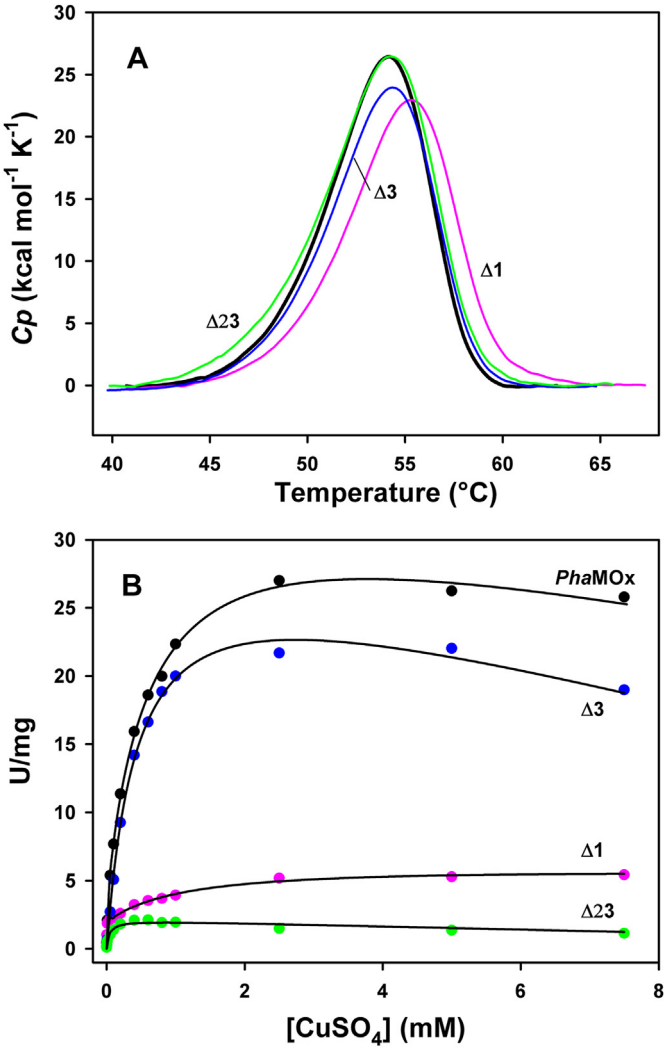

Fig. 6. Stability and laccase-like activity of *Pha*MOx and of its mutants. A: Differential scanning calorimetry of the apoenzymes. Heavy black line: thermogram of the wild-type *Pha*MOx. T_m was measured at the top of the transition and ΔH_{cal} was calculated as the area under the transition. B: Cu(II) dependence of laccase-like activity at 25 °C (1 U = 1 μmole of 2,6-dimethoxyphenol oxidized per min).

Table 4
Stability and laccase-like activity of *Pha*MOx and of its mutants.

	DSC		Laccase-like activity	
	Tm °C	ΔH_{cal} kcal mol^{-1}	V_{max} U mg^{-1}	$K_{d\ app}$ μM
*Pha*MOx	54.2	178	28.8 ± 0.9	334 ± 16
*Pha*MOx Δ 1	55.3	160	5.6 ± 0.2	259 ± 13
*Pha*MOx Δ 3	54.3	158	22.0 ± 0.7	271 ± 13
*Pha*MOx Δ 23	54.1	180	2.1 ± 0.1	53 ± 3

SD are ±0.1 °C on *Tm* and ±5% on ΔH_{cal}.

4. Discussion

Methionin-rich regions are frequently associated with proteins involved in copper trafficking, management and homeostasis. Indeed, the thioether group of methionine has been shown to play a major role in the bioinorganic chemistry of Cu(I) ions [34]. For instance, a simple peptide containing a MXXMXXM motif is sufficient to bind Cu(I) ions with very high affinity [35]. Methionine motifs for copper binding are resistant to oxidation and therefore are mainly found in cell compartments exposed to oxidative environment, in contrast with the oxidation-prone cysteine motifs which are mainly found in the reducing intracellular environment. MCOs from bacterial species which possess Met-rich regions can only be found in the periplasm of prokaryotes where their physiological role is the defense of this important cell compartment against toxic cuprous ions. In CueO, the low coordination number, solvent exposure, and disorder of the methionine-rich binding sites make them suitable for transient copper binding and substrate procurement [14]. Here we have shown that location, size and sequence of these Met-rich inserts are highly variable in bacterial cuproxidases and that they bind specifically Cu(I) with a stoichiometry related to their size and composition in three investigated blue oxidases. It is worth mentioning that Cu(I) binding has been only demonstrated for CueO on the basis of its high resolution crystal structure [14]. Here we provide a new method for cuprous ion binding determination in reducing solution and oxygen-less atmosphere, which can be applied to any potential cuproxidase.

In sharp contrast with most functional motifs which have a well-defined position in protein structures, the Met-rich inserts in bacterial MCOs were found at locations corresponding to six different solvent exposed loops of the cuproxidase CueO (Fig. 2). However, these loops share a close spatial proximity with the strictly conserved blue T1 site which bind the first catalytic copper. It should be noted that all insertions of a Met-rich region (with only one exception at region 5) occur in the cupredoxin domain 2 and as N- or C-terminal tails (Fig. 1). Domain 2 is the longest in the sequence but does not carry any of the active site copper chelating residues. The T1 site is located in the cupredoxin domain 3 and the trinuclear copper binding site is formed at the interface of domains 1 and 3. Accordingly, one can suggest that both cupredoxin domains 1 and 3 are not (or less) amenable to Met-rich loop insertion, whereas domain 2 possesses sufficient structural plasticity to accommodate such insertions.

In the 3 cuproxidases investigated here, these Met-rich regions display a conserved N-terminal M(X)DM(X)G motif (Fig. S4) in which both Met and Asp residues form the outer part of the sCu site in CueO [27]. The involvement of this conserved motif in the sCu site of other bacterial cuproxidases is supported by the Δ23 mutant of *Pha*MOx: deletion of this motif results in a drastic reduction of phenol oxidase activity, which requires Cu(II) binding to this site (Fig. 6B and Table 4). In addition, the 3 blue oxidases possess strongly conserved Asp and Met residues immediately upstream from the strictly conserved histidines of the T1 site (Fig. S4) and forming the buried inner part of the sCu site in CueO [27]. In most cases, the sequence of the outer part was hardly detectable within the primary structures of other cuproxidases. However, the occurrence of M and/or D and/or H immediately upstream of the conserved copper-binding histidines is a novel criterion allowing to distinguish cuproxidases from other MCOs (Figs. S1 and S3). Furthermore, our newly developed method for cuprous ion binding determination will allow to experimentally check this criterion. Altogether, the occurrence of the Met-rich inserts and of both sCu motifs support the possible early events in Cu(I) oxidation proposed for CueO and their generalization in bacterial cuproxidases: the Met-rich regions chelate Cu(I) in the periplasm and are dedicated to feed the sCu site. They provide a first step of electron transfer to the catalytic copper T1 and to the trinuclear center [14,15]. Cuproxidases can then be regarded as molecular octopus with a beak (the sCu site) and tentacles (the Met-rich Cu(I) binding region).

The deletion mutants of *Pha*MOx also provide additional structural and functional information. None of these deletions induce major changes in the CD spectra (Fig. 5) nor in the stability parameters of the mutants (Fig. 6A, Table 4). This indicates that the deleted regions are not closely packed on the core enzyme, but rather are disordered loops as also predicted by PSIPRED. The slight increase of stability (positive shift of ~1 °C in T_m) observed for the mutant Δ1, suggests that this surface loop (devoid of the Met-rich signature) exerts a constraint on the core enzyme, which was relieved upon deletion. This loop is not involved in Cu(I) binding (Table 3) but its deletion results in an 80% loss of laccase-like activity. This indicates that the loop 181–212 specific to *Pha*MOx and not related to the Met-rich region is involved in the phenol-oxidase activity. More importantly, the severe loss of Cu(I) ions bound to mutant Δ3 and Δ23 demonstrates that the Met-rich insert is specifically designed to coordinate several Cu(I) ions.

The physiological relevance of length variability in Met-rich inserts remains unclear. Indeed, long insert sequences potentially binding more Cu(I) are found in bacterium not exposed to high copper concentrations such as *P. haloplanktis* isolated from pristine Antarctic sea ice. Conversely, short insert sequences are noted in thermophiles thriving in metal-rich effluents from hot springs, although this could be possibly related to loop length decreases in thermophilic proteins in order to improve their stability. Nevertheless, variability in location, length and sequence of Met-rich inserts suggests evolutionary trend and selection for the acquirement of copper-binding residues in surface loops close to the blue T1 site.

Finally, we have shown that the three cuproxidases can be produced intracellularly in a functional but almost Cu-depleted form in the absence of copper in the culture medium and that the enzymes can be activated by an exogenous Cu(I) supply. This has at least two physiological consequences. Induction of cuproxidase synthesis is thought to be mediated by the appearance of Cu(I) in the cytoplasm. Accordingly, following cuproxidase synthesis, its copper loading process can already contribute to lower the level of toxic intracellular Cu(I), although CueO from *E. coli* was found to be exported as an apoenzyme [24]. Furthermore, if the induction mechanism is not tightly regulated, a basal level of Cu-depleted cuproxidase can be synthesized and translocated in the periplasm by the Tat secretion apparatus. This pool of poorly active cuproxidase might be regarded as a first line defense, waiting for Cu(I) loading and full oxidase activity.

Authors' contribution

F.R. and A.G. performed the experiments. F.R. and G.F. designed the study and wrote the manuscript. All authors reviewed and approved the final version of the manuscript.

Data availability statement

The data underlying this article are available in the article and in its online Supplementary data.

Declaration of competing interest

The authors declare no conflict of interest.

Acknowledgements

We thanks Dr. Kentaro Miyazaki for providing the *Tth*-MCO expression plasmid. This work was supported by the F.R.S-FNRS, Belgium (Fonds de la Recherche Fondamentale et Collective, contract numbers 2.4535.08, 2.4523.11 and U.N009.13 to G.F.). F.R. and A.G. were FRIA research fellows during this work.

Appendix A. Supplementary data

Supplementary data to this article can be found online at https://doi.org/10.1016/j.biochi.2021.12.015.

References

[1] R.R. Crichton, J.L. Pierre, Old iron, young copper: from Mars to Venus, Biometals 14 (2001) 99–112. http://www.ncbi.nlm.nih.gov/pubmed/11508852.
[2] D. Magnani, M. Solioz, How bacteria handle copper, in: D.H. Nies, S. Silver (Eds.), Microbiology of Heavy Metals, Springer, Berlin, 2007, pp. 259–285.
[3] J.H. Kaplan, S. Lutsenko, Copper transport in mammalian cells: special care for a metal with special needs, J. Biol. Chem. 284 (2009) 25461–25465. http://www.ncbi.nlm.nih.gov/pubmed/19602511.
[4] B.E. Kim, T. Nevitt, D.J. Thiele, Mechanisms for copper acquisition, distribution and regulation, Nat. Chem. Biol. 4 (2008) 176–185. http://www.ncbi.nlm.nih.gov/pubmed/18277979.
[5] S. Tottey, K.J. Waldron, S.J. Firbank, B. Reale, C. Bessant, K. Sato, T.R. Cheek, J. Gray, M.J. Banfield, C. Dennison, N.J. Robinson, Protein-folding location can regulate manganese-binding versus copper- or zinc-binding, Nature 455 (2008) 1138–1142. http://www.ncbi.nlm.nih.gov/pubmed/18948958.
[6] G. Grass, C. Rensing, Genes involved in copper homeostasis in *Escherichia coli*, J. Bacteriol. 183 (2001) 2145–2147. http://www.ncbi.nlm.nih.gov/pubmed/11222619.
[7] C. Rensing, G. Grass, *Escherichia coli* mechanisms of copper homeostasis in a changing environment, FEMS Microbiol. Rev. 27 (2003) 197–213. http://www.ncbi.nlm.nih.gov/pubmed/12829268.
[8] E.I. Solomon, A.J. Augustine, J. Yoon, O_2 reduction to H_2O by the multicopper oxidases, Dalton Trans. 30 (2008) 3921–3932. http://www.ncbi.nlm.nih.gov/pubmed/18648693.
[9] L. Quintanar, C. Stoj, A.B. Taylor, P.J. Hart, D.J. Kosman, E.I. Solomon, Shall we dance? How a multicopper oxidase chooses its electron transfer partner, Acc. Chem. Res. 40 (2007) 445–452. http://www.ncbi.nlm.nih.gov/pubmed/17425282.
[10] D.J. Kosman, Multicopper oxidases: a workshop on copper coordination chemistry, electron transfer, and metallophysiology, J. Biol. Inorg. Chem. 15 (2010) 15–28. http://www.ncbi.nlm.nih.gov/pubmed/19816718.
[11] D. Sirim, F. Wagner, L. Wang, R.D. Schmid, J. Pleiss, The Laccase Engineering Database: a Classification and Analysis System for Laccases and Related Multicopper Oxidases, Database, Oxford), 2011 (2011) bar006, http://www.ncbi.nlm.nih.gov/pubmed/21498547.
[12] C.S. Stoj, A.J. Augustine, E.I. Solomon, D.J. Kosman, Structure-function analysis of the cuprous oxidase activity in Fet3p from *Saccharomyces cerevisiae*, J. Biol. Chem. 282 (2007) 7862–7868. http://www.ncbi.nlm.nih.gov/pubmed/17220296.
[13] K.Y. Djoko, L.X. Chong, A.G. Wedd, Z. Xiao, Reaction mechanisms of the multicopper oxidase CueO from *Escherichia coli* support its functional role as a cuprous oxidase, J. Am. Chem. Soc. 132 (2010) 2005–2015. http://www.ncbi.nlm.nih.gov/pubmed/20088522.
[14] S.K. Singh, S.A. Roberts, S.F. McDevitt, A. Weichsel, G.F. Wildner, G.B. Grass, C. Rensing, W.R. Montfort, Crystal structures of multicopper oxidase CueO bound to copper(I) and silver(I): functional role of a methionine-rich sequence, J. Biol. Chem. 286 (2011) 37849–37857. http://www.ncbi.nlm.nih.gov/pubmed/21903583.
[15] L. Cortes, A.G. Wedd, Z. Xiao, The functional roles of the three copper sites associated with the methionine-rich insert in the multicopper oxidase CueO from *E. coli*, Metallomics 7 (2015) 776–785. http://www.ncbi.nlm.nih.gov/pubmed/25679350.
[16] A.T. Fernandes, C.M. Soares, M.M. Pereira, R. Huber, G. Grass, L.O. Martins, A robust metallo-oxidase from the hyperthermophilic bacterium *Aquifex aeolicus*, FEBS J. 274 (2007) 2683–2694. http://www.ncbi.nlm.nih.gov/pubmed/17451433.
[17] H. Sakuraba, K. Koga, K. Yoneda, Y. Kashima, T. Ohshima, Structure of a multicopper oxidase from the hyperthermophilic archaeon *Pyrobaculum aerophilum*, Acta Crystallogr. Sect. F Struct. Biol. Cryst. Commun. 67 (2011) 753–757. http://www.ncbi.nlm.nih.gov/pubmed/21795787.
[18] S.A. Roberts, A. Weichsel, G. Grass, K. Thakali, J.T. Hazzard, G. Tollin, C. Rensing, W.R. Montfort, Crystal structure and electron transfer kinetics of CueO, a multicopper oxidase required for copper homeostasis in *Escherichia coli*, Proc. Natl. Acad. Sci. U.S.A. 99 (2002) 2766–2771. http://www.ncbi.nlm.nih.gov/pubmed/11867755.
[19] K. Miyazaki, A hyperthermophilic laccase from *Thermus thermophilus* HB27, Extremophiles 9 (2005) 415–425. http://www.ncbi.nlm.nih.gov/pubmed/15999224.
[20] M. Bello, B. Valderrama, H. Serrano-Posada, E. Rudino-Pinera, Molecular dynamics of a thermostable multicopper oxidase from *Thermus thermophilus* HB27: structural differences between the apo and holo forms, PLoS One 7 (2012), e40700. http://www.ncbi.nlm.nih.gov/pubmed/22808237.
[21] C. Medigue, E. Krin, G. Pascal, V. Barbe, A. Bernsel, P.N. Bertin, F. Cheung, S. Cruveiller, S. D'Amico, A. Duilio, G. Fang, G. Feller, C. Ho, S. Mangenot, G. Marino, J. Nilsson, E. Parrilli, E.P. Rocha, Z. Rouy, A. Sekowska, M.L. Tutino, D. Vallenet, G. von Heijne, A. Danchin, Coping with cold: the genome of the versatile marine Antarctica bacterium *Pseudoalteromonas haloplanktis* TAC125, Genome Res. 15 (2005) 1325–1335. http://www.ncbi.nlm.nih.gov/pubmed/16169927.
[22] F. Roulling, A. Godin, A. Cipolla, T. Collins, K. Miyazaki, G. Feller, Activity-stability relationships revisited in blue oxidases catalyzing electron transfer at extreme temperatures, Extremophiles (2016) 621–629. http://www.ncbi.nlm.nih.gov/pubmed/27315165.
[23] T. Palmer, B.C. Berks, The twin-arginine translocation (Tat) protein export pathway, Nat. Rev. Microbiol. 10 (2012) 483–496. http://www.ncbi.nlm.nih.gov/pubmed/22683878.
[24] P. Stolle, B. Hou, T. Bruser, The Tat substrate CueO is transported in an incomplete folding state, J. Biol. Chem. 291 (2016) 13520–13528. http://www.ncbi.nlm.nih.gov/pubmed/27129241.
[25] C.S. Silva, P. Durao, A. Fillat, P.F. Lindley, L.O. Martins, I. Bento, Crystal structure of the multicopper oxidase from the pathogenic bacterium *Campylobacter jejuni* CGUG11284: characterization of a metallo-oxidase, Metallomics 4 (2012) 37–47. http://www.ncbi.nlm.nih.gov/pubmed/22127520.
[26] T. Classen, J. Pietruszka, S.M. Schuback, A new multicopper oxidase from Gram-positive bacterium *Rhodococcus erythropolis* with activity modulating methionine rich tail, Protein Expr. Purif 89 (2013) 97–108. http://www.ncbi.nlm.nih.gov/pubmed/23485678.
[27] S.A. Roberts, G.F. Wildner, G. Grass, A. Weichsel, A. Ambrus, C. Rensing, W.R. Montfort, A labile regulatory copper ion lies near the T1 copper site in the multicopper oxidase CueO, J. Biol. Chem. 278 (2003) 31958–31963. http://www.ncbi.nlm.nih.gov/pubmed/12794077.
[28] G. Feller, Protein stability and enzyme activity at extreme biological temperatures, J. Phys. Condens. Matter 22 (2010), 323101. https://pubmed.ncbi.nlm.nih.gov/21386475.
[29] R. Papa, E. Parrilli, G. Sannia, Engineered marine Antarctic bacterium *Pseudoalteromonas haloplanktis* TAC125: a promising micro-organism for the bioremediation of aromatic compounds, J. Appl. Microbiol. 106 (2009) 49–56. http://www.ncbi.nlm.nih.gov/pubmed/19120609.
[30] T.N. Petersen, S. Brunak, G. von Heijne, H. Nielsen, SignalP 4.0: discriminating signal peptides from transmembrane regions, Nat. Methods 8 (2011) 785–786. http://www.ncbi.nlm.nih.gov/pubmed/21959131.
[31] G. Musci, S. Di Marco, G.C. Bellenchi, L. Calabrese, Reconstitution of ceruloplasmin by the Cu(I)-glutathione complex. Evidence for a role of Mg^{2+} and ATP, J. Biol. Chem. 271 (1996) 1972–1978. http://www.ncbi.nlm.nih.gov/pubmed/8567646.
[32] G. Felsenfeld, The determination of cuprous ion in copper proteins, Arch. Biochem. Biophys. 87 (1960) 247–251. http://www.ncbi.nlm.nih.gov/pubmed/13822131.
[33] D.W. Buchan, F. Minneci, T.C. Nugent, K. Bryson, D.T. Jones, Scalable web services for the PSIPRED protein analysis workbench, Nucleic Acids Res. 41 (2013) W349–W357. http://www.ncbi.nlm.nih.gov/pubmed/23748958.
[34] A.V. Davis, T.V. O'Halloran, A place for thioether chemistry in cellular copper ion recognition and trafficking, Nat. Chem. Biol. 4 (2008) 148–151. http://www.ncbi.nlm.nih.gov/pubmed/18277969.
[35] J. Jiang, I.A. Nadas, M.A. Kim, K.J. Franz, A Mets motif peptide found in copper transport proteins selectively binds Cu(I) with methionine-only coordination, Inorg. Chem. 44 (2005) 9787–9794. http://www.ncbi.nlm.nih.gov/pubmed/16363848.
[36] C. Kim, W.W. Lorenz, J.T. Hoopes, J.F. Dean, Oxidation of phenolate siderophores by the multicopper oxidase encoded by the *Escherichia coli yacK* gene, J. Bacteriol. 183 (2001) 4866–4875. http://www.ncbi.nlm.nih.gov/pubmed/11466290.

Table S1: Primers used in this study. The *Nco*I site in forward primers and the *Xho*I site in reverse primers are underlined. The stop codon is in bold. SP: wild type TAT signal peptide coding sequence.

Coding sequence	Primer	Primer sequence (5' - 3')
*Pha*MOx + SP	Forward	GGTGTAATACCATGGGTTTTAAAAAGTCATTG
*Pha*MOx	Reverse	CCCCTCGAG**TCA**TGATACAACCACCTCTCTAA
PhaMOx	Forward	GGGCCATGGCATCATCTTTAGCGGCTTC
CueO	Forward	GGGCCATGGCAGAACGCCCAACGTTAC
CueO	Reverse	CCCCTCGAG**TTA**TACCGTAAACCCTAACATCATCC
*Pha*MOx Δ1	Forward	GCTGATTTATCGGCTTCGGC
*Pha*MOx Δ1	Reverse	TACAGTGGGCTGATTAAAGTTAAACAC
*Pha*MOx Δ3	Forward	GGTAAAAACCCACTGGCTGTTC
*Pha*MOx Δ3	Reverse	ATTGCCCATCATATCCCGCATT
*Pha*MOx Δ23	Forward	GGTAAAAACCCACTGGCTGTTC
*Pha*MOx Δ23	Reverse	TGCTAACCACTCAACTGGGTC

Table S2: A compilation of previously characterized MCOs used for the multiple sequence alignment in Fig. S1

Name	Pdb	Organism	Gram classification	Signal Peptide identified using SignalP*	Met-rich region location**	References	Uniprot (or GeneBank if noted Gb:)
CueO	3OD3	*Escherichia coli*	-	TAT (Tat/SPI)	4	Singh et al. J Biol Chem. 2011, 286(43), 37849-37857	P36649
OcCueO	6EVG	*Ochrobactrum sp.*	-	TAT (Tat/SPI)	4	Granja-Travez et al. FEBS J. 2018, 285(9), 1684-1700	A6X5N0
Lac15	4F7K	Marine microbial metagenome	NA	TAT (Tat/SPI)	4	Fang et al. PLoS ONE, 2014, 9(7): e102423.	E1ACR6
McoC	3ZX1	*Campylobacter jejuni* CGUG11284	-	TAT (Tat/SPI)	1 - 4	Silva et al. Metallomics, 2012, 4, 37-47	A0A0H3PBA4
K sp. 601 MCO	/	*Klebsiella sp.* 601	-	TAT (Tat/SPI)	4	Li et al. Can J Microbiol, 2008, 54(9), 725-733 - Li et al. BMC Biochemistry, 2011, 12:30	B0FMT2
BmcO	/	*Brucella melitensis* 16M	-	TAT (Tat/SPI)	4	Wu et al. FEMS Microbiology Letters, 2015, 362(12)	Gb:AIJ88386.1
CuiD	/	*Salmonella enterica* serovar typhimurium	-	TAT (Tat/SPI)	4	Achard et al. Infection and Immunity, 2010, 78 (5)	Q8ZRS2
MCO *A. hydrophila*	/	*Aeromonas hydrophila* subsp. hydrophila ATCC 7966	-	TAT (Tat/SPI)	4	Singh et al. Syst Synth Biol, 2012, 6, 51-59	A0KP58
CopA1	/	*Cupriavidus metallidurans* CH34	-	TAT (Tat/SPI)	3 or 4	Monchy et al. Microbiology. 2006, 152(6), 1765-76	Q58AD6
CopA2	/	*Cupriavidus metallidurans* CH34	-	TAT (Tat/SPI)	3 or 4	Janssens et al. PLoS One. 2010, 5(5):e10433	Q1LBE6
PcoA	/	*Escherichia coli* (plasmid-borne pco operon)	-	TAT (Tat/SPI)	3 or 4	Djoko et al. Chem Bio Chem, 2008, 9, 1579 - Xiao and Wedd Aust J Chem, 2011, 64, 231-238	Q47452
CopA	/	*Pseudomonas syringae*	-	TAT (Tat/SPI)	3 or 4	Cha & Cooksey. PNAS, 1991, 88, 8915-8919	P12374
MCO *P. aeruginosa*	/	*Pseudomonas aeruginosa*	-	TAT (Tat/SPI)	3 or 4	Huston et al. Mol Microbiol, 2002, 45, 1741-1750	Q8GP37
Pp-CopA	/	*Pseudomonas putida* KT2440	-	TAT (Tat/SPI)	3 or 4	Granja-Travez et al. Archives of Biochemistry and Biophysics, 2018, 660, 97-107	Q88C03
Pf-CopA	/	*Pseudomonas fluorescens* PF-5	-	TAT (Tat/SPI)	3 or 4	Granja-Travez et al. Archives of Biochemistry and Biophysics, 2018, 660, 97-107	Q4KCN4
Pha MOx	/	*Pseudoalteromonas haloplanktis* TAC125	-	TAT (Tat/SPI)	3 or 4	Roulling et al. Extremophiles, 2016, 20(5), 621-629	Q3ICN9
MCO *S. aureus*	/	*Staphylococcus aureus* ATCC12600	+	Sec/SPI) expected	1	Sitthisak et al. Appl Environ Microbiol, 2005, 71(9), 5650-5653	Q69HT9
GeoLacc	/	*Geobacter metallireducens* GS-15	-	TAT (Tat/SPI)	1	Berini et al. Appl Microbiol Biotechnol, 2018, 102: 2425	Q39TP1
ESU72270	/	*Geobacillus thermopakistaniensis*	+	LIPO (Sec/SPII)	1 - 2	Basheer et al. Extremophiles. 2017, 21(3), 563-571	V6VIX9
Cohnella sp. A01 laccase	/	*Cohnella sp.* A01	+	None	1 - 2	Shafiei et al. Helyon, 2019, 5(9), e02543	A0A0G3VH35
CuOx	/	*Paenibacillus glucanolyticus* SLM1	+	LIPO (Sec/SPII)	2	Mathews et al. Journal of Applied Microbiology, 2016, 121, 1335-1345	A0A165SC98
CutO	/	*Rhodobacter capsulatus* B10	-	TAT (Tat/SPI)	2	Wiethaus et al. FEMS Microbiol Lett, 2006, 256, 67-74	O68054
Lbh1	/	*Bacillus halodurans* HHR028	+	LIPO (Sec/SPII)	2	Ruijssenaars & Hartmans. Appl Microbiol Biotechnol, 2004, 65, 177-182	Q68UP9
CgL1	/	*Corynebacterium glutamicum* ATCC 13032	+	TAT (Tat/SPI)	2	Ricklefs et al. Journal of Biotechnology, 2014, 191, 46-53	Q8NLH5
MmcO	/	*Mycobacterium tuberculosis*	NA	TAT (Tat/SPI)	None	Rowland et al. Journal of Bacteriology, 2013, 195(16), 3724-3733	I6WZK7
MCA2011	/	*Methylococcus capsulatus* (ATCC 33009/Bath)	-	TAT (Tat/SPI)	5	Ward et al. PLoS Biol 2(10): e303	Q606K5
L. plantarum J16 laccase	/	*Lactobacillus plantarum* J16 CECT 8944	+	None	None (6?)	Callejon et al. Appl Microbiol Biotechnol, 2016, 100:3113–3124	Gb:AHN67998.1
P. acidilactici CECT 5930 laccase	/	*Pediococcus acidilactici* CECT 5930	+	None	None (6?)	Callejon et al. PLoS One. 2017; 12(10): e0186019	D2EK17
CueORE	/	*Rhodococcus erythropolis* DSM311	+	LIPO (Sec/SPII)	6	Classen et al. Prot Exp Pur, 2013, 89, 97-108	L7P6C5
Lacc	/	*Thioalkalivibrio sp.* ALRh	-	TAT (Tat/SPI)	3	Ausec et al. Appl Microbiol Biotechnol, 2015, 99(23), 9987–9999	Gb:CCV01628.1
Mrlac	/	*Meiothermus ruber* DSM 1279	-	TAT (Tat/SPI)	3	Kalyani et al. RSC Advances, 2016, 6(5), 3910-3918	D3PLX1
LAC_2.9	/	*Thermus sp. 2.9*	-	TAT (Tat/SPI)	3	Navas et al. AMB Expr, 2019, 9:24	A0A0B0SEJ6
McoA	/	*Aquifex aeolicus* VF5	-	TAT (Tat/SPI)	3	Fernandes et al. FEBS J. 2007, 274(11), 2683-2694	O67206
McoP	3AW5	*Pyrobaculum aerophilum*	-	TAT (Tat/SPI)	3	Sakuraba et al. Acta Cryst, 2011, F67, 753-757	Q8ZWA8
Tth -MCO	2XU9	*Thermus thermophilus* HB27	-	TAT (Tat/SPI)	3	Serrano-Posada et al. Acta Cryst, 2015, D71, 2396–2411	Q72HW2

NA: Not Applicable

*Signal Peptide identification using SignalP-5.0: http://www.cbs.dtu.dk/services/SignalP/

The SignalP 5.0 server can discriminate between three types of signal peptides:

Sec/SPI: "standard" secretory signal peptides transported by the Sec translocon and cleaved by Signal Peptidase I (*Lep*)

Sec/SPII: lipoprotein signal peptides transported by the Sec translocon and cleaved by Signal Peptidase II (*Lsp*)

Tat/SPI: Tat signal peptides transported by the Tat translocon and cleaved by Signal Peptidase I (*Lep*)

**Met-rich region (MR) location was inferred from the alignments, see Fig. S1

A cell colored in column F indicates that the absence of structural information prevent to precisely position the Met-rich region within the secondary structure topology. The localization is in Met-rich region 3 (β18-β19) or in Met-rich region 4 (β20-β21)

Fig. S1: Multiple sequence alignment of the 34 MCOs listed in Table S2

1/ The multiple sequence alignment program Clustal Omega was used (https://www.ebi.ac.uk/Tools/msa/clustalo/).

2/ ESPript 3.0 (Robert and Gouet 2014) was then run using the alignment file generated by Clustal Omega.

Robert, X. and Gouet, P. (2014) "Deciphering key features in protein structures with the new ENDscript server". Nucl. Acids Res. 42(W1), W320-W324 - doi: 10.1093/nar/gku316

http://endscript.ibcp.fr/ESPript/ESPript/index.php

PDB structures 3OD3 (CueO from *E. coli*) and 2XU9 (*Tth* -MCO from *T. thermophilus*) were used for top and bottom secondary structure depictions, respectively.

Red framed residues: strictly conserved. Blue boxed residues in red: similar side chain group. See Fig. 1 for the general location of Met-rich regions

Fig. S2: Structural alignment of MCOs sequences for which the 3D structure has been solved

Name	Pdb	Organism	Met-rich region location	Reference	Uniprot
CueO	3OD3	*Escherichia coli*	4	Singh et al. J Biol Chem. 2011, 286(43), 37849-37857	P36649
OcCueO	6EVG	*Ochrobactrum sp.*	4	Granja-Travez et al. FEBS J. 2018, 285(9), 1684-1700	A6X5N0
Lac15	4F7K	*Marine microbial metagenome*	4	Fang et al. PLoS ONE, 2014, 9(7): e102423.	E1ACR6
McoC	3ZX1	*Campylobacter jejuni* CGUG11284	1 & 4	Silva et al. Metallomics, 2012, 4, 37-47	A0A0H3PBA4
Tth -MCO	2XU9	*Thermus thermophilus* HB27	3	Serrano-Posada et al. Acta Cryst, 2015, D71, 2396–2411	Q72HW2
McoP	3AW5	*Pyrobaculum aerophilum*	3	Sakuraba et al. Acta Cryst, 2011, F67, 753-757	Q8ZWA8

Red framed residues: strictly conserved. Yellow framed residues in red: similar side chain group. See Fig. 1 for the general location of Met-rich regions

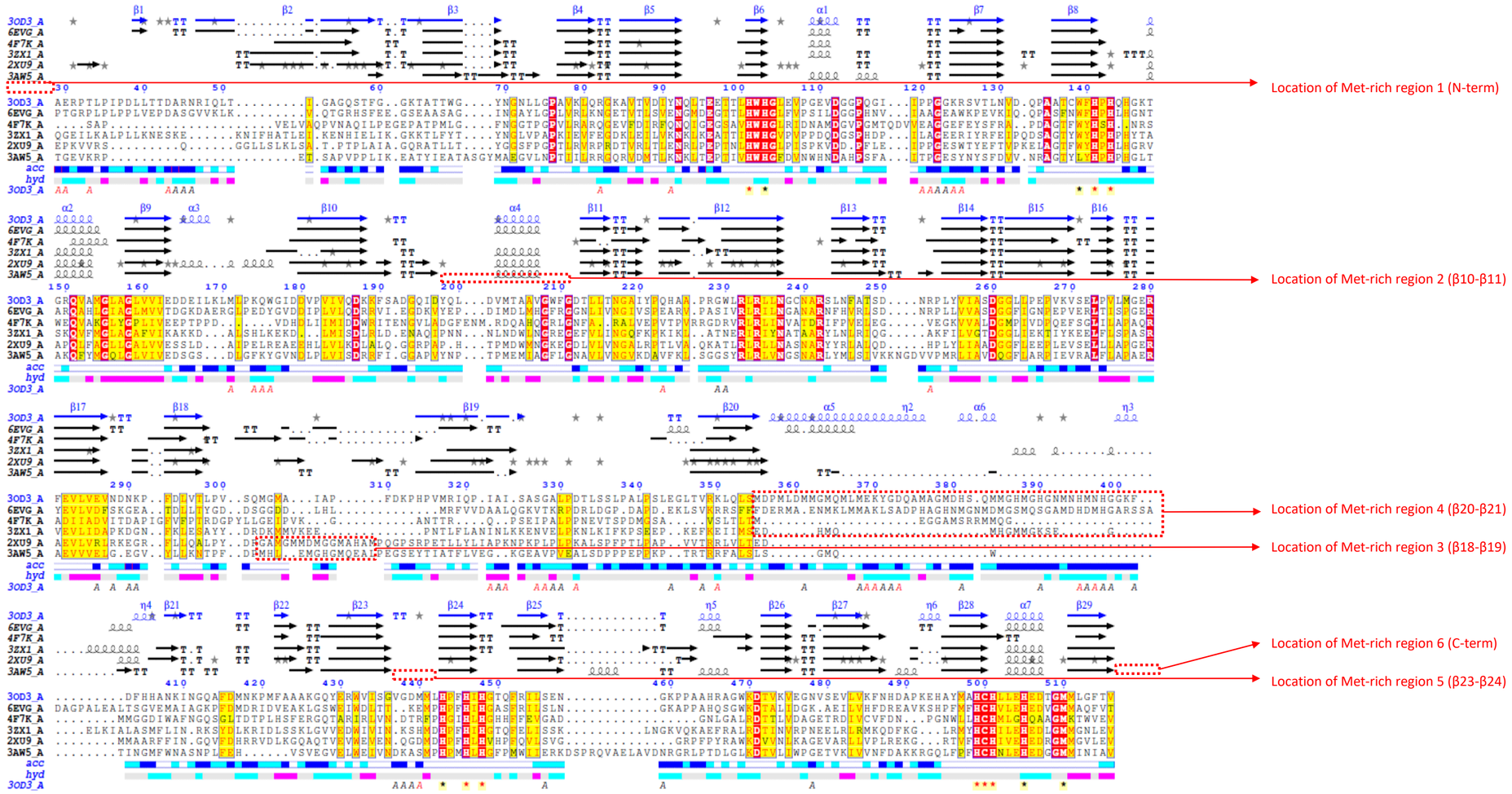

Kept ligands CU*

Figure prepared using ENDscript
http://endscript.ibcp.fr/ESPript/ENDscript/
Robert, X. and Gouet, P. (2014) "Deciphering key features in protein structures with the new ENDscript server". *Nucl. Acids Res* . **42**(W1), W320-W324 - doi: 10.1093/nar/gku316
(freely accessible online)

Fig. S3: Multiple sequence alignment of 93 MCO homologs

1/ The multiple sequence alignment program Clustal Omega was used (https://www.ebi.ac.uk/Tools/msa/clustalo/).
All parameters were kept as default, except for the Order parameter which was changed from "aligned" to "input" for preserving the input order of the sequences.
2/ ESPript 3.0 (Robert and Gouet 2014) was then used using the alignment file generated by Clustal Omega.
PDB structures 3OD3 (CueO from *E. coli*) and 2WZ9 (Tth-MCO from *T. thermophilus*) were used for top and bottom secondary structures depictions, respectively.
EXPert mode was used to select the options "Number sequences" and "Keep the gaps in alignment". The following parameters were modified in the "Alignment output layouts" options: "Paper size" was changed to A0, "Number of columns" was set to 182 and "Gap between blocks" was set to 15. All other parameters were kept with their Default value.
Robert, X. and Gouet, P. (2014) "Deciphering key features in protein structures with the new ENDscript server". Nucl. Acids Res. 42(W1), W320-W324 - doi: 10.1093/nar/gku316
http://endscript.ibcp.fr/ESPript/ESPript/index.php3
Red framed residues: strictly conserved. Blue boxed residues in red: similar side chain group. See Fig. 1 for the general location of Met-rich regions

*: indicates that this MCO has been characterized and is one of the 34 bacterial MCOs listed in Table S1 and in the multiple alignment of Fig. S1

Location of Met-rich region 1 (N-term)

Location of Met-rich region 2 (β10-β11)

Location of Met-rich region 3 (β18-β19)

Location of Met-rich region 4 (β20-β21)

Location of Met-rich region 5 (β23-β24)

Location of Met-rich region 6 (C-Term)

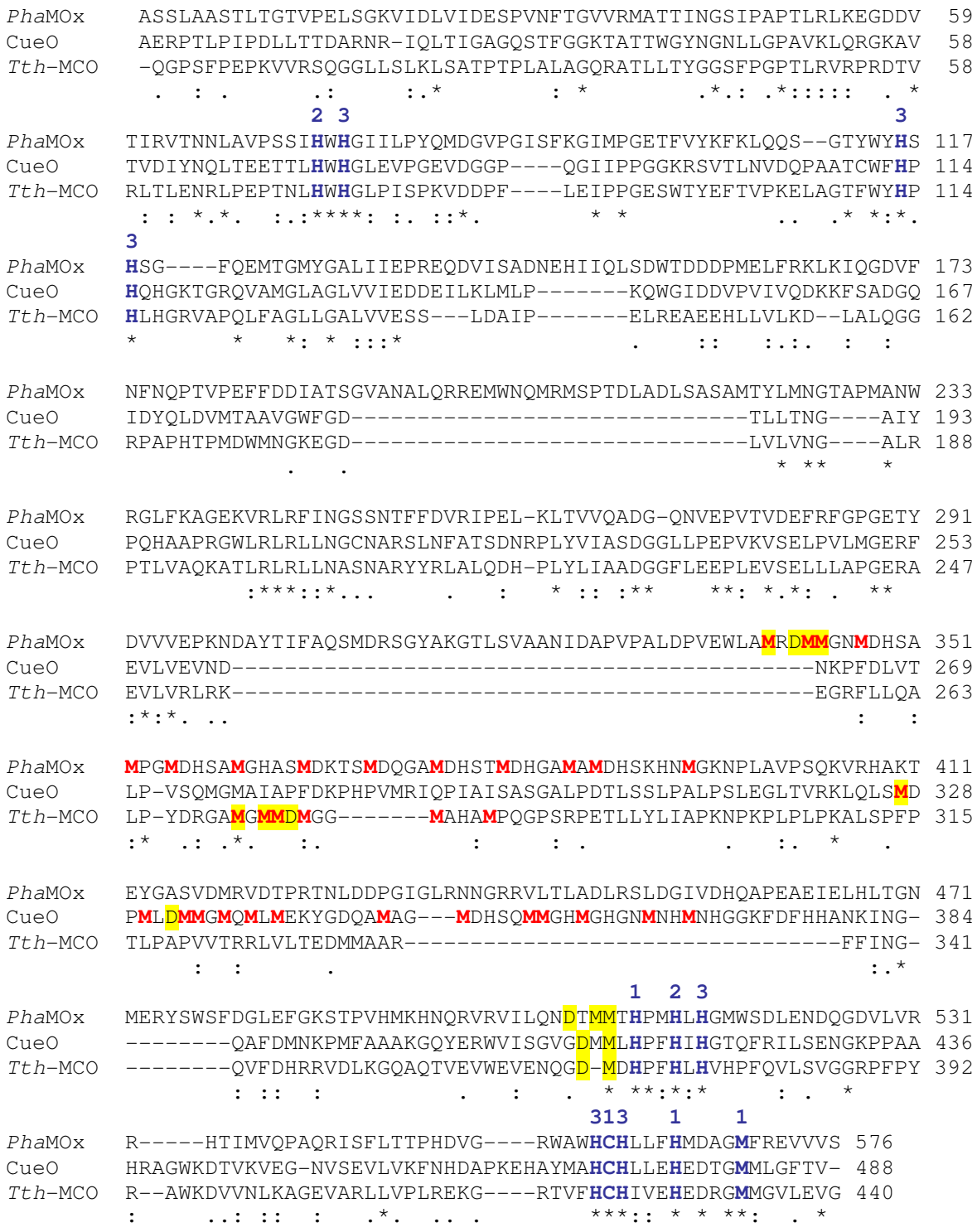

Fig. S4: Amino acid sequence alignment of the investigated blue oxidase mature forms. Ligands of the four catalytic coppers and spectroscopic copper types are indicated in blue. Methionine residues in the Met-rich loops are indicated in red. Asp and Met ligands forming the sCu site in CueO and potential sCu ligands in *Pha*MOx and *Tth*-MCO are highlighted in yellow.

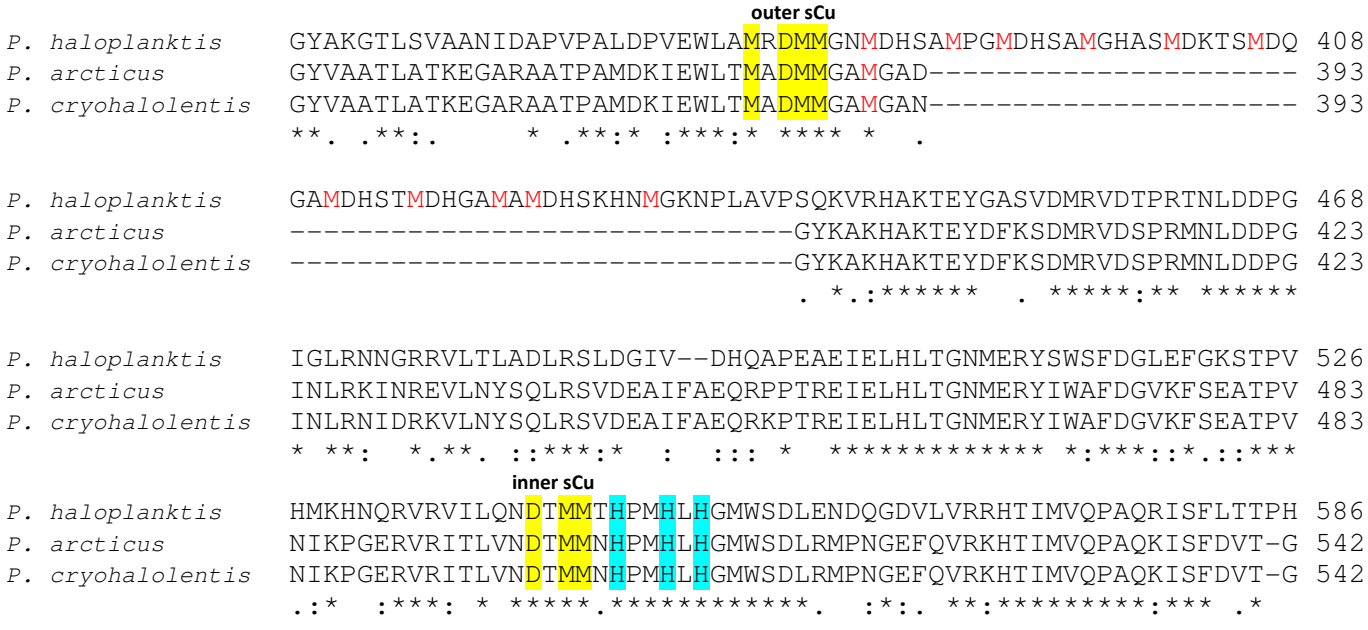

Fig. S5: Partial amino acid sequence alignment of cuproxidases from the psychrophiles *Pseudoalteromonas haloplanktis* TAC125, *Psychrobacter arcticus* 273-4 and *Psychrobacter cryohalolentis* K5. Potential Met and Asp ligands of the sCu site (yellow), Met residues in the Met-rich insert (red) and ultra-conserved His residues of the catalytic copper binding sites (blue). Amino acid numbering of the precursors.

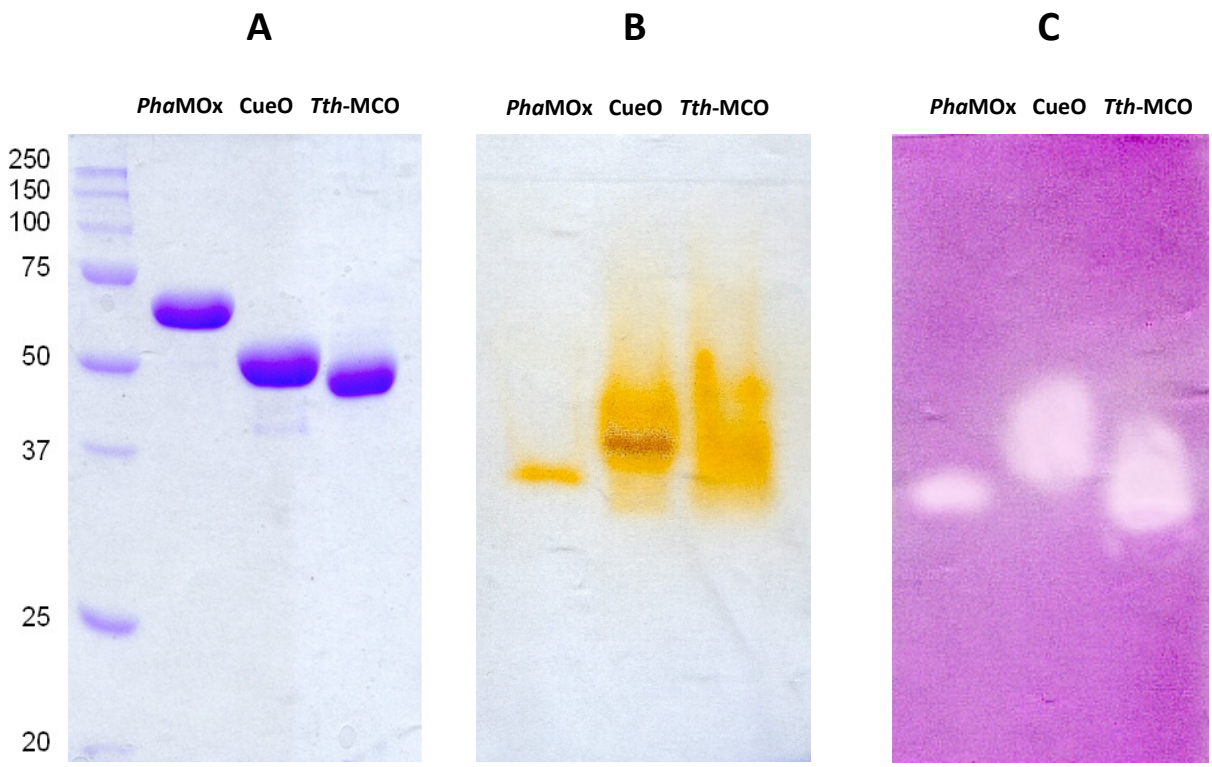

Fig. S6: Electrophoretic characterization of the investigated cuproxidases.

A: Coomassie blue stained SDS-PAGE of the purified blue oxidases. Left lane, molecular weight markers (in kDa).

B: Phenol oxidase activity after non-denaturing gel electrophoresis, revealed by oxidation of 3 mM 2,6-dimethoxyphenol in 50 mM Na-acetate, 0.5 mM $CuSO_4$, pH 5.0.

C: Ferroxidase activity after non-denaturing gel electrophoresis, revealed by oxidation of 0.2 mM $FeSO_4$ in 50 mM Na-acetate, 0.5 mM $CuSO_4$, pH 5.0. Ferrozine (15 mM) produces a purple coloration with remaining reduced iron ions.

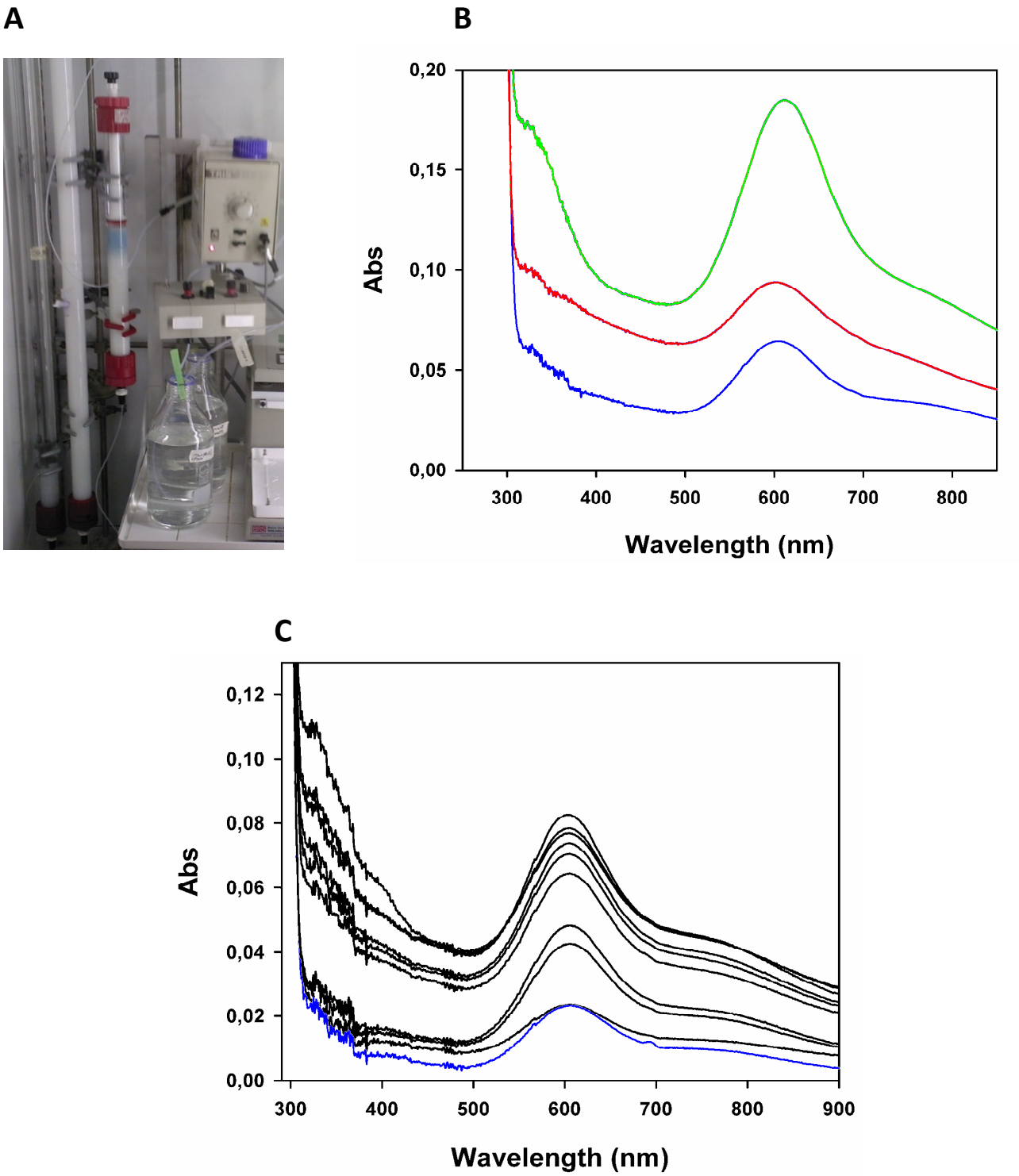

Figure S7: Spectroscopic characterization of the investigated cuproxidases.

A: a blue oxidase loaded on a chromatographic column; the blue color is produced by the T1 copper binding site.

B: UV-Vis spectra of *Pha*MOx (blue), CueO (green) and *Tth*-MCO (red) at 15 µM each and loaded with four Cu(I) equivalents. The main signal centered at 610 nm is produced by the T1 copper binding site. The contribution of the T3 binuclear copper binding site is observed around 340 nm.

C: UV-Vis spectra of *Pha*MOx after purification (blue) titrated by Cu(I) up to 225 µM $[Cu(I)(MeCN)_4]^+$ (upper spectrum, 15 Cu(I) equivalents).

Chapter V – General conclusions and perspectives

This study was undertaken to analyze the adaptive strategy to temperature of enzymes involving electron transfer in catalysis. The model enzymes chosen are homologous periplasmic cuproxidases: CueO from the mesophilic bacterium *Escherichia coli*, the thermophilic *Tth*-MCO from *Thermus thermophilus*, and PhaMOx, the corresponding psychrophilic enzyme from the Antarctic bacterium *Pseudoalteromonas haloplanktis*. We have shown that these enzymes demonstrate a specific adaptive pattern, distinct from the one observed in enzymes possessing a well-defined active site and relying on conformational changes such as for the induced fit mechanism. In fact, and in contrast with many previous studies on extremozymes, the stability of the extremophilic cuproxidases examined is correlated with neither activity, nor flexibility. One of the most striking observation is that despite large differences in stability, the flexibility of the cold-adapted PhaMOx and that of the thermophilic *Tth*-MCO are identical. This tends to indicate that the firm and precise bindings of the four catalytic copper ions are essential to ensure the proper functioning of the oxidases, *i.e.* substrate oxidation by the T1 site, positioned close to the protein surface, and oxygen reduction to water by the trinuclear cluster, located in the core enzyme. Still, the psychrophilic cuproxidase display a low stability and it remains to be clarified if it is due to a lack of selective pressure or if it is an essential component for its function.

The cuproxidases are found in prokaryotes and form a subgroup of the blue multicopper oxidase (MCO) family. Their role is to oxidize toxic Cu(I) ions into less harmful Cu(II) and they are part of the copper resistance mechanism of bacteria. In contrast to other MCOs such as laccase or ascorbate oxidase where a depression near the T1 site creates a substrate specific site for phenolic compounds or ascorbic acid, respectively, cuproxidases display disordered methionine-rich loops of variable length that restricts accessibility to the T1 site. In CueO, the Met-rich region had been demonstrated to bind Cu(I) ions which are subsequently oxidized by the enzyme. We found that the location of the Met-rich regions in the primary structure is highly variable in bacterial cuproxidases, but always inserted in solvent exposed surface loops, at close proximity of the conserved T1 site. Taking advantage of the large loop length differences in the three model cuproxidases and by studying PhaMOx variants, we showed that the number of Cu(I) bound is nearly proportional to the size of the Met-rich loops and to the number of potential Cu(I) ligands (Met, His, Asp). These results demonstrate that Met-rich loops in cuproxidases are essential components of bacterial copper resistance. They can be seen as tentacles that feed the Cu(I) substrate binding site (sCu), regarded as a beak located between the protein surface and the T1 site, and fancying cuproxidases as molecular octopus chasing toxic cuprous ions in bacterial periplasm.

As a possible follow-up to this work, there is a key point that still needs to be cleared up: the determination of the kinetic parameters of the actual *in vivo* activity, namely the catalysis of Cu(I) oxidation. Several experimental attempts were made to measure Cu(I) oxidation catalyzed by the enzymes of this study: by using an oxygen electrode to monitor O_2 consumption during catalysis or with the help of color developing reagents for time-specific determination of Cu(I) or Cu(II) concentrations. Despite some positive results were obtained, they were difficult to reproduce mostly due to the Cu(I) instability and so not conclusive enough. Due to time limit, the cuproxidase activity assay experiments were stopped in the favor of other characterization works. Later on, after the experimental part of this work had been completed, a research group published a novel and reliable method for determining the cuprous oxidase activity of CueO (Djoko *et al.*, 2010; Cortes *et al.*, 2015). They found that the purple complex anion $[Cu^{I}(Bca)_2]^{3-}$ satisfied the requirements for a chromophoric model substrate. Bca (Bicinchoninic acid) is a bidentate ligand having a Cu(I) affinity comparable to those of periplasmic Cu(I) binding proteins (Xiao & Wedd, 2011). The $[Cu^{I}(Bca)_2]^{3-}$ complex is a robust reagent, it resists air oxidation in common biological buffers, including

Cu(II)-binding buffers such as BisTris (2-[Bis(2-hydroxyethyl)amino]-2-(hydroxymethyl)-1,3-propanediol) but is oxidized readily with CueO as a catalyst. It was shown that the enzyme could extract Cu(I) from the air-stable pseudo-substrate efficiently for the oxidation (Figure V.1). The associated bleaching of the solution allows the cuprous oxidase reaction to be followed conveniently with a spectrophotometer. These advantages allowed, for the first time, a reliable and quantitative investigation of both the thermodynamics and the kinetics of CueO acting as a cuprous oxidase (Djoko *et al.*, 2010).

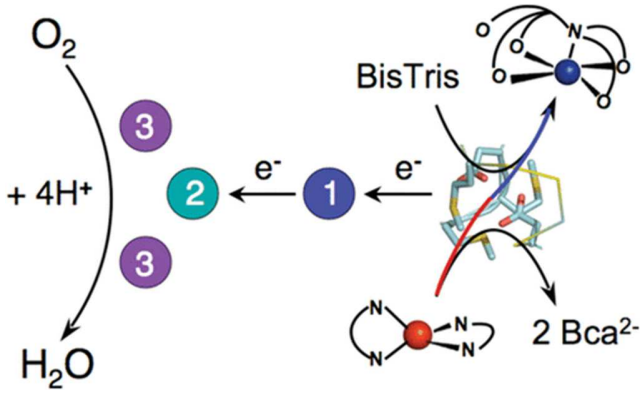

Figure V.1 - Model of the cuprous oxidase reaction mechanism of CueO using the $[Cu^{I}(Bca)_2]^{3-}$ complex. Copper centers are represented by circled numbers (T1, blue; T2, teal; T3 (binuclear), purple). The cuprous oxidase activity relies on the capability of the oxidation site, here the sCu site with ligands shown as sticks, to extract Cu(I) (red sphere) from its carrier (two Bca molecules) and is optimized in weak Cu(II) binding buffer BisTris that promotes removal of inhibiting product Cu(II) (blue sphere) from the reaction site. The model was subsequently further refined by the same research group and they showed that the sCu (called also Cu5) site is an essential electron-transfer mediator, not a substrate reaction site and that Cu6 and Cu7 are the two reaction sites for Cu(I) loading and oxidation (Cortes *et al.*, 2015; see Chapter I.II – Part B, Figure I.II.8, page 42).
(Figure from Djoko *et al.*, 2010).

It would be of high interest to test this method in order to further characterize *Tth*-MCO and PhaMOx and its variants. It could bring invaluable insights on the temperature adaptation strategy and on the effect of the composition and length of the Met-rich region on enzymatic catalysis.

A comparative structural study of the three homologous cuproxidases would also provide a better understanding of their mode of action. The crystal structures of CueO and *Tth*-MCO are available, but this is not the case for PhaMOx. While X-ray crystallography is the most widely used method to determine the 3D structure of protein molecules, this could sometimes prove to be difficult and time-consuming with no guarantee of success. On the other hand, it became recently possible to predict a 3D structure of a protein only from its amino acid sequence thanks to the release of the artificial intelligence system Alphafold (Jumper *et al.*, 2021; Varadi *et al.*, 2022). Superposition of the 3D structures of the three cuproxidases allows to highlight both their similarities and divergences, particularly visible is the huge difference in the Met-rich region (Figure V.2). These very preliminary observations would definitely deserve further study.

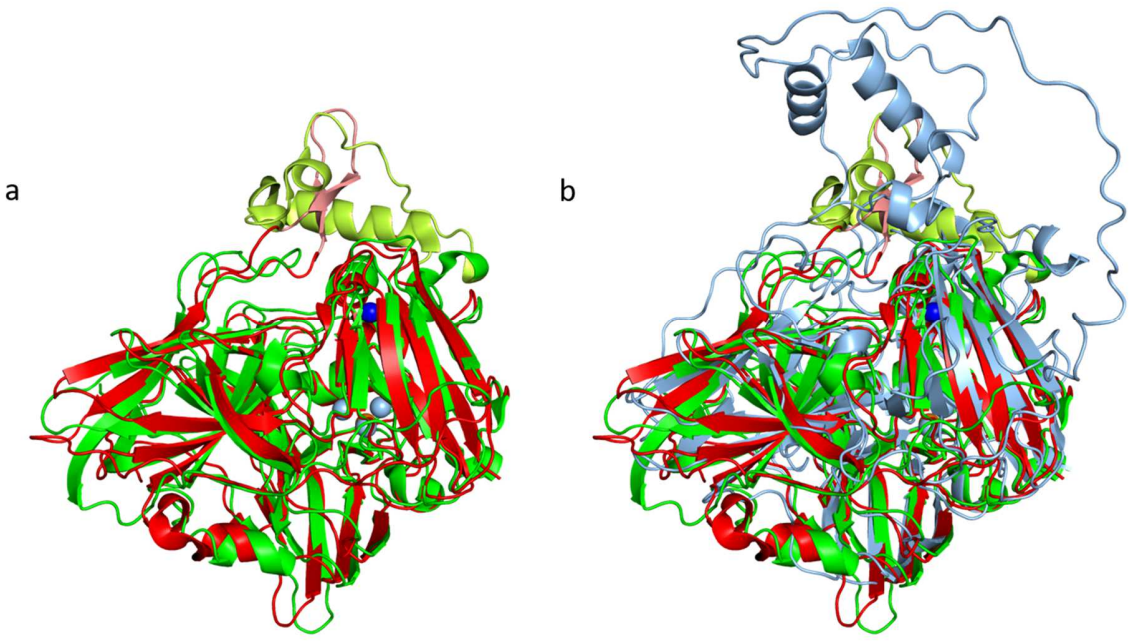

Figure V.2 – Ribbon models of CueO, *Tth*-MCO and PhaMOx.
The spheres are the copper centers associated with MCO activity (T1, blue; trinuclear cluster, grey). (a) Superposition of CueO from *E. coli* (PDB: 3OD3) colored in green and *Tth*-MCO from *T. thermophilus* (PDB: 2XU9) colored in red. The Met-rich region, covering the T1 Cu, is colored in light green and in light red in CueO and in *Tth*-MCO, respectively. (b) Same as (a) with the additional superposition of PhaMOx from *P. haloplanktis* colored in light blue. The structure prediction of PhaMOx was obtained from the AlphaFold Protein Structure Database at https://alphafold.ebi.ac.uk/ using UniProt accession number Q3ICN9 (the signal peptide was removed from the structure). The model confidence score is very high for the PhaMOx core enzyme structure and very low for the Met-rich loop covering the T1 Cu, indicating that this region may be unstructured in isolation.

As other perspectives to the work, there are a couple of intimately linked questions that still greatly spark curiosity:

1. What is the physiological relevance of length variability in Met-rich inserts? Is it "the longer the better" in terms of copper resistance function of cuproxidases?
2. Why can cuproxidases and by extension elaborated copper resistance systems be found in prokaryotes whose habitats are pristine -and then at first sight low-copper- environments?
3. Is there a specific mechanism controlling the length of the Met-rich region that may contribute to an adaptive response to elevated copper?

It is clear that the variability in location, length and sequence of Met-rich inserts suggests evolutionary trend and selection for the acquirement of copper-binding residues in surface loops close to the blue T1 site. Long insert sequences potentially binding more Cu(I) are found in bacterium not expected to be exposed to high copper concentrations such as *P. haloplanktis* isolated from pristine Antarctic sea ice. The cuproxidase PhaMOx from this bacterium displays a long 55 residue Met-rich insert whereas both cuproxidases from the Arctic *Psychrobacter arcticus* 273-4 and *Psychrobacter cryohalolentis* K5 from Siberian permafrost are devoid of the Met-rich region and only display the conserved motifs of the sCu site in their cuproxidases, although the three enzymes share 55% identity (82% similarity) in the core enzyme. Conversely, short insert sequences are noted in thermophiles thriving in metal-rich effluents from

hot springs, although this could be possibly related to loop length decreases in thermophilic proteins in order to improve their stability. Finally, the occurrence of a cuproxidase in bacteria is unpredictable: whereas the investigated *Tth*-MCO was isolated from *T. thermophilus* HB27, the genome of *T. thermophilus* HB8 is devoid of a cuproxidase coding sequence.

A phylogenetic analysis is presented below to understand the possible evolution of MCOs having a Met-rich region (Figure V.3). Despite the fact that CueO and PhaMOx possess a long Met-rich region with 14 methionines in both cases, CueO appears more evolutionary related to *Tth*-MCO which possesses however a short Met-rich region with only 7 methionines. When compared with the protein sequence of CueO, the psychrophilic PhaMOx shows 53.5 % sequence similarity (24.6 % identity), and the thermophilic *Tth*-MCO exhibits 59.9 % similarity (30.5 % identity). The cladogram also reveals that MCOs employing a Met-rich region in location MR2 (Met-rich Region 2) tend to be more widely distributed within the phylogenetic tree compared to the other MCOs which are forming clear groups according to their Met-rich region location. Whether this tend to indicate a convergent evolution for the appearance of Met-rich sequences particularly in this loop would still need to be further investigated.

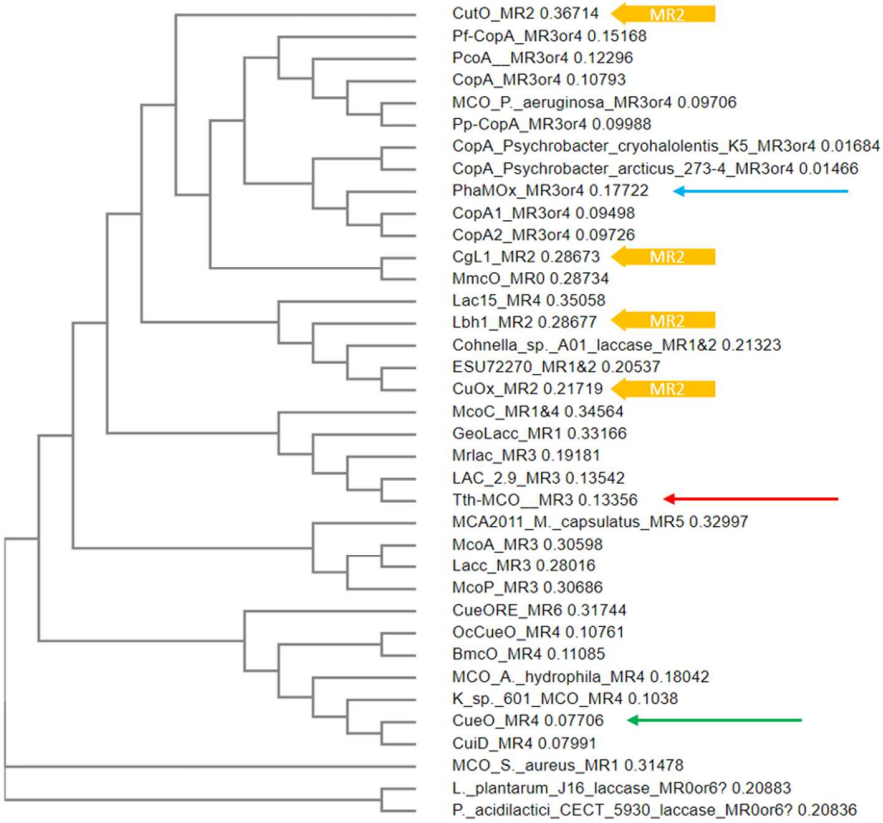

Figure V.3 - Unrooted cladogram constructed with the MCOs characterized by the presence of a methionine-rich region and/or by an experimentally confirmed cuprous oxidase activity.
This representation was constructed with the Neighbour-joining tree method without distance corrections of Clustal Omega and using the sequences of MCOs listed in Table S2 (Chapter IV, page 68), and also the MCOs sequences from *Psychrobacter arcticus* 273-4 and from *Psychrobacter cryohalolentis* K5. The number right after the MR (Met-rich Region) indication succeeding each sequence name specifies the location of the Met-rich region according to Table S2. The blue arrow, the red arrow and the green arrow indicate the position of the PhaMOx sequence, the *Tth*-MCO sequence and the CueO sequence, respectively. The orange arrows indicate the positions of the MCOs displaying a Met-rich region in location MR2.

The reasons for a cuproxidase to be part of the copper defense arsenal of prokaryotes and the physiological relevance of length variability in Met-rich inserts in this enzyme could potentially be explained by the silent, sometimes unsuspected, microscopic war that has been going on for 2 billions of years. Here we are referring to the interaction of bacteria and protists which is considered to be one of the oldest prey-predator interactions in nature. In aquatic environments, soil or anthropogenic ecosystems, predation by phagocytic protists is a major cause of bacterial mortality and a significant driving force of the genetic and functional structure of bacterial communities (Amaro *et al.*, 2015). It is also well known that human macrophages pump copper into their phagosomes after engulfing pathogenic bacteria to induce oxidative stress and bacterial cell death (Besold *et al.*, 2016). Hao and coworkers hypothesized that such a mechanism, where bacterial killing occurs through accumulation of Cu(I) in the phagosome/vacuole, originated in protozoa long before multicellular life arose and that it later evolved in eukaryotic phagocytes (Hao *et al.*, 2016). By examining survival of bacteria differing in their copper resistance determinants in two distinct unicellular eukaryote models, *Dictyostelium discoideum* and *Paracercomanas*, they could conclusively show the role of Cu(I) (and Zn(II)) in protozoan predation of bacteria, confirming their original hypothesis (Figure V.4).

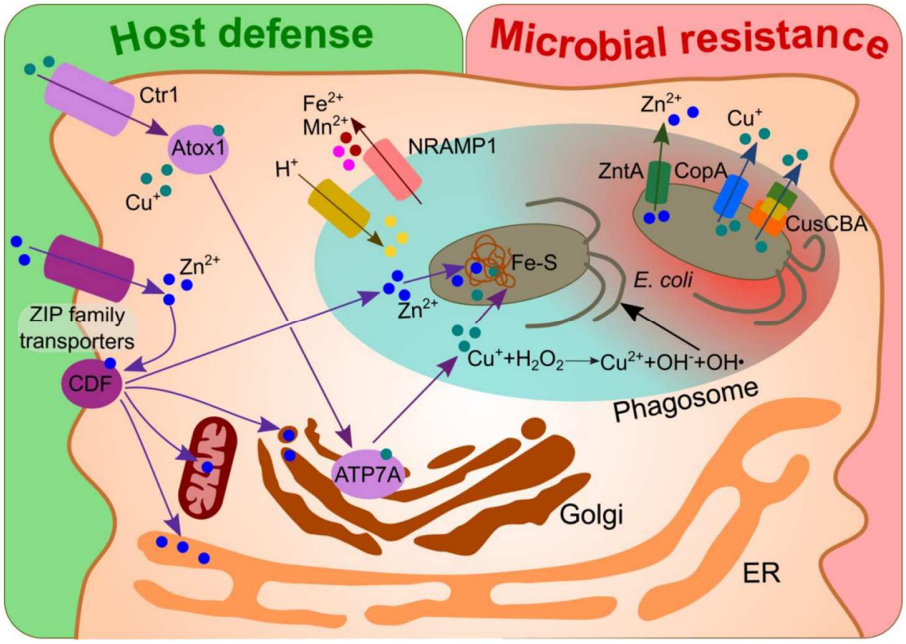

Figure V.4 - A sdchematic overview of Zn and Cu involvement in phagosomal killing of bacteria.
Macrophages and amoeba can exploit similar molecules for Zn^{2+} and Cu^{+} trafficking. ZIP family transporters allow Zn^{2+} uptake into the cytoplasm, and cation diffusion facilitator proteins (CDF) could deliver Zn^{2+} to the phagosome and other organelles, like mitochondria, Golgi, and endoplasmic reticulum (ER). Cu^{+} uptake and delivery to phagosomes occur due to copper transporter 1 (Ctr1, in amoeba known as P80), antioxidant 1 copper chaperone (Atox1), and in human macrophages, the P-type ATPase ATP7A. H^{+}-ATPase causes acidification of the phagosomal milieu, while natural resistance-associated macrophage protein 1 (NRAMP1) removes Fe^{2+} and Mn^{2+}, which are needed to protect (Mn^{2+}) and rebuild degraded Fe-S clusters of bacteria (Fe-S clusters are essential for bacterial survival). In addition, Cu^{+} amplifies toxicity of reactive oxygen species (hydroxyl radical (°OH) and hydroxide anion (OH^{-})). *E. coli* express genes encoding ZntA for Zn^{2+} efflux, CopA for Cu^{+} efflux, and the CusCBA complex for periplasmic Cu^{+} efflux, but virulent strains have additional copper resistance systems. In *E. coli*, the periplasmic cuproxidase CueO (not visible on the figure) which converts Cu(I) into less toxic Cu(II) is certainly an additional key determinant of copper resistance.
(Figure from Hao *et al.*, 2015).

Protozoan predation is then a major selection factor for maintenance and acquisition of copper resistance determinants and can explain their widespread presence in environments where copper concentrations are very low, such as in a deep ocean, and where the effect of anthropological factors on copper resistance development is also minimal (Hao *et al.*, 2017). Since these determinants would aid survival in both protozoans and macrophages, one could expect a higher occurrence of additional copper resistance determinants in virulent bacteria. For example in *Salmonella enterica*, the pathogenic serovars take copper resistance a step further through the expansion of the anti-copper arsenal via the partial duplication of the cue system and the presence of additional periplasmic and cytosolic copper chaperones, most likely to escape intracellular killing by macrophages (Giachino & Waldron, 2020). Besides the use of copper and zinc as poisons to target notably the Fe-S clusters, mechanisms of bacterial killing in the phagosomes of macrophages and protozoa also include low pH, iron and manganese starvation, generation of reactive oxygen and nitrogen species, and the engagement of a battery of acidic hydrolases (Festa & Thiele, 2011; Soldati & Neyrolles, 2012; German *et al.*, 2013; Barisch *et al.*, 2018).

In view of these evidences, one can imagine different type of experiments to examine the physiological role of the cuproxidases and particularly of their Met-rich region, such as assessing the survival rate of different bacterial strains when exposed to increasing copper concentration or to protozoan predation. The strains would only differ in the length of the Met-rich region within the cuproxidase. This could bring interesting insights on the role of this peculiar region and how it can contribute to copper resistance.

To the question whether there is a specific mechanism controlling the length of the Met-rich region that may contribute to an adaptive response to elevated copper, we see two important prerequisites.
Firstly, it is based on the fact that there is a survival advantage for the bacterium of having a higher number of Cu(I) binding sites in the Met-rich region of periplasmic cuproxidase when exposed to higher copper concentrations. The idea of attracting extra harmful Cu(I) and defuse them to less dangerous Cu(II) is very attractive and makes a lot of sense, but as discussed above, it is still an assumption.
Secondly, the underlying mechanism must be at the gene level, in the DNA, to allow an expansion of the Met-rich region. Using model peptides, previous studies demonstrated that motifs of the type $MX_{1-2}MX_{1-2}M$ are specific for Cu(I) and Ag(I) with no affinity for divalent metals, and they require at least three methionine residues for effective copper binding. Furthermore, their affinity for Cu(I) is independent of pH, motif arrangement, and composition of intervening amino acids. These studies have shown that methionine-rich sites provide a unique environment that stabilizes Cu(I) and provides exquisite selectivity over competing, biologically-relevant metal ions (Rubino & Franz, 2012). This tends to demonstrate that increasing the number of repetitions of short DNA sequences coding for linear methionine-rich Cu(I) binding motifs could readily allow to expand the number of Cu(I) binding sites in the Met-rich loop located at the cuproxidase surface and close to the T1 site. This potential process raises the question of whether it already exists distinctive regulation mechanisms that are known for copper resistance proteins. There is an interesting case of programmed ribosomal frameshifting which allows to generate two copper resistance proteins from the same gene. As described in the introduction chapter (I.II.A.5, Figure I.II.4, page 37), one component of the copper homeostasis in bacteria is the membrane integral protein CopA which pumps copper ions from the cytosol. In a number of bacteria, a small soluble copper binding protein (metallochaperone) that transfers copper to the CopA efflux pump is encoded by a *copZ* gene distinct from *copA*. In *E. coli* no separate copper chaperone has been identified, though a copper binding domain was identified at the N-terminus of its copper efflux pump protein (Atkins *et al.*, 2017). Some ribosomes translating *copA* undergo programmed frameshifting, terminate translation in the -1 frame, and generate the 70 amino acid-long polypeptide CopZ (Figure V.5). The high efficiency of frameshifting is achieved by the combined stimulatory action of a ‘slippery’ sequence, an mRNA pseudoknot, and the CopA nascent chain. Further research is needed to elucidate if copper itself or a copper binding protein could directly

regulate the frameshift mechanism by potentially interacting with the mRNA structure or the nascent CopA protein (Meydan *et al.*, 2017). For instance, it was shown that bacterial riboswitches cooperatively bind Ni^{2+} or Co^{2+} ions and control expression of heavy metal transporters to respond to toxic levels of these metals (Furukawa *et al.*, 2015).

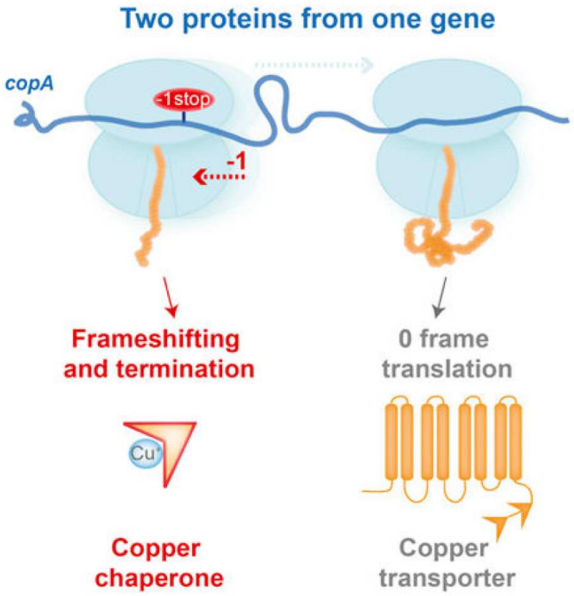

Figure V.5 - Programmed ribosomal frameshifting into the -1 reading frame where a stop codon is immediately encountered and results in the synthesis of the CopZ protein from the CopA mRNA.
(Figure from Meydan *et al.*, 2017).

It is tempting to imagine that a somehow resembling process might take place at the DNA level thereby allowing to expand the number of DNA sequence repeats coding for linear methionine-rich Cu(I) binding motifs in cuproxidases, in response to a copper stress. It is well known that Tandem Repeats (TR) are prone to DNA polymerase slippage during replication and to increased recombination, ultimately leading to expansion or deletion of TR sequences (Zhou *et al.*, 2014). It is an important mechanism in bacterial adaptation and numerous examples illustrate that bacteria can exploit TRs to adapt to changing environments on short evolutionary time scales. However, in general, it remains unclear how environmental signals are transduced to modulate the switching rate of TR-containing genes (Zhou *et al.*, 2014). Whether this is a mechanism explaining the high length variability of the Met-rich regions in cuproxidases has still to be uncovered.

References

Subsection I.I.1, section I.II and chapter V:

Amaro F, Wang W, Gilbert JA, Roger Anderson O, Shuman HA. Diverse protist grazers select for virulence-related traits in Legionella. ISME J 2015;9(7):1607-1618.

Andrei A, Öztürk Y, Khalfaoui-Hassani B, Rauch J, Marckmann D, Trasnea P-, et al. Cu homeostasis in bacteria: The ins and outs. Membr 2020;10(9):1-45.

Atkins JF, Loughran G, Baranov PV. A [Cu]rious Ribosomal Profiling Pattern Leads to the Discovery of Ribosomal Frameshifting in the Synthesis of a Copper Chaperone. Mol Cell 2017;65(2):203-204.

Baldrian P. Fungal laccases-occurrence and properties. FEMS Microbiol Rev 2006;30(2):215-242.

Barisch C, Kalinina V, Lefrançois LH, Appiah J, López-Jiménez AT, Soldati T. Localization of all four ZnT zinc transporters in Dictyostelium and impact of ZntA and ZntB knockout on bacteria killing. J Cell Sci 2018;131(23).

Bento I, Martins LO, Lopes GG, Carrondo MA, Lindley PF. Dioxygen reduction by multi-copper oxidases; a structural perspective. Dalton Trans 2005(21):3507-3513.

Besold AN, Culbertson EM, Culotta VC. The Yin and Yang of copper during infection. J Biol Inorg Chem 2016;21(2):137-144.

Collins JF, Klevay LM. Copper. Adv Nutr. 2011;2(6):520-2.

Cortes L, Wedd AG, Xiao Z. The functional roles of the three copper sites associated with the methionine-rich insert in the multicopper oxidase CueO from E. coli. Metallomics 2015;7(5):776-785.

Crichton RR, Pierre J-L. Old iron, young copper: From Mars to Venus. Biometals 2001;14(2):99-112.

Davis AV, O'Halloran TV. A place for thioether chemistry in cellular copper ion recognition and trafficking. Nat Chem Biol 2008;4(3):148-151.

Decker H, Hellmann N, Jaenicke E, Lieb B, Meissner U, Markl J. Minireview: Recent progress in hemocyanin research. Integr Comp Biol 2007;47(4):631-644.

Dick GJ, Torpey JW, Beveridge TJ, Tebo BM. Direct identification of a bacterial manganese(II) oxidase, the multicopper oxidase MnxG, from spores of several different marine Bacillus species. Appl Environ Microbiol 2008;74(5):1527-1534.

Djoko KY, Chong LX, Wedd AG, Xiao Z. Reaction mechanisms of the multicopper oxidase CueO from Escherichia coli support its functional role as a cuprous oxidase. J Am Chem Soc 2010;132(6):2005-2015.

Dong Y, Liao M, Meng X, Somero GN. Structural flexibility and protein adaptation to temperature: Molecular dynamics analysis of malate dehydrogenases of marine molluscs. Proc Natl Acad Sci U S A 2018;115(6):1274-1279.

Dupont CL, Grass G, Rensing C. Copper toxicity and the origin of bacterial resistance - New insights and applications. Metallomics 2011;3(11):1109-1118.

Enguita FJ, Martins LO, Henriques AO, Carrondo MA. Crystal structure of a bacterial endospore coat component: A laccase with enhanced thermostability properties. J Biol Chem 2003;278(21):19416-19425.

Ferreira PHB, Freitas FC, Mccully ME, Slade GG, De Oliveira RJ. The Role of Electrostatics and Folding Kinetics on the Thermostability of Homologous Cold Shock Proteins. J Chem Inf Model 2020;60(2):546-561.

Festa RA, Thiele DJ. Copper: An essential metal in biology. Curr Biol 2011;21(21):R877-R883.

Finney LA, O'Halloran TV. Transition metal speciation in the cell: Insights from the chemistry of metal ion receptors. Science 2003;300(5621):931-936.

Furukawa K, Ramesh A, Zhou Z, Weinberg Z, Vallery T, Winkler WC, et al. Bacterial Riboswitches Cooperatively Bind Ni2+ or Co2+ Ions and Control Expression of Heavy Metal Transporters. Mol Cell 2015;57(6):1088-1098.

Galli I, Musci G, Bonaccorsi Di Patti MC. Sequential reconstitution of copper sites in the multicopper oxidase CueO. J Biol Inorg Chem 2004;9(1):90-95.

German N, Doyscher D, Rensing C. Bacterial killing in macrophages and amoeba: Do they all use a brass dagger? Future Microbiol 2013;8(10):1257-1264.

Giachino A, Waldron KJ. Copper tolerance in bacteria requires the activation of multiple accessory pathways. Mol Microbiol 2020;114(3):377-390.

Grey B, Steck TR. Concentrations of Copper Thought to Be Toxic to Escherichia coli Can Induce the Viable but Nonculturable Condition. Appl Environ Microbiol 2001;67(3-12):5325-5327.

Gupta SD, Lee BTO, Camakaris J, Wu HC. Identification of cutC and cutF (nlpE) genes involved in copper tolerance in Escherichia coli. J Bacteriol 1995;177(15):4207-4215.

Gupta P, Lakes A, Dziubla T. A Free Radical Primer. Oxidative Stress and Biomaterials; 2016. p. 1-33.

Hao X, Lüthje F, Rønn R, German NA, Li X, Huang F, et al. A role for copper in protozoan grazing – two billion years selecting for bacterial copper resistance. Mol Microbiol 2016;102(4):628-641.

Hao X, Li X, Pal C, Hobman J, Larsson DGJ, Saquib Q, et al. Bacterial resistance to arsenic protects against protist killing. Biometals 2017;30(2):307-311.

Hellman NE, Gitlin JD. Ceruloplasmin metabolism and function. Annu Rev Nutr 2002;22:439-458.

Imahara H, Wakatsuki T, Kitamura T, Tanaka H. Effect of copper on growth of yeast. Agric Biol Chem 1978;42(6):1173-1179.

Jumper J, Evans R, Pritzel A, Green T, Figurnov M, Ronneberger O, et al. Highly accurate protein structure prediction with AlphaFold. Nature 2021;596(7873):583-589.

Koch KA, Peña MMO, Thiele DJ. Copper-binding motifs in catalysis, transport, detoxification and signaling. Chem Biol 1997;4(8):549-560.

Liu J, Chakraborty S, Hosseinzadeh P, Yu Y, Tian S, Petrik I, et al. Metalloproteins containing cytochrome, iron-sulfur, or copper redox centers. Chem Rev 2014;114(8):4366-4369.

Lu Y. Electron Transfer: Cupredoxins. In McCleverty JA, Meyer TJ, editors. Comprehensive Coordination Chemistry II; Vol. 8 (Bio-coordination Chemistry; Que JL, Tolman WB, editors). Elsevier, Oxford, U.K., 2003. p. 91-122.

Magnani D, Solioz M. How bacteria handle copper. In Nies DH, Silver S, editors. Molecular microbiology of heavy metals. Springer, Berlin, Heidelberg, 2007. p. 259-285.

Marcus RA, Sutin N. Electron transfers in chemistry and biology. Biochim Biophys Acta Rev Bioenerg 1985;811(3):265-322.

Mayer AM, Staples RC. Laccase: New functions for an old enzyme. Phytochemistry 2002;60(6):551-565.

Meydan S, Klepacki D, Karthikeyan S, Margus T, Thomas P, Jones JE, et al. Programmed Ribosomal Frameshifting Generates a Copper Transporter and a Copper Chaperone from the Same Gene. Mol Cell 2017;65(2):207-219.

Moss GP, Smith PAS, Tavernier D. Glossary of class names of organic compounds and reactive intermediates based on structure (IUPAC recommendations 1995). Pure Appl Chem 1995;67(8-9):1307-1375.

Outten FW, Outten CE, Hale J, O'Halloran TV. Transcriptional activation of an Escherichia coli copper efflux regulon by the chromosomal MerR homologue, CueR. J Biol Chem 2000;275(40):31024-31029.

Pearson RG. Hard and Soft Acids and Bases. J Am Chem Soc 1963;85(22):3533-3539.

Rapuano R, Graziano G. Some Clues about Enzymes from Psychrophilic Microorganisms. Microorg 2022;10(6).

Rosenzweig AC, Sazinsky MH. Structural insights into dioxygen-activating copper enzymes. Curr Opin Struct Biol 2006;16(6):729-735.

Rubino JT, Franz KJ. Coordination chemistry of copper proteins: How nature handles a toxic cargo for essential function. J Inorg Biochem 2012;107(1):129-143.

Saavedra HG, Wrabl JO, Anderson JA, Li J, Hilser VJ. Dynamic allostery can drive cold adaptation in enzymes. Nature 2018;558(7709):324-328.

Sakuraba H, Koga K, Yoneda K, Kashima Y, Ohshima T. Structure of a multicopper oxidase from the hyperthermophilic archaeon Pyrobaculum aerophilum. Acta Crystallogr Sect F Struct Biol Cryst Commun 2011;67(7):753-757.

Sakurai T, Kataoka K. Basic and applied features of multicopper oxidases, CueO, bilirubin oxidase, and laccase. Chem Rec 2007;7(4):220-229.

Sakurai T, Yamamoto M, Ikeno S, Kataoka K. Amino acids located in the outer-sphere of the trinuclear copper center in a multicopper oxidase, CueO as the putative electron donor in the four-electron reduction of dioxygen. Biochim Biophys Acta Proteins Proteomics 2017;1865(8):997-1003.

Sanchez-Amat A, Solano F. A pluripotent polyphenol oxidase from the melanogenic marine Alteromonas sp shares catalytic capabilities of tyrosinases and laccases. Biochem Biophys Res Commun 1997;240(3):787-792.

Sehnal D, Bittrich S, Deshpande M, Svobodová R, Berka K, Bazgier V, et al. Mol∗Viewer: Modern web app for 3D visualization and analysis of large biomolecular structures. Nucleic Acids Res 2021;49(W1):W431-W437.

Sen S, Sarkar M. Insights on Rigidity and Flexibility at the Global and Local Levels of Protein Structures and Their Roles in Homologous Psychrophilic, Mesophilic, and Thermophilic Proteins: A Computational Study. J Chem Inf Model 2022;62(8):1916-1932.

Serrano-Posada H, Centeno-Leija S, Rojas-Trejo SP, Rodríguez-Almazán C, Stojanoff V, Rudiño-Piñera E. X-ray-induced catalytic active-site reduction of a multicopper oxidase: Structural insights into the proton-relay mechanism and O2-reduction states. Acta Crystallogr Sect D Biol Crystallogr 2015;71:2396-2411.

Shleev S, Tkac J, Christenson A, Ruzgas T, Yaropolov AI, Whittaker JW, et al. Direct electron transfer between copper-containing proteins and electrodes. Biosens Bioelectron 2005;20(12):2517-2554.

Silva CS, Durão P, Fillat A, Lindley PF, Martins LO, Bento I. Crystal structure of the multicopper oxidase from the pathogenic bacterium Campylobacter jejuni CGUG11284: Characterization of a metallo-oxidase. Metallomics 2012;4(1):37-47.

Smith AW, Camara-Artigas A, Wang M, Allen JP, Francisco WA. Structure of phenoxazinone synthase from Streptomyces antibioticus reveals a new type 2 copper center. Biochemistry 2006;45(14):4378-4387.

Sočan J, Isaksen GV, Brandsdal BO, Åqvist J. Towards Rational Computational Engineering of Psychrophilic Enzymes. Sci Rep 2019;9(1).

Sočan J, Purg M, Åqvist J. Computer simulations explain the anomalous temperature optimum in a cold-adapted enzyme. Nat Commun 2020;11(1).

Solano F, Lucas-Elío P, López-Serrano D, Fernández E, Sanchez-Amat A. Dimethoxyphenol oxidase activity of different microbial blue multicopper proteins. FEMS Microbiol Lett 2001;204(1):175-181.

Soldati T, Neyrolles O. Mycobacteria and the Intraphagosomal Environment: Take It With a Pinch of Salt(s)! Traffic 2012;13(8):1042-1052.

Solomon EI, Sundaram UM, Machonkin TE. Multicopper oxidases and oxygenases. Chem Rev 1996;96(7):2563-2605.

Stoj CS, Augustine AJ, Zeigler L, Solomon EI, Kosman DJ. Structural basis of the ferrous iron specificity of the yeast ferroxidase, Fet3p. Biochemistry 2006;45(42):12741-12749.

Tian S, Jones SM, Solomon EI. Role of a tyrosine radical in human ceruloplasmin catalysis. ACS Cent Sci 2020;6(10):1835-1843.

Ueki Y, Inoue M, Kurose S, Kataoka K, Sakurai T. Mutations at Asp112 adjacent to the trinuclear Cu center in CueO as the proton donor in the four-electron reduction of dioxygen. FEBS Lett 2006;580(17):4069-4072.

Underwood E J. Trace elements in human and animal nutrition. 4th ed. Academic Press: New York, 1977.

Van Der Ent F, Lund BA, Svalberg L, Purg M, Chukwu G, Widersten M, et al. Structure and Mechanism of a Cold-Adapted Bacterial Lipase. Biochemistry 2022.

Varadi M, Anyango S, Deshpande M, Nair S, Natassia C, Yordanova G, et al. AlphaFold Protein Structure Database: Massively expanding the structural coverage of protein-sequence space with high-accuracy models. Nucleic Acids Res 2022;50(D1):D439-D444.

Wang H, Liu X, Zhao J, Yue Q, Yan Y, Gao Z, et al. Crystal structures of multicopper oxidase CueO G304K mutant: structural basis of the increased laccase activity. Sci Rep 2018;8(1).

Xiao Z, Wedd AG. Metallo-oxidase enzymes: Design of their active sites. Aust J Chem 2011;64(3):231-238.

Zhang Z, Xia Y, Dong G, Fu Y, Liu S. Exploring the cold-adaptation mechanism of serine hydroxymethyltransferase by comparative molecular dynamics simulations. Int J Mol Sci 2021;22(4):1-19.

Zhou K, Aertsen A, Michiels CW. The role of variable DNA tandem repeats in bacterial adaptation. FEMS Microbiol Rev 2014;38(1):119-141.